The Development of Multi - Compartmentalised Systems for the Directed Organisation of Artificial Cells

---

Tabea Kirchhofer

Univ. Diss.

zur Erlangung des akademischen Grades
“doctor rerum naturalium”
(Dr. rer. nat.)
in der Wissenschaftsdisziplin “Kolloid- und Grenzflächenwissenschaften”

eingereicht an der
Mathematisch - Naturwissenschaftlichen Fakultät
Institut für Chemie
der Universität Potsdam
und
dem Max - Planck - Institut für Kolloid- und Grenzflächenforschung

Disputation: 27.10.2021

Erster Betreuer: Prof. Ilko Bald
Zweiter Betreuer: Dr. Tom Robinson

Erster Gutachter: Prof. Ilko Bald
Zweiter Gutachter: Dr. Tom Robinson
Externe Gutachterin: Prof. Patricia Bassereau

Published online on the
Publication Server of the University of Potsdam:
https://doi.org/10.25932/publishup-52842
https://nbn-resolving.org/urn:nbn:de:kobv:517-opus4-528428

Abstract

Membrane contact sites are of particular interest in the field of synthetic biology and biophysics. They are involved in a great variety of cellular functions. They form in between two cellular organelles or an organelle and the plasma membrane in order to establish a communication path for molecule transport or signal transmission. These sites are characterised by being tethered in close apposition (10 - 80 nm) without membrane fusion and are composed of specific lipids and proteins.

The development of an artificial membrane system which can mimic membrane contact sites using bottom up synthetic biology was the goal of this research study. For this, a multi - compartmentalised giant unilamellar vesicle (GUV) system was created with the membrane of the outer vesicle mimicking the plasma membrane and the inner GUVs posing as cellular organelles. The multi - compartmentalised system, also called vesosome was formed in a multi step process starting with the formation of electroformed GUVs. These GUVs were afterwards encapsulated in the outer GUVs created from the inverted emulsion method to form the desired vesosomes. The study revealed different factors influencing the creation of vesosomes e.g. the centrifugation speed used for the inverted emulsion method.

In the following steps, three different strategies were used to achieve an internal membrane - membrane adhesion. The first one established a biotin streptavidin bridge between both GUV membranes. For this, both GUV types contain a biotinylated lipid. Streptavidin is encapsulated in the outer GUV along with the electroformed vesicles. The membrane adhesion includes a large contact angle and an enlarged adhesion area often leading to a membrane deformation of either of the two GUVs. A directed membrane - membrane adhesion could be formed by the employment of liquid - liquid membrane phase separations of either of the vesicle types. The biotinylated lipid, only partitioning into the liquid disordered phase, restricts the adhesion to the same.

The second strategy employed DNA oligonucleotides which were biotinylated and attached to the membrane via a biotin streptavidin bridge. Two different strands (different sequences) binding to either of the GUV types, were paired with a third strand, establishing the membrane - membrane adhesion. The great advantage was the observation of the adhesion in the moment its formation. The adhesion can (in theory) also be reversed through the addition of a competitive oligonucleotide. The membrane adhesion showed a more narrow adhesion area compared to the former system and a small contact angle. A directed membrane - membrane adhesion could not be established. This strategy still needs further investigation, parameter changing and experiments in the future.

The last strategy used two proteins which bind when they are irradiated by light with a wavelength of 488 nm and dissociate again in the dark. They are called iLID and Nano and were provided by the group of S. Wegner. Carrying a His - tag, they were attached to the membranes of GUVs through the incorporation of Ni^{2+}-NTA lipids which form a complex with the His - tags. The membrane - membrane adhesion was afterwards triggered by light irradiation and reversed again by incubating the sample in the dark. The membrane adhesion also showed a small adhesion area and a small contact angle. A directed membrane - membrane adhesion could not be established. The inverted emulsion GUVs of this system had stability issues, leading to transient pore formation, budding, fusion and bursting which affected the experimental work.

Mimicking membrane contact sites by forming an internal membrane - membrane adhesion with multi - compartmentalised GUVs, was to some extend successful. Specific agents were used on both GUV membranes binding to each other and in this way forming a “contact site”. A communication between both GUVs could not be established.

Zusammenfassung

Viele bedeutende Prozesse einer Zelle spielen sich an den Berührungsstellen zwischen Zellmembranen und auch zwischen Zellmembranen und der Plasmamembran ab. An diesen, aus spezifischen Lipiden und Proteinen aufgebauten Kontaktstellen, können auf Grund der geringen Entfernung Signale und auch Moleküle ausgetauscht werden.

Ziel dieses Forschungsprojektes war die Entwicklung eines künstlichen Zellmembransystems, das in der Lage ist diese Kontaktstellen nachzubilden. Dafür wurden multikompartmentalisierte riesige unilamellare Vesikel (GUVs) aufgebaut. Dies bedeutet, dass sich ein GUV innerhalb eines anderen GUVs befindet. Das äußere Vesikel bildet in diesem System die Plasma Membran, während das Innere als Zellorganelle fungiert. Dieses System wird auch als Vesosom bezeichnet und in einem mehrschrittigen Prozess hergestellt (Eischluss von GUVs in andere GUVs mittels der invertierten Emulsionsmethode). Im Rahmen dieser Studie konnte gezeigt werden, dass die Herstellung von Vesosomen mittels dieser Methode unter anderem von der verwendeten Zentrifugationsgeschwindigkeit im letzen Schritt der invertierten Emulsionsmethode abhängt.

Im Folgenden wurden drei verschiedene Strategien entwickelt, um interne Haftung (Adhäsion) zwischen den Membranen zu erzeugen.

1) Aufbau einer Verbindung durch die Verwendung von Biotin und Streptavidin: Dafür wurden mit Biotin funktionalisierte Lipide in die Membranen eingebracht und Streptavidin in das Innere des äußeren GUVs mit eingeschlossen. Die Adhäsion erfolgte durch die Bildung eines Komplexes zwischen Biotin und Streptavidin.
2) Aufbau einer Verbindung unter Verwendung von kurzen DNA - Strängen (Oligonukleotide, einsträngig): Die Adhäsion erfolgte in diesem Fall durch die Bindung der DNA - Stränge zueinander.
3) Aufbau einer Verbindung durch lichtsensitive Proteine: Bei dieser Strategie wurden zwei Proteine verwendet, welche unter Lichteinfluss aneinander binden. Die Bindung zerfällt in der Dunkelheit wieder.

Mit Hilfe der gewählten Strategien konnten die Kontaktstellen zwischen Zellmembranen und der Plasmamembran zum Teil nachgebildet werden. Eine Optimierung der Stabilität von z.B. dem Proteinsystem und das Erreichen einer Kommunikation zwischen den Vesikeln sind zukünftige Forschungsziele.

Besonders die Nutzung von DNA - Nukleotiden undlichtsensitiven Proteinen erscheint lohnenswert durch eine mögliche Reversibilität und sogar Schaltbarkeit. Für die Etablierung einer Kommunikation eignet sich das System aus Biotin und Streptavidin mit großer Wahrscheinlichkeit am meisten.

Table of contents

Declaration

Die Vorliegende Arbeit entstand im Zeitraum zwischen Mai 2017 und Juni 2021 am Max-Planck-Institut für Kolloid- und Grenzflächenforschung in der Abteilung für Theorie und Biosysteme.

Ich, Tabea Kirchhofer, erkläre hiermit, dass die vorliegende Arbeit an keiner anderen Hochschule eingereicht sowie selbstständig von mir angefertigt wurde. Ebenso wurden nur die hier angegebenen Hilfsmittel und Literaturen verwendet wurden.

The present work was carried out and written during May 2017 and June 2021 at the Max Planck Institute of Colloids and Interfaces in the department of Theory and Biosystems.

I, Tabea Kirchhofer, hereby declare that neither I nor anybody else has submitted this thesis to any other university. I have produced this work independently, using only literature and other aids as described and listed here.

Tabea Kirchhofer

Acknowledgement

In the beginning, I would like to thank the people near and dear to me.
I like to thank my family, for all their support in needed times, for all their pushing me and still never letting go of me completely. I would like to thank my friends for accepting me the way I am and always looking out for me when I'm too busy doing it myself, for distracting me from the one life that is work and dragging me into another that is…not work but just simple life.
One does not need a lot of people in their life, only the right ones.

My gratitude goes to all the people of the MPIKG, the ones who were always up for discussions on all things work related, the ones who were always there for a short or not so short break from work (especially the ones with tea and sweets), the ones who helped when things would not go as planned and needed.
I would like to thank everybody from the theory department, from the IT group, from the library, the store, the workshop, the administration, but especially the members of my group and the best secretary of all.

I would like to give my gratitude to Dr. Tom Robinson for giving me the chance to work on this exciting project at this amazing research institute. Thank you for the support, the discussions, the motivation and the patience.
I want to thank Prof. Ilko Bald for all the help, the mentoring, the trust and for keeping me connected to the University for more than just on paper.

I also want to thank Prof. Patricia Bassereau and JProf. Henrike Müller-Werkmeister for agreeing to act as reviewers on my thesis and effort and interest to it.

And last but not least, I want to thank Jack for being my loyalest companion, for spending more time with me than anybody else, for cuddling, purring, playing and meowing. You are the best cat in this world!

1. Introduction

1.1. Cells

1.1.1. Prokaryotes and Eukaryotes

These days, the scientific community estimates that some 3.8 billion years ago, first life evolved in form of single cell organisms. However, what happened is still a matter of speculation and countless theories are discussed but none can be proven. And since evolution is not something one can easily recreate in the lab, the future will probably hold more questions than answers for this particular topic.[1]

So what does the scientific community agree on (mostly) these days?

Cells are living things or to use the words of B. Alberts "the individual cell is the minimal self-reproducing unit of living matter […]" with the ability to divide into two as their form of reproduction. They process information, respond to stimuli and organise a wide range of chemical reactions. They have a plasma membrane which is mostly made of phospholipids and creates a selective barrier between the interior and the exterior of the cell.[2,3] There are three different types of cells: prokaryotes, archaea and eukaryotes. Archaea are a special type of prokaryotic cells, forming a separate class and will not be discussed here.[2]

Prokaryotic cells, in most cases, live as single cell individuals meaning, they can live in colonies or close association with other organisms but they often live isolated[3]. In general, these cells are spherical, rod-shaped, or spiral and are smaller compared to eukaryotic cells usually, within a diameter of 1 to 10 μm (see Figure 1.1.a)[1,2]. They are less complex in structure comprising a single compartment, containing all needed live sustaining components like DNA, RNA, proteins and so on. Being simpler in structure, they show a much greater biological diversity than eukaryotes, including the ability to survive in the most hostile environments[2]. Typical prokaryotes are almost all bacteria, the most studied here being Escherichia coli, or E.coil for short.

Eukaryotes, other than prokaryotes, are more often found in multicellular organisms, forming astonishing structures like plants, animals or fungi. In general, eukaryotic cells are bigger and of a more complex design compared to prokaryotic cells (see Figure 1.1.b).[1,2] But the main difference is for them to be multi - compartmentalized. Eukaryotic cells keep especially their DNA in the nucleus, separated by a double membrane from the cytoplasm and the other organelles like the mitochondria or the endoplasmic reticulum (ER). All the different organelles being involved in the cell's digestion and secretion processes, are enclosed by membranes. These membranes function as selective barriers between the interior of the different organelles and the interior of the cell itself

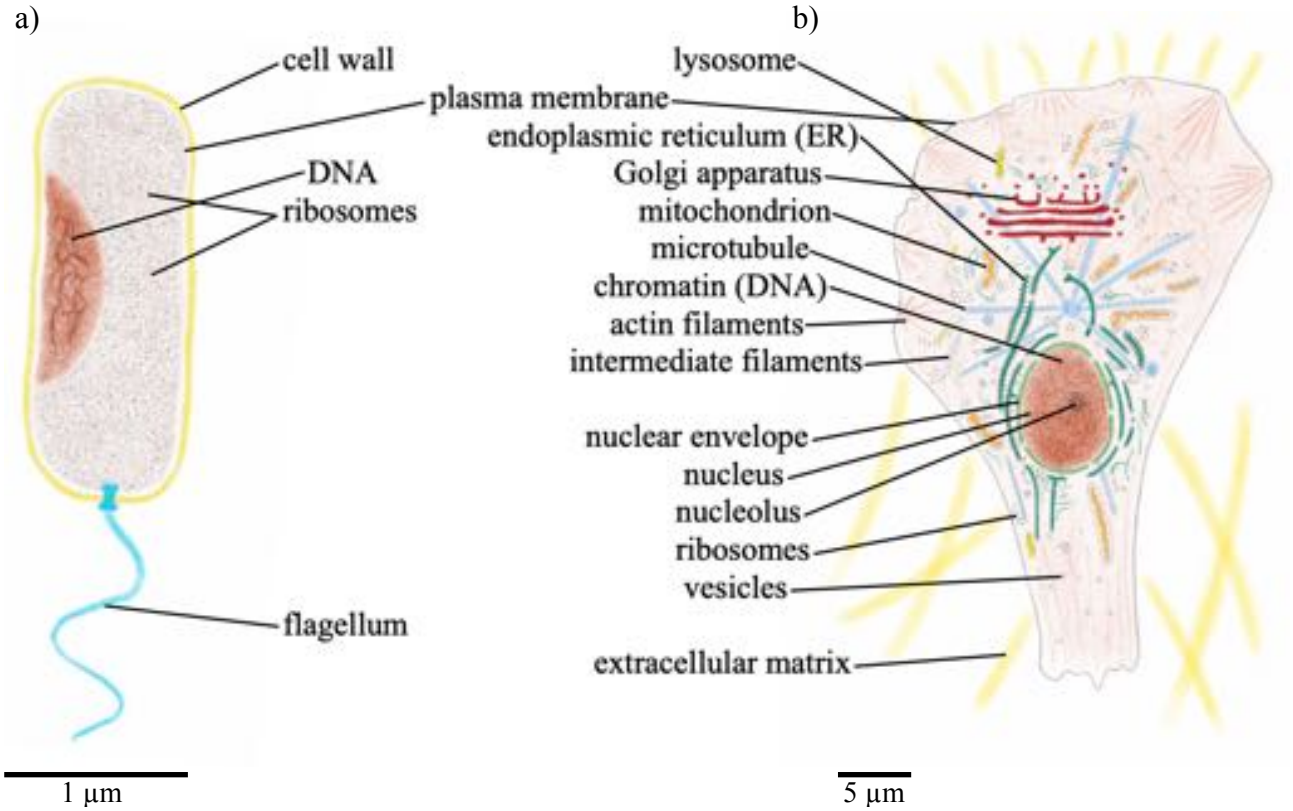

Figure 1.1: a) Schematic of a bacterium (Vibrio cholerae) as an example of a prokaryotic cell. b) Schematic of an animal cell (no specific species) as an example of an eukaryotic cell. Adapted from [2].

and confine specific molecules in their interior, creating compartments with specific chemical identities. Also, a distinct key feature of eukaryotes is the actin cytoskeleton which is the cell equivalent to the human skeleton, helping to maintain its shape and size, providing mechanical strength. It is important for the cell's movement and even involved in processes like exocytosis[2,4].

All in all, one can say that cells, prokaryotes and eukaryotes, are the most astonishing thing evolution came up with. The complexity of these systems is, to this day, not completely understood, not for the simplest but much more diverse prokaryotes nor for the more elaborate but less diverse eukaryotes. And to this day, no scientist was able to reproduce the evolution of cells or parts of it nor can we build our own fully functional synthetic cell in the laboratory.[1] There is much left to learn particularly about the communication between cells, and cells and their organelles in case of eukaryotes[3].

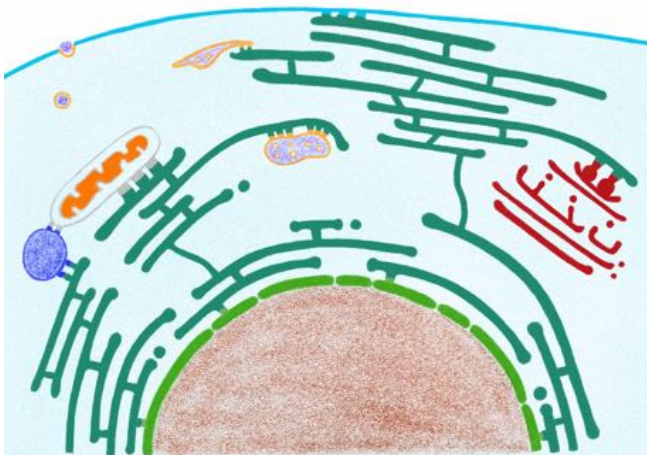

Figure 1.2: Schematic of contact sites between different cellular organelles and the plasma membrane of an eukaryotic cell. Adapted from [5].

This work was inspired by the ability of

communication that a cell is capable of. The different membranes that a cell contains can form so called membrane contact sites with each other (see Figure 1.2 for examples). Briefly, membrane contact sites are special areas at which two membranes of two organelles (or the membranes of an organelle and the plasma membrane) come into close apposition (in the range of 10 - 80 nm distance) without membrane fusion. They serve specific functions like bidirectional molecule transport, signal transmission and enzyme positioning for activity regulation.[6,7] It is very likely for these contact sites to be composed of functional proteins and/or specific lipid compositions especially, “lipid rafts” are discussed in this context[6,7,8,9]. Membrane contact sites can occur between many organelles and also between organelles and the plasma membrane. Well studied examples are contact sites between the endoplasmic reticulum and the plasma membrane, the Golgi apparatus, mitochondria and more[5,6,7,10,11]. But there are also contact sites between mitochondria and vacuoles, mitochondria and lysosomes, the plasma membrane and mitochondria.[5,6,7,10,11]

For this study, membrane contact sites involving the plasma membrane are of particular interest. There is a high level of organisation of the cellular organelles to prevent hindrance of diffusive transport processes and in some cases, cells even consist of a cell polarity which is critical for its functionality[12]. To understand the mechanisms behind the process of organelles getting in close proximity with the plasma membrane and the requirements of the two membranes to establish a contact site in between to accomplish a way for communication, is of extensive relevance in order to one day fully comprehend eukaryotic cells in detail. For that, one needs to take a closer look at biological membranes.

1.1.2. Biological Membranes

In 1972, Singer and Nicolson published a model representing the structure and dynamics of the cell membrane of eukaryotic cells[13]. They called it the fluid mosaic model. Almost 50 years later, their model still has its place in modern membrane science despite adaptations. It still shows the basic idea of a biological membrane (see Figure 1.3). The plasma membrane composes of phospholipids, glycolipids, sterols, different types of proteins and polysaccharides. The membrane itself is built as an oriented bilayer made of two leaflets of different lipids, a high density of

Figure 1.3: Schematic of the Singer-Nicolson model updated and extended by Engelmann showing the lipid bilayer (yellow) and intrinsic as well as peripheral proteins (green). Adapted from [13,14].

proteins, and polysaccharides. The proteins associated with biological membranes can be classified into three different categories. There are integral proteins which are embedded in the lipid bilayer, lipid anchored proteins which are bound to the head group of single or multiple lipids of one leaflet and a third type called peripheral proteins which can either be associated with the membrane through interactions with one of the other two protein types or by interactions with the head groups of the lipids. The polysaccharides are bound to specific lipids, the glycolipids.[2,3,13]

The lipids, providing the fundamental structure/backbone of the membrane, are of an amphiphilic nature which means a lipid molecule contains a water soluble part (polar head group) and a water insoluble part (non polar tail group) (see Figure 1.4.a). This includes phospholipids, glycolipids, sphingolipids and sterols. Although, sterols are somewhat of an exception because they are mostly

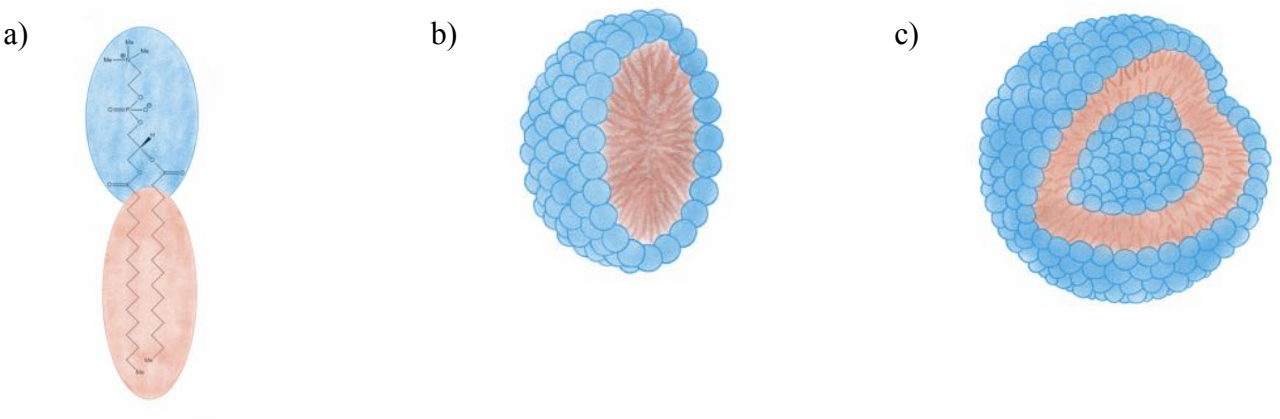

Figure 1.4: a) Chemical structure of the phospholipid 1,2-dipalmitoyl-sn-glycero-3-phosphocholine (DPPC) with the polar phosphocholine head group marked in blue and the two non polar carbon chain tail group marked in red. Chemical structure from Avanti® Polar Lipids; ©2021 Merck KGaA, Darmstadt, Germany. b) Schematic of a micelle (lipid monolayer) in an aqueous solution with the polar head groups (blue) facing the exterior and the non polar tail groups (red) facing the interior. Adapted from [2]. c) Schematic of a lipid vesicle (lipid bilayer) in an aqueous solution with the polar head groups (blue) facing the exterior as well as the interior and the non polar tail groups (red) averted from the aqueous phase. Adapted from [2].

hydrophobic and carry only one hydroxyl group as hydrophilic (polar) part.[2,3,13] In an aqueous medium which represents a polar solvent, lipids will self assemble into a form where the water insoluble tail groups are assembled close to each other facing the core of the structure while the water soluble head groups will face the solvent. Structures like micelles (monolayer) (see Figure 1.4.b), vesicles (bilayer) (see Figure 1.4.c) or flat lamellar bilayers can form this way.[2,3] The formation of these structures depends on different conditions and most amphiphilic molecules can form such phases. In all cases, the critical micelle concentration (CMC), being the minimal concentration of amphiphiles in a solution to form micelles, must be exceeded. Below this

concentration the molecules will be dispersed as free molecules in solution. A bilayer structure can be favoured, if the head and the tail groups of the lipids are of a similar area.

In case of biomembranes like the plasma membrane, the lipids are to a great extend phospholipids meaning, they have a phosphate containing head group usually bound to an organic rest such as serine, choline, ethanolamine or others and usually two hydrocarbon chains mostly fatty acids (acyl chains) as tail group (see Figure 1.5). They display a great versatility because of that. Phospholipids are subdivided into phosphoglycerides also called glycerophospholipids, and sphingolipids. Both types are similar in structure except for one group. The phosphate group which carries the head group on one side, is on its other side attached to a glycerol (two marked groups in red in structures in Figure 1.5) connected to the fatty acid tails in case of the phosphoglycerides while, in case of sphingolipids, it is sphingosine (two marked groups in dark blue in structures in Figure 1.5) linking the fatty acids to the phosphate group. Sphingosine itself carries one unsaturated fatty acid chain by default. Glycolipids on the other hand are very similar to sphingolipids but do not include the

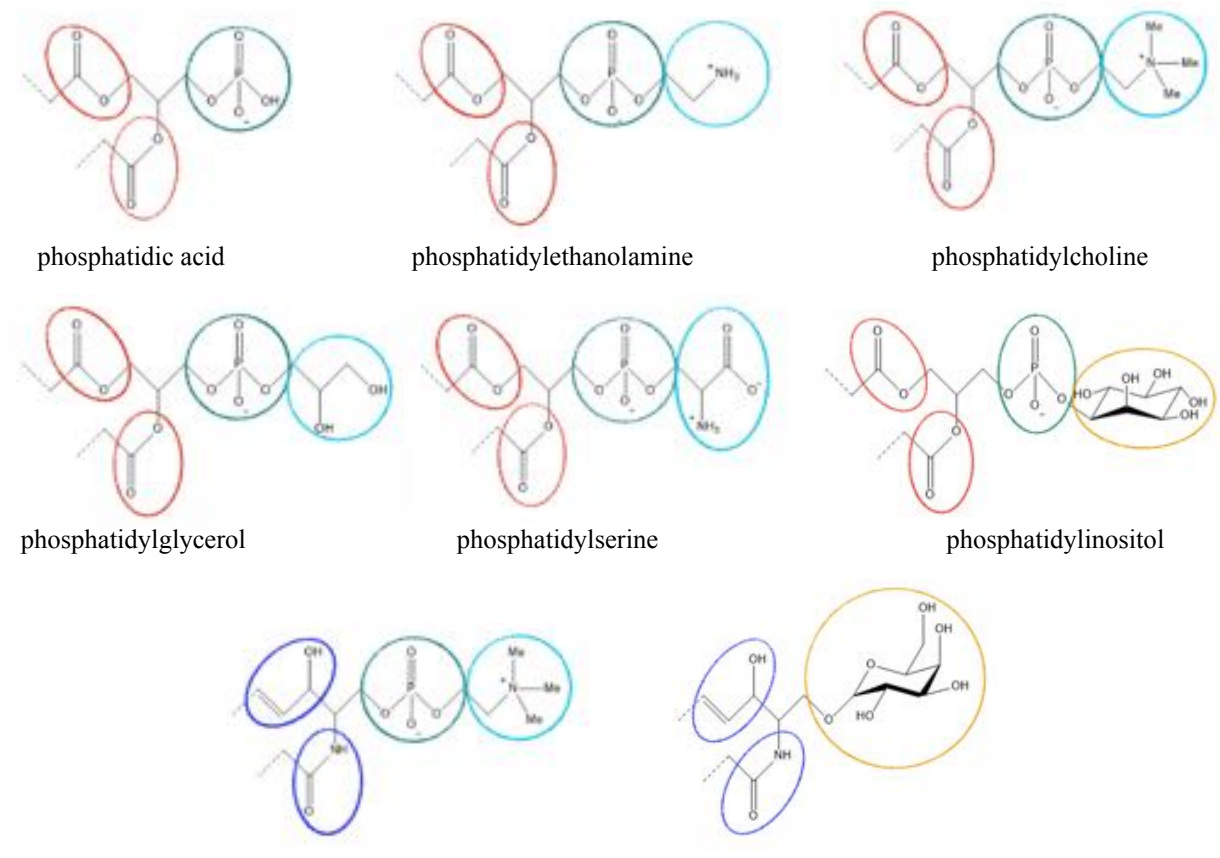

Figure 1.5: Chemical structures of a variety of lipid head groups. Phosphate groups marked in green, ester bond connecting the fatty acid tails to the lipid marked in red, additional neutral or positively charged head groups connected to the phosphate group marked in light blue, amino alcohol group connecting fatty acid tails to the lipid marked in dark blue (also called sphingosine) and sugar groups marked in yellow. Chemical structures from Avanti® Polar Lipids; ©2021 Merck KGaA, Darmstadt, Germany.

phosphate group. Instead, they carry saccharides (mono- or oligosaccharides marked in yellow in Figure 1.5) attached to sphingosine (in case of glycolipids from animal cells). There are also many different types of head groups (in case of phospholipids) with different charges, different sizes, different characteristics in general, as can be seen in Figure 1.5.[15] When considering the distribution of the different lipids within the two leaflets of a biomembrane, the asymmetry of the lipid distribution is a clear indicator of specific functionalities rooted to certain lipids.[2,3] Phosphatidic acid is the simplest of the phospholipids. And although it displays as one of the minor components of the natural lipids within biomembranes (1 - 4 %[16]), its diverse biological functions are still not completely understood. Next to its role as a precursor for the biosynthesis of other phospholipids, phosphatidic acid is involved in cell proliferation, vesicular trafficking, it works as a second messenger and it modulates the membrane shape.[16,17,18,19] In the processes of membrane fusion and fission which are mostly regulated by certain proteins, there are also specific lipids involved. One of them is phosphatidic acid next to phosphoinositides, diacylglycerol and also sterols[16]. Phosphoinositol (PI), also called phosphoinositide, is a more special type of lipid involved in several cellular functions. Carrying a sugar group connected to the phosphate group, three of the hydroxyl groups can be phosphorylated by a specific group of enzymes called PI kinases. Resulting from that, there are seven distinct phosphoinositides in addition to the non phosphorylated version.[20,21,22] Phosphatidylcholine (PC) is the most common phospholipid in the plasma membrane and the different endomembranes next to -ethanolamine and -serine. Among other things, these lipids influence membrane fluidity and membrane curvature. At this point, the varieties of the tail groups are of importance too. Tail groups which are usually fatty acid groups can be of different chain length, can have a different degree of saturation and there can be one chain (lysophospholipid) or two chains (see Figure 1.6). Depending on the length of the fatty acid (usually even numbered like C_{14}, C_{16}, C_{18}, C_{20}) and the saturation of the carbon chain, the forming bilayer (or monolayer) can vary in thickness, fluidity and membrane curvature.

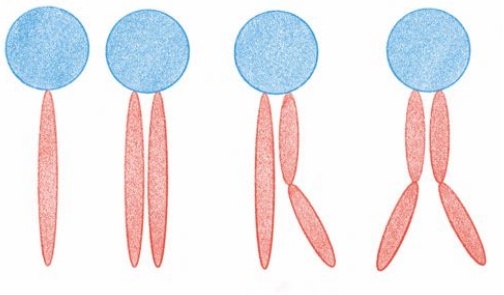

Figure 1.6: Schematics of different lipids. From left to right: with one fatty acid tail group and two fatty acid tail groups where both chains are saturated, one of two is unsaturated and both are unsaturated. Adapted from [2,3,23,24].

The whole bilayer structure is stabilised via van der Waals forces between the carbon chains and hydrogen bonds and ionic bonds between the phosphate groups and the aqueous (polar) solvent. This is the basis of the organisation of all biological membranes.

As mentioned before, every eukaryotic cell is contained by a barrier, the plasma membrane and the profound difference between prokaryotes and eukaryotes are the cellular organelles of which some are also enclosed by a biomembrane. It is important to notice that membranes are asymmetric, not only in terms of composition (lipids and proteins) but also relative to their individual leaflets.[2,3,13]

The most essential purpose of a membrane with all its diversities in lipids and proteins is its function as a semi permeable barrier, permeable to only specific agents and controlled in both ways. This permeability in the case of the plasma membrane ensures the communication of the cell with its environment and other neighbouring cells, for example.[3] The exchange of molecules of all sorts is included in the term communication.[6] The barrier function of the membrane is of particular importance due to concentration differences of ions, for instance. In the case of Na^+, the concentration in the cytoplasm i.e. inside of the cell is several times lower compared to the exterior. The concentration of K^+ on the other hand is several times lower in the exterior. Many proteins being part of the plasma membrane, are relevant for the controlled transport of ions and other molecules. Some of these proteins can transport ions against the concentration gradient across a membrane which requires energy. Other transport processes like ion transport with a concentration gradient, release energy.[2,3] When talking of communication between cells or a cell and its organelles, this always includes a signal transduction of some sort. It can be an electrical potential in form of ions or the transport of essential nutrients. These processes can require specific conditions like membrane contact sites.[6,25] For example, chemical reactions in cellular organelles can produce toxic waste products which the cell has to be able to discard without compromising the cell itself.[1,2,3] Processes like that need to have a high level of control considering the organelles involved as well as the time and place within the cell. Several factors like the presence of specific proteins, a definite membrane composition of the involved membranes are of crucial importance here.[8,9,26]

Scientists can employ different strategies to gain deeper knowledge of processes like nutrient transport, the communication between cellular organelles and the plasma membrane or all the other functions of a eukaryotic cell. The approach in this study is mimicry. A simplified model membrane system was created in the laboratory which is supposed to act like a plasma membrane interacting with the membranes of cellular organelles in a controlled way. What this means and how it was done is topic of this thesis. The next section will give an insight into model membrane systems and how they can be used to mimic cell and cellular processes.

1.2. Model Systems of Biological Membranes and Cells

It takes a great effort to even just create single accurate parts of cells in a lab and especially for those to be close to the original in structure and function. But why do we even try to create synthetic versions of cells?

One of the essential reasons is understanding. A single eukaryotic cell is a sophisticated machinery with countless of specialised functions and characteristic structural features that provide these functions. In order to fully comprehend someday, how a cell is able to reproduce, to evolve, to take up energy, basically to live, we need to look deeper. Model systems allow us to do exactly that and can even lead to unexpected discoveries. Scientists study cells, cellular functions and cellular structures through reversed engineering in a controlled (laboratory) environment, to learn more about actual living cells. A second reason is to gain a broader knowledge about the evolution of cells. It is clear that the living evolved at a certain point of time from the non - living. In molecular evolution, it is generally agreed upon that there was a common ancestor for all living cell types today, that is bacteria, archaea and eukaryotes. It is called LUCA (last universal common ancestor) and represents the “root of the tree of life” (D. Penny, A. Poole 1999).[27,28,29] Because of that, there has to be a protocellular system basically, only a few steps away from being classified as a living cell. Being alive in a most minimal way is defined as the ability to self - maintain that means, a cell needs to have some sort of metabolism, to self - reproduce, so the capability to recreate all components and growing before undergoing division, and the possibility to evolve in a Darwinian way through selective processes[30]. The creation of a minimal cell, a cell that is able to perform these basic functions with only a minimal genome could therefore give a major insight into cellular evolution, the minimal genome, cell division and cell sustainability[30]. A third point why researchers want to create synthetic cell - like systems is the development of new pharmaceuticals, the ability to replace damaged or deficient cells, and create new pathways for drug delivery.[31]

The formation of a minimal cell model can be conducted in two different ways, one is the top - down method and the other the bottom - up approach. The top - down method uses cells and modifies them by removing, reducing or replacing the genome[30]. This way the product can be a minimal cell, only able to perform the basic processes in order to be called living[31]. Several researchers use this approach to create cells with a further and further reduced genome. The bacterium *Mycoplasma genitalium* is one frequently utilised for this task, since it has a genome of only 582 kilobase pair (kbp) and therefore one of the smallest genomes known in nature[32]. In 2010, Hutchison, Smith and Venter reported the first creation of a bacterial cell with a complete synthetic genome JCVI-syn1.0 which is able to self - replicate[33]. This cell is controlled by the synthetic

chromosome and was the first of its kind. In 2016, the same group of Hutchison and co - workers published the synthesis of the first minimal bacterial cell. They were able to take their research even further by reducing the genome even more compared to JCVI-syn1.0 with 1079 kbp down to 531 kbp and created JCVI-syn3.0[34]. With this attempt, they were not just able to synthesise a complete genome which will control the cell but to take out more genes from the genome which are not needed for the basic functions of the cell. This is the first minimal cell created from the top - down synthetic biology approach described in literature. But there are still some genes with unknown functions which means a complete comprehension of the system is still missing. Because of that scientists also use a different approach which is bottom - up synthetic biology.

When using the bottom - up approach, the goal is to build a minimal cell - like system from scratch using only non - living components. This presents a very different task of creating a minimal cell which could be attributed to as “living”. The biomembrane, as the cell’s boundary, displays in an artificial form therefore the “boundary of the reaction vessel”. Knowing that biomembranes are composed of large amounts of phospholipids next to proteins and polysaccharides, the employment of these lipids was a logical consequence. The key result was the development of lipid vesicles (see Figure 1.4c) and their usage as artificial membrane systems[35,36,37] to study membrane phase behaviour[38] and different membrane processes like the fusion of membranes[39,40,41,42] or membrane adhesion[43,44,45,46,47] and more[37]. After the accomplishment of synthesising lipid vesicles in the laboratory from different lipid compositions using different methods like gentle hydration[48,49,50], the electroformation method[51,52], the inverted emulsion method[53] and the continuous droplet interface crossing encapsulation (cDICE) method[54,55], pulsed jetting technics[56], or other microfluidic techniques[57,58,59,60,61,62,63,64,65], many research groups were working on using giant vesicles as model platform to study and mimic cell membranes. Lipid vesicles, also called liposomes, have a crucial advantage, they can self - replicate under the right conditions[66]. Although, it requires physical forces, this is a vital aspect for the possible creation of a minimal cell. The plasma membrane is a very complex part of the cell with countless properties specifically evolved for the various functions (see Chapter 1.1.2.). Through different studies and modifications of liposomes over the last decades, there was an enormous increase in knowledge here. Testing specific features on lipid vesicles or mimicking cellular functions can allow to draw parallels to living cells. The following studies demonstrate the large variety of lipid vesicles and their applications in bottom - up synthetic biology.

Scientists analysed the diffusion of lipid monomers from vesicle to vesicle[67], as well as lateral diffusion within a lipid bilayer[68,69,70]. Microinjections[71,72] and even picoinjections[62] of reagents

into a single vesicles were possible, showing the feasible manipulation of a single vesicle while observing the process in real time via light microscopy and without effecting neighbouring vesicles. Using micromanipulation techniques like optical tweezers[72,73], micropipettes[74] or entrapping vesicles within microfluidic devices[75,76], it was now achievable to work on a single vesicle base next to bulk experiments (groups of vesicles)[77], exposing the vesicles to variable stressors i.e. mechanical influences[40,44,76], thermal variances[76], illumination with different wavelengths[72] as well as chemical changes[45,78,79], examining for example morphological changes[40], adhesion[45,46,47,72,74], fusion[41,42,72,76], budding[80] or division.[74,77,81] Bulk experiments lead also to experiments on vesicle assemblies to mimic cell tissue - like structures and behaviour[82,83]. One alteration of vesicle membranes to allow more control of the permeability of the vesicles, is the formation of transmembrane pores. This can be achieved by the use of pore forming proteins like α - hemolysin[84,85,86,87,88] or DNA origami[89,90,91,92]. With this method, it is now possible to release content from within the lumen of a vesicle in a controlled way without membrane disruption as well as introducing small molecules to the lumen after vesicle formation[90]. Further developments here were the introduction of not just membrane pores to the vesicles but also blocker molecules like TRIMEB (heptakis(2,3,6-tri-O-methyl)-β-cyclodextrin) to close the pores again in a reversible way[93,94,95].

A more severe modification is the exchange of the lipid bilayer with a bilayer formed from polymers. Block copolymers with an amphiphilic character can also self - assemble into closed vesicular structures like lipid vesicles. The polymer vesicles can be formed from a polymer monolayer or bilayer depending on the polymer molecular structure. Polymersomes are structurally very similar to lipid vesicles in general but they show a higher stability as well as a lower permeability and lateral fluidity of the membrane[96,97,98,99]. Liposomes are often described as leaky for those reasons[100]. These typical properties of vesicles (liposomes and polymersomes) highly depend on the molecular weight and the nature of the membrane building components, on the preparation method and the storage[98,101]. Phospholipids for example, have an average molecular weight of about 100 - 1000 g/mol while the molecular weight of a block copolymer like polyethylene glycol - polylactic acid (PEG - PLA) is significantly higher, with > 1000 g/mol[101]. This difference leads to a distinction in membrane thickness from usually around 3 - 5 nm in liposomes to 5 - 50 nm in polymersomes[96]. The membrane thickness is related to the type of the hydrophilic head group but mostly on the hydrophobic tail group. As a result, the overall stability in sense of lifetime and resistance against chemical or mechanical changes of polymersomes is significantly higher.[96,97,98,99,100,101] Coming out of that part of research, scientists today use both

vesicle types for all different applications and model systems. Polymersomes opened up new possibilities to mimic cellular functions and properties of the cell membrane[102]. They were exposed to temperature changes[103,104], pH changes[105,106], different chemicals[107,108] and light[109] to study and compare their response behaviour. Also, non - spherical polymersomes were formed since biological cells in most cases are not spherical but highly structurally asymmetric[110]. Not only the shape of cells is asymmetric also, the building blocks forming the membrane are distributed in an asymmetrical way. Therefore, researchers created asymmetric polymer membranes, which is one of the essential features of biological membranes[111,112]. Another one is the functionality of the membrane coming from proteins like pore forming proteins[113] or the incorporation of biotin moieties[114] to name just a few. Overall, polymersomes next to liposomes play a vital and promising role in the bottom - up approach of the creation of synthetic protocells/ minimal cells.

The compartmentalisation in eukaryotic cells, as mentioned before, is another essential feature for the cell's survival. Therefore the creation of multi - compartmentalised vesicle systems was inevitable. Today, scientists can choose different forms of compartmentalisation for example, the assembly of two or more compartments within one vesicle where, the compartments share an internal lipid bilayer, using vesicles produced by the inverted emulsion method[65,115], or with the employment of microfluidic technics[116]. Another form is the encapsulation of small unilamellar vesicles (SUVs) to create compartments within a giant unilamellar vesicle (GUV)[117]. Since chemical reactions are executed in dedicated compartments within a cell in order to contain toxic byproducts and other waste products, it is important to be able to use vesicles as isolated microcompartments for chemical reactions, especially biochemical reactions[118] such as the polymerase chain reaction[119,120], enzymatic RNA replication[121,122,123], protein synthesis and expression[42,124,125], or two parallel reactions in two different compartments of the same vesicle[126]. More advanced after achieving single reactions was the creation of a complete reaction cascade within vesicles[127].

This shows the great platform vesicles present in recreating and mimicking cellular functions which is why they were used in this study.

1.2.1. Lipid Vesicles as Artificial Membranes

Lipid vesicles (liposomes) are for many decades now one method of choice when studying cells, cellular functions and cellular structures through reversed engineering. They can be of different sizes which puts them in different categories. Liposomes from sizes of 20 - 100 nm fall in the group

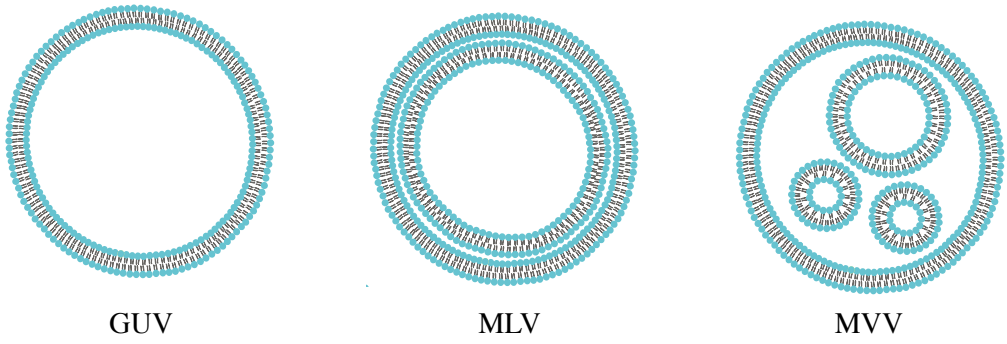

Figure 1.7: Schematic of different vesicle forms. A giant unilamellar vesicle (GUV) with a single lipid bilayer, a multilamellar vesicle (vesosomes) including multiple lipid bilayers and a multivesicular vesicle (MVV) where there are GUVs inside of another GUV. Adapted from [101,128].

of small unilamellar vesicles (SUVs), from 100 - 1000 nm they are called large unilamellar vesicles (LUVs), while for sizes > 1 µm we talk about giant unilamellar vesicles (GUVs)[101,128]. Next to unilamellar vesicles, there are also vesicles containing more than one bilayer like multilamellar vesicles (MLVs) or vesicles inside of vesicles known as multivesicular vesicles (MVVs) or vesosomes (see Figure 1.7). Of all these types, GUVs are employed in a large number of studies because they are nearly cell sized and can therefore be visualised by light microscopy. They can be prepared in an easy and quick way, the variety of lipid compositions is astonishing (natural and synthetic lipids), giving the opportunity to build GUVs for precise purposes and functions. The pH can be varied, buffers, salts, sugars, proteins and other additives can be mixed with them, encapsulated or even integrated into their membranes. The possibilities of modifications and manipulations are manifold.[101,129]

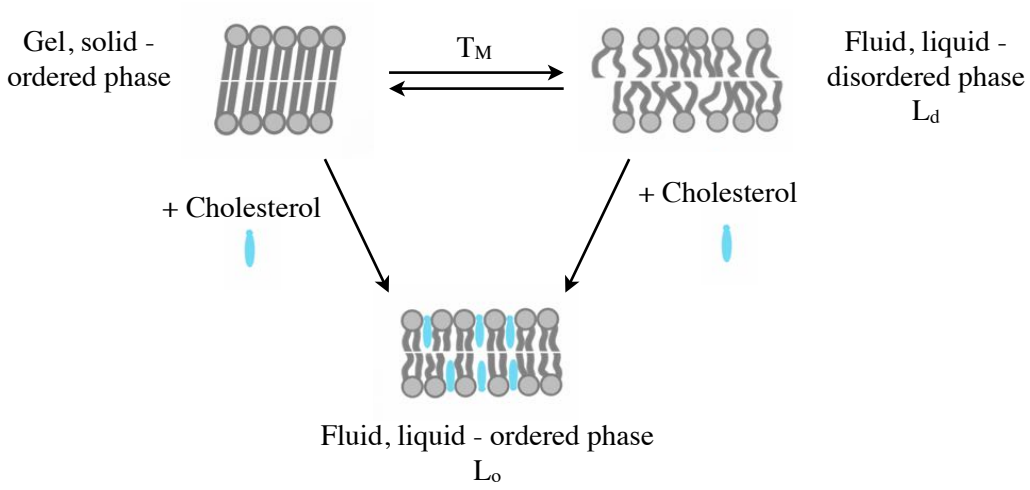

Figure 1.8: Illustration of phospholipid membrane phase behaviour in aqueous solutions. Three lamellar phases (solid - ordered, liquid - ordered and liquid - disordered) depending on the temperature, lipid type and cholesterol concentration. The fluidity of the membrane increases with increasing temperature. Adapted from [37,130].

Looking at the building blocks of biomembranes and liposomes (described in section 1.1.2.), phospholipids, glycolipids and sterols are amphiphilic molecules with a hydrophilic (polar) head group and a hydrophobic (non polar) tail group. All functions of a membrane like the thickness, the fluidity and the membrane curvature depend on the lipid composition but are also intertwined with factors like temperature, ionic strength and pH for example[37]. Especially the fluidity of a membrane is of great importance and correlates directly with the saturation of the fatty acids and therefore the degree of order/packing of the tail groups within the membrane. Completely saturated tail groups will be tightly packed resulting in a higher degree of order forming a crystalline or gel - like structure (Figure 1.8 top left). Introducing unsaturated bonds (usually *cis* - double bonds) within a carbon chain, lead to a kink in the fatty acid chain giving room to a more disordered alignment of the lipids and a higher fluidity (Figure 1.6 and 1.8 top right and bottom). The

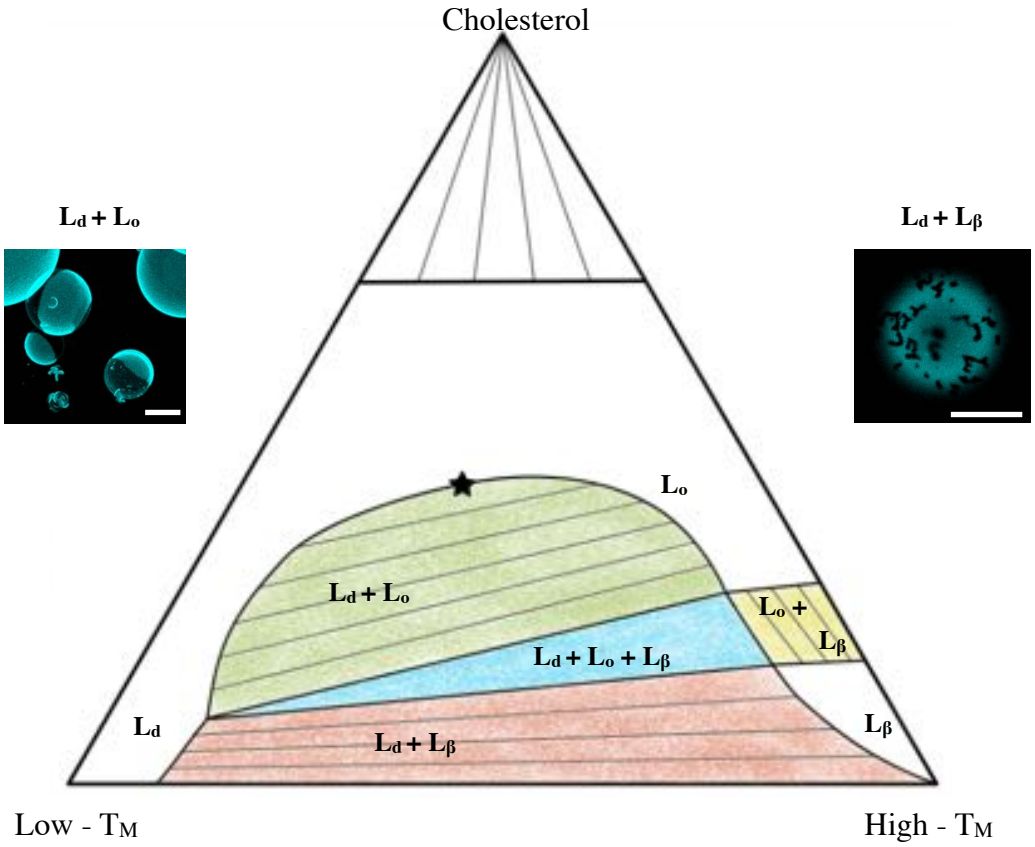

Figure 1.9: Phase diagram of a ternary phospholipid mixture including one low - melting temperature lipid, one high - melting temperature lipid and cholesterol. Membrane phases depend on the lipid composition. Two - and three phase regions are marked in different colours (liquid - disordered / liquid - ordered coexistence in green (fluorescence confocal microscopy image shown), liquid - disordered / liquid - ordered / solid - ordered coexistence in blue, liquid - disordered / solid - ordered coexistence in red (fluorescence confocal microscopy image shown), liquid - ordered / solid - ordered coexistence in yellow). Star shows the critical point with ~ 40 mol% cholesterol. At this point the phases become indistinguishable. Lipid composition L_o/L_d - membrane phase separation GUVs: 30 mol% DOPC, 44.9 mol% DPPC, 25 mol% cholesterol and 0.1 mol% Atto 633 DOPE Lipid composition L_β/L_d - membrane phase separation GUVs: 30 mol% DOPC, 65.9 mol% DPPC, 4.0 mol% cholesterol and 0.1 mol% Atto 633 DOPE. Scale bars: 10 µm. Adapted from [131].

formation of domains can be the consequence and this depends to a great extent on the temperature as well as the lipid composition. Membrane domains are areas that show a distinct fluidity. A liquid ordered (L_o) phase has a higher degree of order leading to a decrease in fluidity while a liquid disordered (L_d) phase has a lower degree of order and an increased fluidity. The solid ordered (L_β) phase or gel phase has the highest degree of order and therefore the lowest fluidity (in some cases also called S_o phase). Every lipid has a certain transition temperature (T_M) or chain melting temperature depending strongly on the acyl chains (the length, the saturation even the asymmetry of the two chains attached to the lipid) but also on the polar head group (size).[23,24] The resulting membrane phases show distinct lipid compositions. While L_d phases are built from low - melting temperature lipids like phosphatidylcholines, L_o phases comprise of high - melting temperature lipids like sphingomyelin and cholesterol[131]. Cholesterol plays an important role here and will be discussed later on in more detail. Because the different phases influence the fluidity of the membrane, it has a strong influence on the lateral as well as the rotational diffusion of the lipids. The more fluid a membrane phase is, the faster lipid diffusion can be[37]. Figure 1.9 shows a typical phase diagram which is used to depict the different phases and phase transitions, vesicles can undergo when created from ternary lipid mixtures composed of one low - melting temperature lipid, one high - melting temperature lipid and cholesterol. There are regions with only one phase but also regions where vesicles can show phase coexistence. The vesicles formed with these lipid compositions (for example 1,2-dioleoyl-sn-glycero-3-phosphocholine (DOPC), sphingomyelin (SM) and cholesterol) can show a L_d/L_o - membrane phase separation (example see Figure 1.9) depending on the molar ratio of the constituent lipids, where ordered phases are macroscopic and visible as round domains or a L_β/L_d - membrane phase separation (example see Figure 1.9) can occur with visible “flower” - like gel shapes on the vesicle membrane (of course a coexistence of all three phases is also possible as well as L_β/L_o coexistence).[131] In other cases, it is also possible to have a membrane phase separation with nanometer - sized domains which can not be resolved by optical microscopy. To prove phase coexistence in those cases other analytical methods like Foerster resonance energy transfer (FRET) or fluorescence correlation spectroscopy (FCS) are needed[132,133].

Sterols, although their structure looks completely different (see structure of cholesterol in Figure 1.10), play an important role in biological as well as artificial membranes. Cholesterol as the most abundant sterol in mammalian cells will pose as example here. The basic structure, like the structure of all lipids, is consisting of a hydrophobic and a hydrophilic moiety. Other than in phospholipids or glycolipids, the hydrophobic part is not a fatty acid but a rather rigid polycyclic structure and the

hydrophilic head group consists but of a single hydroxyl group.[2,3,14,15] Within a membrane the majority of the cholesterol molecule lies within the tail group region of the other lipids. Only the hydroxyl group links it to the polar head group area. By that, it stiffens up the tail groups leading to a higher degree of order although, this is composition - dependent[134]. One has to differentiate at this point between the effects of cholesterol added to membranes constructed from high - melting temperature lipids and membranes from low - melting temperature lipids.[14,131,135,136] Although, there is still a debate on the actual effects on the different lipids and there are still experiments to conduct to prove these theories, it seems that cholesterol acts in a form of “push” and “pull” mechanism. That is, low - melting temperature lipids “push” cholesterol away while high - melting temperature lipid phases favour cholesterol interaction. Experiments with the nearest - neighbour recognition (NNR) technique have shown repulsive interactions of low - melting temperature lipids and attractive interactions with high - melting temperature lipids which supports the theory of a “push” and “pull” mechanism.[14] The permeability is a feature of the membrane influenced by the fluidity too and therefore by the degree of order meaning, a higher order leads to a lower permeability because it decreases the ability of water molecules to penetrate the membrane[135,136]. Considering the influence of cholesterol on the different lipid types, it is theoretically possible to tune the permeability of a vesicle membrane to some extent. In general, a lot of the natural lipids, building up biomembranes, have unique biophysical and chemical properties[137] and can therefore be chosen according to the specific modelling purposes when employed for artificial membranes.

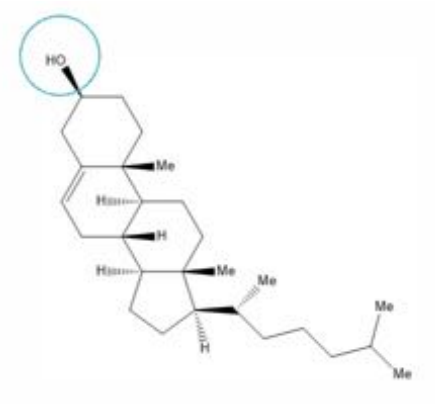

Figure 1.10: Chemical structure of cholesterol. Polar hydroxyl group is marked in green. Chemical structure from Avanti® Polar Lipids; ©2021 Merck KGaA, Darmstadt, Germany.

All features a vesicle membrane can possess depend on several factors besides the lipid composition like, the medium the GUVs are prepared in, the pH and the preparation method. There are many variables a scientist can choose from.

1.2.1.1. Preparation Methods for GUVs

After the decision about the lipid composition, one needs to think about the method for vesicle synthesis. Because this thesis concentrates on GUVs, I will only talk about relevant methods for their formation.

Since the 1960s, vesicles can be formed deliberately in a laboratory environment. In the beginning, the established method was, what is now called gentle swelling. Basically, lipid films are created from lipid solutions by evaporating the organic solvent. Afterwards, an aqueous solution is carefully poured on top which leads to swelling of the lipid films, forming vesicles over several hours.[48,138,139] This method is used to the day because it allows for GUVs to form in most aqueous solutions, like solutions with high ion concentrations. One of the disadvantages nevertheless is the long preparation time, when high yields want to be achieved.[48,49,50,138,139]

The probably most used method in present times is the electroformation method which was first published in 1986 by the group of Angelova and Dimitrov[51]. It is based on the gentle swelling method (for that reason it is sometimes also referred to as electroswelling) but uses an external alternating current (AC) during the swelling process. Because of that, it requires a specific chamber with electrically conductive surfaces. One example are indium tin oxide (ITO) coated glass plates. The plates, separated by a thin spacer made of a non - conducting material like teflon, form a reaction chamber where the vesicles can grow. Electroforming GUVs is certainly advantageous in comparison to the gentle swelling method in terms of preparation time. After two hours of electroformation, there can be as many GUVs as there are after 24 hours of gentle swelling. On the other hand, ionic solutions like buffers for example can not or only at very low ionic strengths be used with this method because of the charged particles in combination with an electric current. In 2018, the group around Stéphane Arbault published a slightly changed protocol for the electroformation of GUVs in physiological buffer concentration (phosphate - buffered saline)[140]. Other than that, if the vesicles are needed in combination with a buffer solution or in presence of some sort of ions, they have to be transferred after their formation or gentle swelling should be used.[51,52,129]

Another method of GUV formation that are based on the principles which uses either a water/oil (w/o) emulsion or an oil/water (o/w) interface including lipids passing an interfacial lipid monolayer wrapping around the aqueous droplets of the emulsion in order to build a proper bilayer (see Figure 1.11)[129]. Within this category fall methods like the inverted emulsion transfer[53]. These concepts are usually two - phase systems of which one is a polar phase (usually an aqueous phase) and the second is an oil (non polar) phase. For the oil phase, organic solvents are employed like mineral oil[53,61], n - decane[56], liquid paraffin[141], mixtures of different

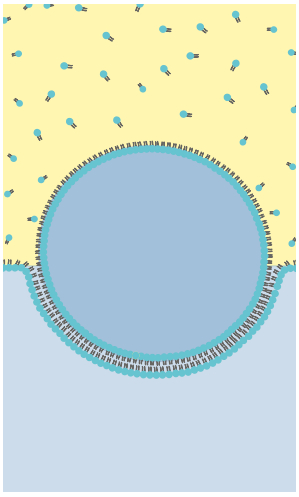

Figure 1.11: Passing of an aqueous droplet with lipid monolayer from an oil phase through an interfacial lipid monolayer into an aqueous phase. A lipid bilayer forms while droplet passes through the interface. Adapted from [139].

organic solvents[59] and even olive oil[142]. The w/o emulsions can be prepared by vortexing, shaking, pipetting, sonication[141] or actually rubbing a tube over a tube rack (only for plastic tubes) [143]. For the aqueous phase, basically any solution is suitable (even high ionic strength solutions) as long as the osmolarity is balanced with the solution the formed GUVs will end up in. Considering the lipids, not all suit this method (when the membrane is formed only by one lipid) although, the exact reasons are unknown. There might be a connection to the emulsification ability. Some lipids do not form stable emulsions. Properties like the size and the affinity of the lipids to the interfacial region within the w/o emulsion affect the adsorption and therefore the formation of stable droplets. [129,144] One feature that cannot be realised through gentle swelling or electroformation is the preparation of asymmetric vesicle membranes. By using a different lipid composition for the emulsion and for the creation of the interfacial lipid monolayer, the resulting bilayer can be made asymmetric[53,145,146]. The amount of produced GUVs is smaller compared to other preparation methods but it provides advantages other methods do not have. Encapsulating specific solutions or molecules (even macromolecules) is a valuable feature opening up many more possibilities for experiments especially in minimal cell research for example[147,148,149,150,151]. Microfluidic approaches and the cDICE assembly allow the production of GUVs with a much narrower size distribution, while the other methods give more polydisperse vesicles with near to no way of controlling the vesicle size[54,58,129]. Certainly, using these strategies of vesicle formation, one should also be aware that the chances are quite high for oil traces ending up within the lipid bilayer and influencing the membrane's behaviour and dynamical properties in experiments[129,152]. Although, the thickness of the membrane is not affected as well as the biocompatibility[152,153].

The wide range of preparation methods give the opportunity to an even wider range of research and many different types of experiments. Depending on the nature of the experiment, one can choose the best fitting vesicle type considering lipid composition, the solution in which the vesicles will be experimented on, the solution within the vesicle lumen, the possibility to have asymmetric membranes and the formation method.

1.2.1.2. Modifications of GUVs

Some modifications have already been mentioned before. Modifications in vesicle applications can be basically of two sorts, lipid modifications or vesicle modifications. Lipid modification means that one or more types of lipids can have a specific modification either to their head group or to their tail group. The list of molecules which can be attached to a lipid molecule is large and many of them are commercially available (see Figure 1.12) and if not, many companies offer reagents for

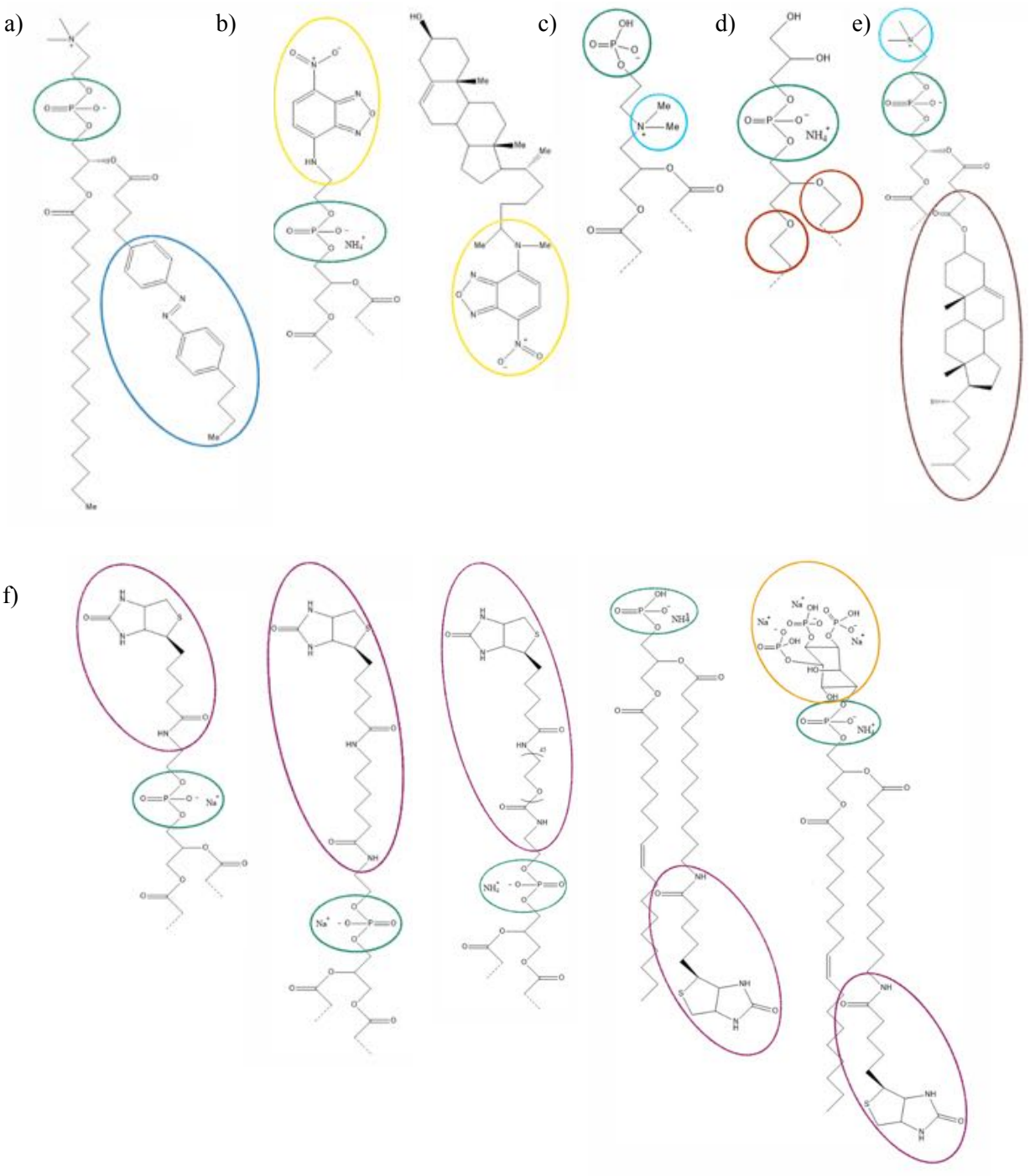

Figure 1.12: Chemical structures of different modifications in common lipids. a) 18:0 phosphocholine carrying an azobenzene moiety (blue) which can be switched between cis - and trans - isomerisation by light irradiation. b) Phosphatidic acid and cholesterol labelled with a nitrobenzoxadiazole (NBD) fluorophore (yellow). c) Inverted phosphocholine (iPC) with inverted phosphate - (green) and choline (light blue) moiety changing the charge distribution of the lipid. d) Diether phosphoglycerol with ether bond (red) instead of ester bond connecting the fatty acid tail groups to the lipid head group. e) Phosphocholine with one fatty acid group functionalised with cholesterol (brown). f) Different functionalisations of lipids with biotin (purple) at the lipid head groups either directly attached or with a spacer of varying length, or bound to one of the fatty acid tail groups. Chemical structures from Avanti® Polar Lipids; ©2021 Merck KGaA, Darmstadt, Germany.

click chemistry for the scientist to modify lipids themselves[154]. There are enantiomers of natural lipids[155], lipids with photo - switchable moieties (Figure 1.12a) that can activate or deactivate a certain function[156,157], fluorescently labelled lipids with different types of dyes covering different wavelengths (Figure 1.12b), lipids with inverted head groups (Figure 1.12c)[158], the ester group connecting the fatty acid tail to the phosphate head group can be reduced to an ether group[159] (Figure 1.12d) and lipids with all different sorts of functional groups even cholesterol can be connected to a phospholipid (Figure 1.12e)[160]. One of the most known and used functionalisations is biotinylation (Figure 1.12f). Biotin can be attached to different types of lipids, it can be directly attached to the head group or with a spacer like polyethylene glycol (PEG) in between and it can be attached to the tail group. Biotinylation in lipids can be used for protein recruitment, for example, by using its ligand avidin. In nature, the binding affinity of biotin and avidin is the strongest known with a K_D value of ~ 10^{-16} M. The K_D value (also called dissociation constant) gives information about the binding affinity between a ligand and a receptor. The higher the value is, the more likely it is for the components to dissociate, meaning the smaller the value, the stronger the binding state.[2,3] The same applies for the bacterial version of avidin, called streptavidin. Both avidin and streptavidin are tetrameric proteins (see Figure 1.13) composed of four identical monomer units (with two on opposite sites) from which each can bind to one biotin molecule[162,163,164]. Biotin and avidin (or streptavidin) bind in a non - covalent way, but only through polar and hydrophobic interactions like hydrogen bonds. In case of streptavidin, the binding is marginally weaker due to fewer hydrophobic and hydrophilic groups. While for avidin, the carboxylate group of the biotin molecule forms five hydrogen bonds when binding to it, in case of streptavidin, there are only two. This leads to a slightly higher affinity constant for avidin, leading to K_D values of $6 \cdot 10^{-16}$ M and for streptavidin $4 \cdot 10^{-14}$ M respectively.[162]

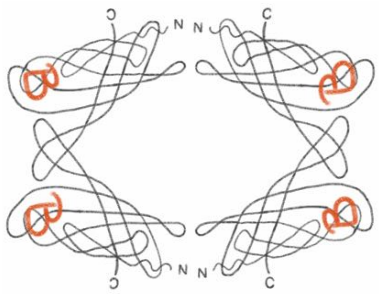

Figure 1.13: Schematic of the β sheet folding pan of a streptavidin tetramer with one biotin (red) bound to one monomer. Adapted from [161].

Because of this, biotin and avidin (or streptavidin) are used very often in research and in case of vesicles, for example, for the adhesion on to specific (also biotinylated) surfaces (e.g. for immobilisation)[129,165] or for the adhesion of single vesicles to each other[166] or the creation of larger assemblies[167]. It is also widely used because the binding is not just strong but also hardly effected by other influences like pH changes, temperature changes or even organic solvents. For all those systems, visualisation can simply be achieved by using labelled avidin (or streptavidin).

Another positive aspect of biotinylated lipids is the low tension affecting the vesicle membrane since, the lipids still have a significant flexibility.[129]

When thinking of modifications of vesicle membranes, there are, for example, pore forming agents or proteins changing the membrane curvature which can lead to membrane budding or fusion. Consequences of changes in membrane fluidity were already explained in section 1.2.1. and although, cholesterol can be added to already formed GUVs to cause a membrane phase separation, achieving this is much easier by choosing the right lipid composition in the first place (see Figure 1.9). All the forms of membrane phase separations are highly dependent on the lipid composition and the molar ratio of the lipid constituents. In cases where a phase separation is induced after vesicle formation, it has been triggered through a component within the vesicle membrane. In 2012, Haluska et al. published a method triggering the phase separation by light irradiation. This was possible due to the addition of a photosensitive porphyrinated lipid[168].

The deliberate formation of membrane pores (mentioned in section 1.2.) allows a controlled exchange of certain agents through a bilayer. The pore forming strategies are proteins like α - hemolysin, melittin or bax and bak[83,84,85,86,169,170,165,171,172] and antimicrobial peptides[173,174] which can also lead to vesicle rupture when used in high concentrations. But it is also possible to create membrane pores using certain detergents[175], DNA origami[88,89,90,91] or mechanical stimuli via electroporation[176,177], stretching of the membrane[178,179] and photosensitive reactions[180]. Depending on the lipid composition and the poration method the pores show different stabilities meaning, a membrane pore is also changing after its formation. It can change in size over time and even close completely. In extreme cases, the vesicles burst. Using α - hemolysin as a pore forming agent is also used to show the unilamellarity of vesicles.[180,181] Another factor is the pore size in general. Every agent generates not just different pores in structure but also in size considering the channel diameter. For some agents like bax and bak proteins the concentration affects the pore diameter, leading to smaller pores of ~ 3 nm at low protein concentrations and for high protein concentrations $\geq$ 8 nm[172]. This does not apply for poring agents like α - hemolysin. Pores created from that have a fixed pore size of ~ 1.4 - 4.6 nm in diameter[85,86,87,92]. In membrane research, α - hemolysin is probably the most used pore forming agent. It is also compatible with molecules like TRIMEB which can block the pores again after their formation. TRIMEB is an oligosaccharide able to reversibly bind in a non - covalent way to the inside of the pore and therefore inhibiting the leakage of molecules through the channel. The blocker itself can not translocate through the pore due to its size[93,94,95].

A lot of the mentioned manipulations can be executed in bulk experiments as well as in single vesicle experiments with the employment of micropipettes or microfluidic devices.[73,93] One special feature of vesicles is their ability to exhibit multi - compartmentalisation which is of particular interest in this study and will be discussed in the next section.

1.2.1.3. Multi - Compartmentalisation as a Special Modification

Creating a multi - compartmentalised vesicle system became more popular in recent years. It displays the essential step in mimicking eukaryotes with their cellular organelles. A system like this is generally a GUV system with separated compartments. A vesosome is the closest membrane model to the actual cell but also difficult to create. Much easier are multi - compartmentalisations of two or more compartments within the same vesicle separated by the same lipid bilayer. This way, the compartments can contain different solutions but the bilayer separating the compartments comprises of the same lipid composition. This form of multi - compartment vesicles is actually called multi - compartment vesicle.[115,116,127,128] Other arrangements are defined as higher - order structures and mean hierarchical systems with encapsulated vesicles either SUVs, LUVs or GUVs called multivesicular vesicles as well as multilamellar vesicles (see Figure 1.7). The most interesting form for this work is the multivesicular type with GUVs encapsulated in GUVs. In the past, this was achieved via the influence of osmotic stress leading to invagination of the vesicle membrane followed by budding thus creating a GUV in a GUV[182]. Equally to the multi - compartment vesicle, the membranes of the different compartments comprise of the same lipid composition. A very sophisticated method of vesosome production is using a microfluidic approach. The group of Wilhelm Huck published in 2016 their method of GUV formation using microfluidics[117]. The same approach was used by them to create multi - compartmentalised vesicles encapsulating GUVs inside of GUVs. Using microfluidics, they were able to control not just the size of the inner and outer GUVs but also the number of encapsulated vesicles including the solutions within the vesicle lumen from all the vesicles. With the incorporation of membrane pores with the usage of α - hemolysin and melittin, they showed the unilamellarity of the vesicle membranes.[183] In 2020, a novel method for the creation of vesosomes was published using gel - assisted swelling to form multi - compartmentalised GUV - in - GUV systems under physiological conditions. The yield is rather low as is the stability of the vesosomes unless PEG is added. On the other hand, this method allows the formation of vesosomes without a microfluidic setup.[184]

1.3. Analytics

1.3.1. Optical and Fluorescence Confocal Microscopy

Optical microscopy allows the observation and examination of samples and their microstructure by taking advantage of the different interactions of light with materials. Light can be diffracted and refracted within a microscope setup. Thereby, the diffraction describes the light bending around the objects which is supposed to be magnified. The diffracted light pattern is travelling through lenses refracting the light meaning, the direction is changed which allows focusing. The size of the object is directly related to the resulting diffraction pattern. Smaller objects result in higher diffraction which can only be resolved by a microscope to a certain limit.[185,186,187] The resolution (r) of an optical microscope defining the minimum distance of two points at which they can be distinguished, depends on the light wavelength, the numerical aperture (NA) of the lens system and the correct alignment of the whole optical system. Equation 1.1 (see Figure 1.14) shows that at shorter wavelengths the resolution is increased and with a lower numerical aperture the resolution decreases. The numeric aperture basically defines the ability of a medium to focus light and depends on its refractive index. Mathematically, the numeric aperture is the product of the refractive index (n) of the imaging medium and half the angular aperture (α) of the objective (Equation 1.2, Figure 1.14). This means, the resolution can be increased by changing the imaging medium. Often in optical microscopy the imaging medium is air which has a refractive index of n ~ 1. Exchanging the medium with water (n ~ 1.3) or an immersion oil (n ~ 1.5) increases the numeric aperture and therefore the resolution.[185,186,187,188,189]

$$r = \frac{0.61\lambda}{NA} \qquad \textbf{1.1}$$

$$NA = n \cdot \sin\alpha \qquad \textbf{1.2}$$

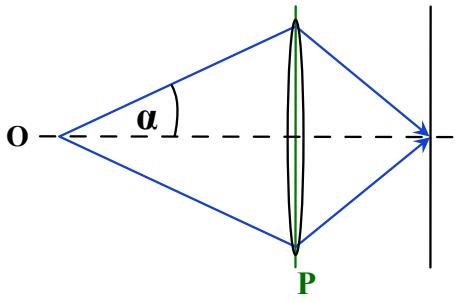

Figure 1.14: Equation **1.1** for calculating the resolution r of an optical microscope from the wavelength λ and the numerical aperture NA. Equation **1.2** for calculating the numerical aperture NA of an optical microscopy from the refractive index n and half the opening angular of the aperture α. The schematic on the left depicts the opening angular of an aperture used for Equation **1.2** with the object plain O and the objective plain P. Adapted from [185,186].

Most of the microscopes today are compound microscopes which use a series of lenses to create a magnified image of an object (see Figure 1.15). A condenser lens focuses the light coming from the light source. The light is diffracted by the specimen before passing the optical pathway of the

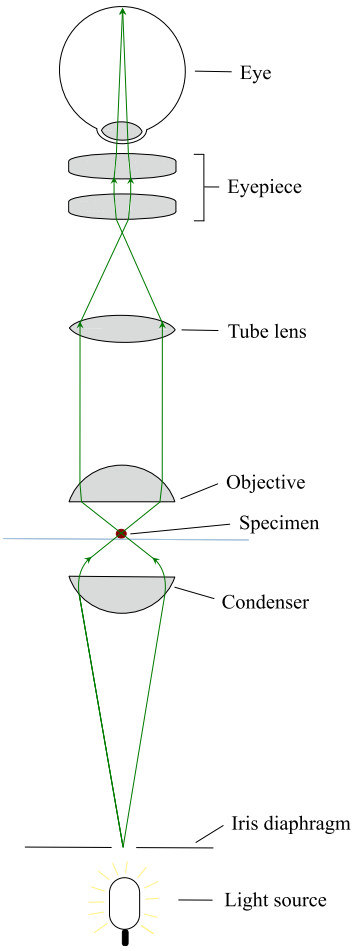

Figure 1.15: Schematic of the light path (green) of an optical microscope. Light emits from the light source and is focused on the sample through lenses within the condenser. Diffracted light goes through the objective, tube lenses and the lenses of the eyepiece where the magnification takes place before it can be detected either by eye or a detector. Adapted from [2,185].

microscope tube with the objective lenses where the image is being magnified. The ocular or eyepiece is composed of a second set of lenses which enlarge the image even further before it is reproduced in front of the focal plane, where it can be seen by eye or camera (for example a charge - coupled device (CCD)). This describes the general alignment of an upright microscope. There is also inverted microscopy with the objective underneath the specimen instead of above. This allows to image samples which are in solution and would sink to the bottom of the chamber because of gravity (sample sinks towards the objective) making the imaging process easier. This also makes is possible to image samples in all sorts of sample chambers like petri dishes, bottles or microtiter plates, other than for upright microscopy, where a specimen is usually imaged on a glass slide.[129,185,186,187,188,189]

Brightfield microscopy is the simplest of these techniques with white light illuminating the sample from below while the imaging is done from above. Imaging GUVs by using brightfield microscopy can be difficult due to the lack of contrast. Instead of using normal brightfield microscopy, phase contrast microscopy can be employed. This technique uses two additional ring plates to create a phase shift of the diffracted light pattern which changes the intensity of the light that is detected. This means, a difference in refractive index is converted into a contrast. In the case of GUVs prepared with different internal and external solutions, creating a sharp contrast of the vesicle membrane.

Another microscopy method which is often used to image GUVs is fluorescence microscopy. Fluorescence is the spontaneous emission of radiation in form of light by an electronically excited molecule. The absorption of energy in form of a photon ($h \cdot \nu$) excites a molecule to a higher electronic state, as shown in the simplified Jablonski diagram (Figure 1.16). In a non - radiative way, the molecule loses small amounts of energy afterwards through collisions with surrounding molecules before falling down several vibrational levels to the lowest one of the S^* state. To relax down to the ground electronic state S, the molecule spontaneously emits a photon of lower energy

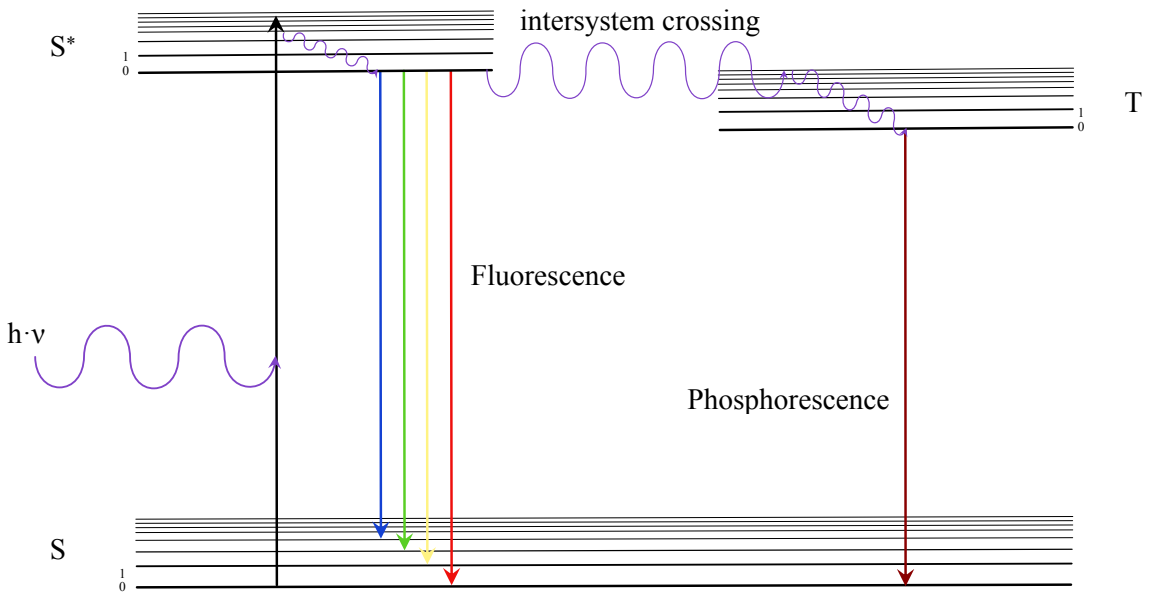

Figure 1.16: Simplified Jablonski diagram picturing the absorption of light (h·ν) by a molecule though exciting it from the singlet ground electronic state S to the first singlet excited electronic state S*. All electronic states comprise of several vibrational levels (0, 1 and so on). Adapted from [187,189]

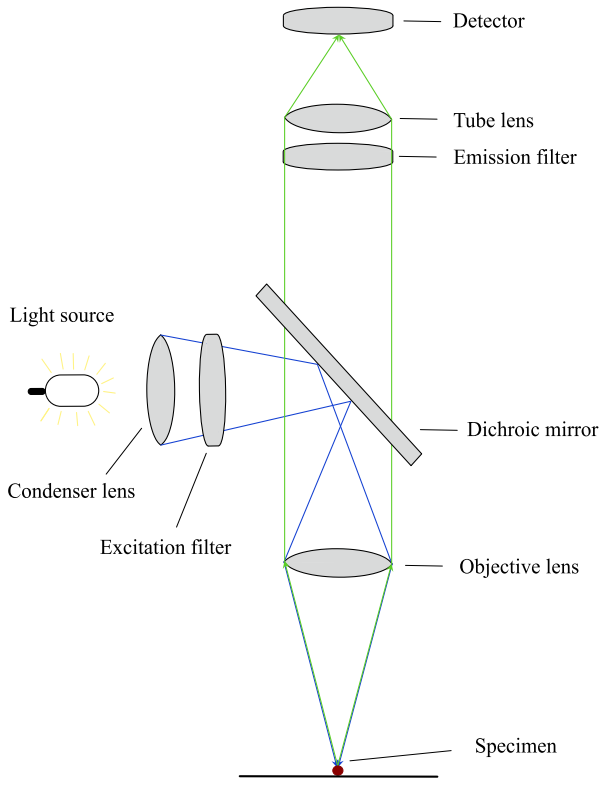

Figure 1.17: Schematic of the light path of a fluorescence microscope. Light emits from the light source (blue) and passes through the excitation filter before being reflected onto the sample through the dichroic mirror. Sample emits fluorescence signal (green) which travels through the objective and is transmitted by the dichroic mirror through the emission filter and focused on the detector. Adapted from [185,187,190]

(and higher wavelength). Fluorescence is typically short lived with a lifetime in the range of ns. In case of phosphorescence, the molecule, when on the first singlet excited state S* undergoes a spin flip. In the non - excited state the spins of two electrons in a coupled electron cloud are oriented antiparallel. When a spin flip occurs the spin - orbit coupling is dissipated and the molecule enters the triplet electronic state T, where it is trapped until the spin can flip back into the antiparallel configuration. This is spin - forbidden until another spin - orbit coupling occurs. Because of that, the lifetime of phosphorescence is prolonged and more in the range of µs even up to ms.[185,186,187,189]

The setup for fluorescence microscopy (see Figure 1.17) uses an excitation filter placed in front of the light source which allows only a specific wavelength to pass through. The light is

reflected by a dichroic mirror through the objective and onto the sample. The fluorophores of the specimen are excited by light absorption and emit light of a higher wavelength which passes back through the objective and will not be reflected by the dichroic mirror but transmitted and directed further through the emission filter before the signal is focused on the detector.[185,186,187]

GUVs can easily be created with the addition of fluorophores like rhodamine, Texas Red, dialkylcarbocyanine (DiI), Alexa Fluor, Atto (all commercially available) and many others, giving a clear advantage when imaging GUVs. In addition, they are very sensitive which means only very small mole fractions are needed next to the lipids the membrane is composed of. They can either be attached to a lipid (e.g. rhodamine) or have a structure that is similar to lipids (like DiI).[129] In the case of GUVs showing a membrane phase separation, fluorophores, depending on their structure, can be incorporated preferentially (but typically not exclusively) into one phase, giving images with distinct visible patterns of the different phases.[129] It is also possible to detect more than one fluorophore in one experiment when using more than one detector. This requires fluorophores which excite and emit at different wavelengths so every detector will only detect one of them. Fluorescence microscopy can also easily be combined with phase contrast microscopy.[129, 187,190]

For many applications and experiments the optimal way to image biological samples like GUVs is confocal microscopy (see Figure 1.18). This technique is a special form of fluorescence microscopy. Compared to conventional microscopy, the specimen is here imaged in optical "slices". The light hitting the sample is not in total collected by the detector. A pinhole aperture which is positioned before the detector filters the signal, letting only light through coming from the focal plane and allows to view single sections of the specimen at a time. This opens up the opportunity to stack the sections in the end, creating a 3D view of the sample.[185,189,191,192]

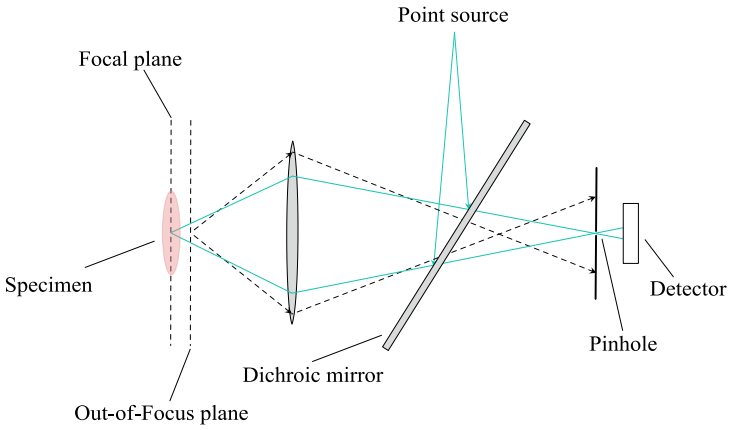

Figure 1.18: Schematic of the light path in confocal microscopy. Light path in dotted lines coming from the out - of - focus plane will be excluded by the pinhole and not detected. Adapted from [2,191,192].

Fluorescence confocal microscopy was extensively used in this particular work to image the created GUVs in high resolution and with optical sectioning to reduce background signal and quantify the fluorescence intensities. This technique is particularly suitable because several fluorescent dyes

were used to label the different components which could be detected simultaneously with multiple detectors.

1.3.2. Microfluidic chips

Microfluidic technologies are also called “lab - on - a - chip”. As it already gives away in its name, it uses fluids as working medium. One can think of a microfluidic device in a similar way as of a microchip, a small device transporting information in the form of electrical signals through defined channels (see Figure 1.19a and b). In the same way, a fluid sample is transported through the channels of a microfluidic chip. In general, microfluidic devices can perform a great variation of tasks caused by the properties of a laminar flow, a related mass transfer by diffusion, as well as a low volume - to - area ratio. Among possible applications are fluid transport and mixing, fluid valving, detection/biosensing, separation, sample preparation and concentration. The use of microfluidic devices can be of great advantage in several ways. For once, these technologies process very small amounts of fluids from nanolitres to microlitres through channels of lengths between one up to hundreds of micrometres. The pressure - controlled flow within the channels can be regulated by a syringe pump either through a connection in a pushing mode from the inlet or a drawing mode from the outlet (see Figure 1.19c). Most of the time, microfluidic devices are made

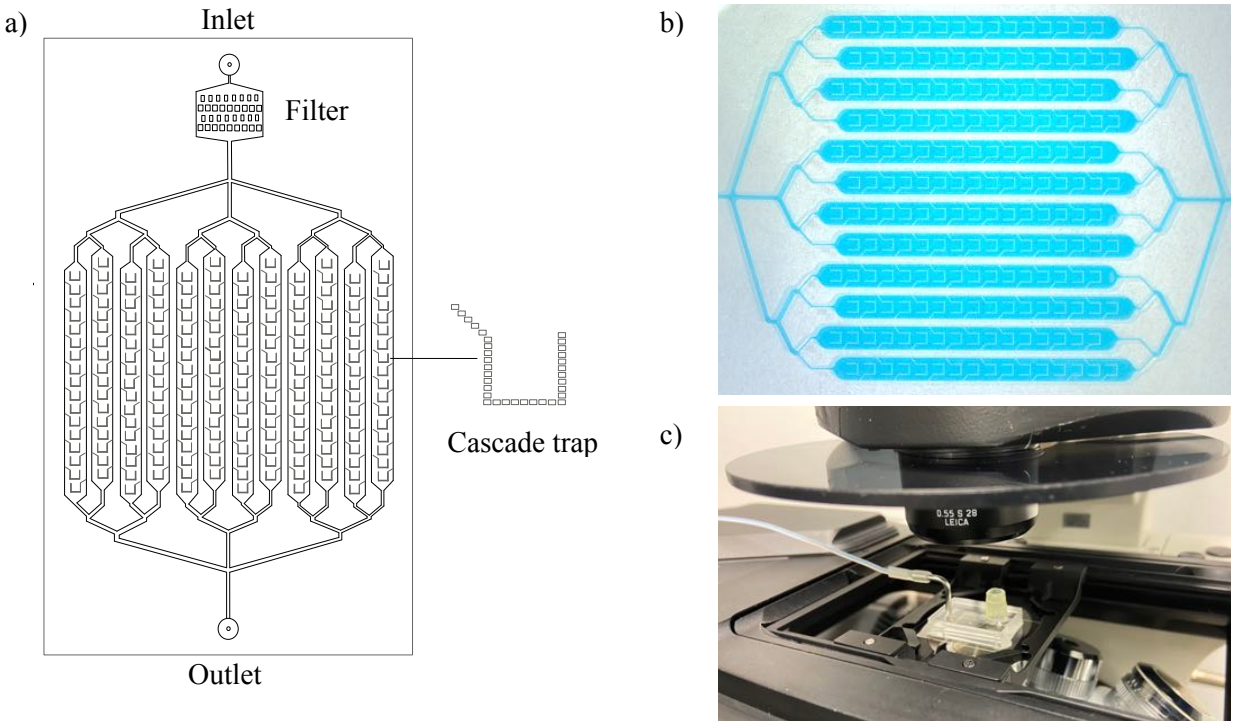

Figure 1.19: a) Schematic of a microfluidic chip with a cascade design from the Robinson group.[76] The chip has a filter unit and 12 lines with 17 traps per line. b) Microscopy image of a cascade microfluidic chip filled with a blue dye for better visibility of the channels. c) Photograph of the same microfluidic chip mounted on the microscope stage, connected to a syringe pump.

of poly(dimethylsiloxane) (PDMS). PDMS is an optically transparent elastomer which allows for imaging samples within the device. This makes it very easy and practical to work with and also a low cost technology. In an analytical context, microfluidics can be seen as somewhat related to methods like gas - phase chromatography and capillary electrophoresis. They share a high sensitivity, a high resolution and the use of very small amounts of sample.[75,76,193,194]

In GUV research, microfluidic devices are used frequently today[195]. It allows the production of GUVs, the trapping of several or just single vesicles and their manipulation as well as long term observation. The devices are small and can be produced with a glass slide on the bottom to fit microscopy stages (see Figure 1.17c) for imaging. During this study, microfluidic chips were used to trap GUVs and immobilise them for imaging. The chip which is shown in Figure 1.19a and b is called “cascade” (due to the cascade style filling) and was used for different experiments. It is composed of 12 lines with 17 traps per line. The traps are designed in a cascade way to help entrap the GUVs. The flow within the chips forces the vesicles into a form of slalom motion around the traps which increases the likelihood of the GUVs getting into the traps[77].

Using microfluidic chips is an easy way to immobilise GUVs to a certain extend but it should be mentioned that single GUVs are not completely immobilised. Unless the fluid flow is stopped, the GUVs are exposed to a frequent spinning motion which can influence imaging in specific cases.

1.4. Aim of the Study

The study focuses on specific membrane - membrane interactions by taking interactions from the cell plasma membrane with membranes of cellular organelles as an example. Several functions within eukaryotic cells require a communication of cellular organelles and the plasma membrane which was already discussed in Chapter 1.1.1. Membrane contact sites are a prominent example which was discussed in this context and was used in this study as an example of a minimal cell system. There are still many unknown facts about membrane contact sites especially, when it comes to the plasma membrane e.g., what is the leading factor for the region where and if a contact site evolves. It is known that in this case, both the participating organelle and the plasma membrane use specific lipids like PI and proteins to establish a contact site[6,7]. In the case of the process of exocytosis where exocytotic vesicles dock to the plasma membrane before fusion to excrete the vesicle’s content, the docking is believed to function by molecular recognition and therefore, in a directed (targeted) way.[196] This process involves an organelle (a vesicle) moving to a specific point of the plasma membrane and docking to it in order for the membranes to fuse.

Mimicking this process means, creating a GUV multi - compartmentalised system which includes an outer GUV functioning as the plasma membrane and an inner GUV as internal organelle. Both membranes then need to come into close proximity in a controlled manner and dock to each other, in other words, adhere. For this study, fusion is not included since it focuses on the mimicry of membrane contact sites, but the recognition between organelles and the plasma membrane was adapted into the system in order to achieve a directed adhesion rather than a random adhesion.

The first step to model a membrane contact site between cellular organelles and the plasma membrane is, the design of a suitable vesosome system. With the inverted emulsion method, it is possible to encapsulate buffers, proteins, other biomolecules and even GUVs singly or even all at the same time. Because of that, the method is used to encapsulate electroformed GUVs within the inverted emulsion vesicles to create vesosomes.

The second step is, to think of a method to adhere the inner GUV's membrane to the outer GUV's one. A clear choice for this is, the employment of the biotin streptavidin system. This strategy has the ability to form a strong adhesion of vesicles to surfaces or other vesicles and is easily realised by the use of biotinylated lipids in both lipid membrane compositions and the addition of streptavidin to bridge the biotin moieties of the vesicles. The adhesion resulting here will be specific, strong, easily established and irreversible.

Another possibility is the use of single - stranded DNA (ssDNA).[197] Different modifications of ssDNA like biotinylation[197] or cholesterol linked to it[198], allow the attachment to a vesicle membrane. In case of the biotinylation, the ssDNA needs a biotin streptavidin bridge to be linked to a likewise biotinylated lipid. Since the two ssDNA strands bind in a specific way only (adenine to thymine and cytosine to guanine), two strands of custom made ssDNA bind reliably but not necessarily irreversibly. By introducing a competitive ssDNA strand, the binding can be reversed. This system is more advanced compared to the first adhesion method considering the complexity of the adhesion and the possible reversibility. The advantage of a strategy like this is, one can trigger the adhesion directly through the addition of the complementary strand. This gives a certain control of the time when the adhesion is supposed to form and makes it possible to observe the adhesion in the moment when it is established.

A third way to create a membrane - membrane adhesion works by the binding of two proteins which can be attached to the membrane lipids by the use of a Ni^{2+} - nitrilotriacetic acid (Ni^{2+} - NTA) moieties. The proteins are called Nano (wild - type SspB) and iLID (improved light - induced dimer protein). What makes these proteins special is their property of binding only under the illumination of light with a wavelength of about 488 nm and unbinding in the dark[199]. This cycle can be

activated several times leading to a switch - ability of the adhesion putting this method another step further.[199,200]

With now three different approaches to establish a way of adhering the membrane of the inner GUV to the membrane of the outer GUV, all that is left is a way of directing the adhesion to a specific area of the membranes. This ideally requires for the membrane to exist in a state which allows the lipids responsible for the adhesion (like biotinylated lipids) to accumulate in a specific area of the membrane and be excluded from the rest. To achieve this, the membrane phase separation can be employed. Since the biotinylated lipids as well as lipids carrying Ni^{2+} - NTA are commercially available, the lipid here can be chosen accordingly, so it will partition into a specific membrane phase. For reasons of a more clear distinction of a later adhesion area, it is easier to employ a liquid ordered - liquid disordered membrane phase separation with clear bigger round shaped liquid ordered phases (see Figure 1.20a) instead of a liquid disordered - gel ordered membrane phase separation where the gel phases show as small flower like patches on the membrane (see Figure 1.20b). Depending on the lipid carrying the biotin moiety and its partitioning into either of the membrane phases, the adhesion will occur to the liquid ordered or the liquid disordered phase of the vesicle membrane, respectively.

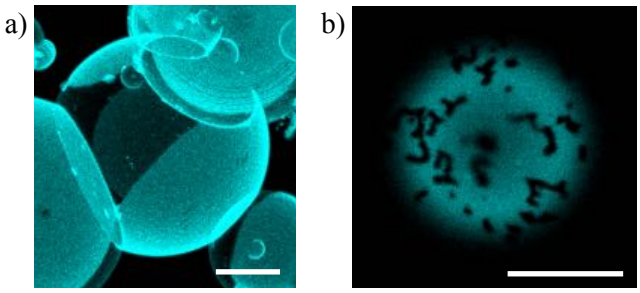

Figure 1.20: Fluorescent confocal microscopy images (Atto 633 channel) of GUVs showing a) a liquid ordered - liquid disordered membrane phase separation (lipid composition: 30 mol% DOPC, 44.9 mol% DPPC, 25 mol% cholesterol and 0.1 mol% Atto 633 DOPE) and b) a liquid disordered - gel ordered membrane phase separation (lipid composition: 30 mol% DOPC, 65.9 mol% DPPC, 4.0 mol% cholesterol and 0.1 mol% Atto 633 DOPE). Atto 633 DOPE partitions into the liquid disordered phase. GUVs created from the electroformation method. Scale bars: 10 µm.

This last part of the project ensures the direction of the adhesion and completes the process of targeted docking of an “organelle” to the “plasma membrane” in a model membrane system.

2. Multi - compartmentalised cell models and coexisting membrane phases

2.1. The Formation of Multi - Compartmentalised GUVs

To form an appropriate vesosome system, the required vesicles were formed by two methods. The inner GUVs are created from the electroformation method (step 1 Figure 2.1) in a sucrose solution (see Chapter 7.2.) and have to be formed before the outer ones. They do not require specific features that cannot be incorporated by this method.[51] The outer vesicles are afterwards formed using the inverted emulsion method (see Chapter 7.2.).[53,143] After harvesting the electroformed GUVs, they are used to prepare the w/o emulsion which is needed to form the outer GUVs (step 2 Figure 2.1). That way, the aqueous droplets which are confined by a lipid monolayer and being dispersed in the oil phase contain the electroformed vesicles from step one. The centrifugation step forces the aqueous droplets to cross the interfacial lipid monolayer. This lipid monolayer forms at the interface

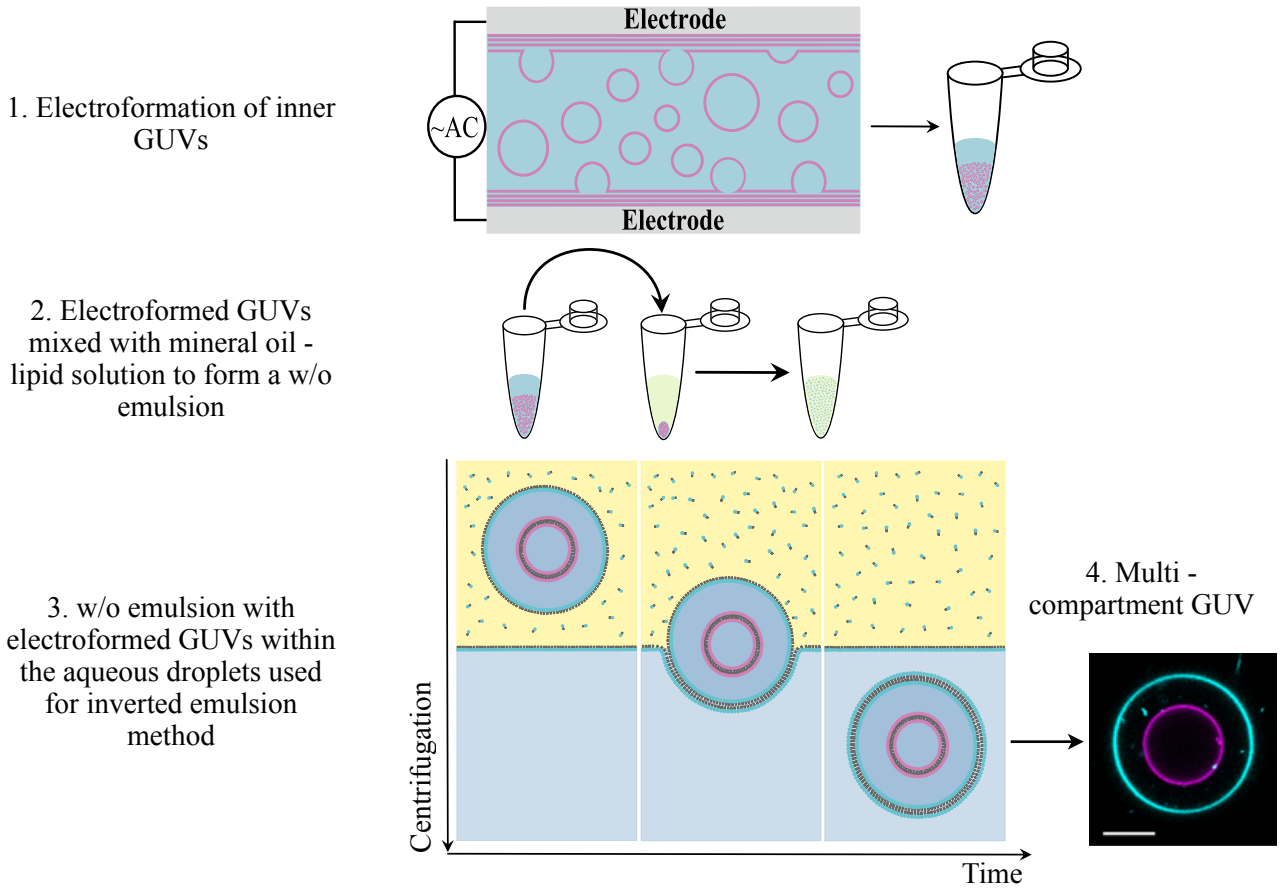

Figure 2.1: Schematic of the process of forming multi - compartmentalised GUVs. The first step is the creation of the inner GUVs from electroformation before in step two these harvested GUVs will be mixed with a mineral oil - lipid solution to create a w/o emulsion. The emulsion is in the third step poured on top of an aqueous phase and centrifuged to form the outer vesicles while encapsulating the electroformed ones. The resulting multi - compartment GUV is shown in step 4 (fluorescence confocal microscopy image, merge). Electroformed inner GUV labelled with 0.1 mol% $DiIC_{18}$ (magenta), the inverted emulsion outer GUV is labelled with 0.1 mol% Atto 633 DOPE (cyan). Scale bar 10 µm

of the upper oil phase (emulsion) and the bottom aqueous phase and wraps around the aqueous droplets confined by a lipid monolayer, completing the formation of the vesicle bilayer (step 3 Figure 2.1). The vesicles end up in the bottom aqueous phase which is usually a sugar solution. The preparation is carried out using a 96 well microtiter plate coated with a solution of β - casein. The great advantage is the possibility of imaging directly in the microtiter plate right after GUV/ vesosome preparation without harvesting the vesicles and transferring them onto a glass slide or another imaging system which for some preparation methods is known to induce GUV rupture and therefore, a decrease in vesicle yield.

The electroformation method is not as sensitive considering the formation of the vesicles and the conditions they need to grow in besides the absence of salts when compared with the inverted emulsion method. The inverted emulsion method by itself is influenced by several different factors like the organic solvent (oil phase), the sugar concentration used for the aqueous phase (if sugars are used) and also the centrifugation speed. Moga et al. described the yields of GUVs at varying sugar concentrations when created from the inverted emulsion method. Concentrations of 600 - 900 mM sugars lead to the highest yields of GUVs which is why for this thesis the same concentrations were employed.[143] The suitable organic solvents which are used for the inverted emulsion method were mentioned in Chapter 1.2.1.1. They display a high variety in viscosity, boiling temperature, polarity and composition since, not all are pure solvents like n - decane. There are also mixtures of different organic compounds like mineral oil or olive oil. Another factor which is depending on different properties is the solubility for lipids. A mineral oil solution has a significantly lower solubility for lipids compared to n - decane. To dissolve a lipid film in n - decane, it just needs to be added. In case of mineral oil, a solution with an equal concentration of lipids has to be sonicated for some time to dissolve the lipids properly. The solubility of the emulsion produced from a certain organic solvent is important.

In this study, mineral oil was mostly used and different lipid compositions tested. The emulsions created with a mineral oil lipid solution (oil phase) and a 600 - 900 mM sucrose solution (aqueous phase) are very stable which was rather randomly tested by incubating the emulsions at room temperature for 2 minutes, 5 minutes and up to 10 minutes without a distinct change in the formed vesicles from these specific emulsions. The number of GUVs as well as the size was not influenced (see Figure 2.2). For the average experiment for this study, there was no incubation time used for the emulsion. The emulsions were prepared and used instantly. The emulsion's stability would be different with other oil phases, leading to the resulting GUVs differing in certain properties like size and robustness perhaps. Considering the lipid composition, the inverted emulsion method can be

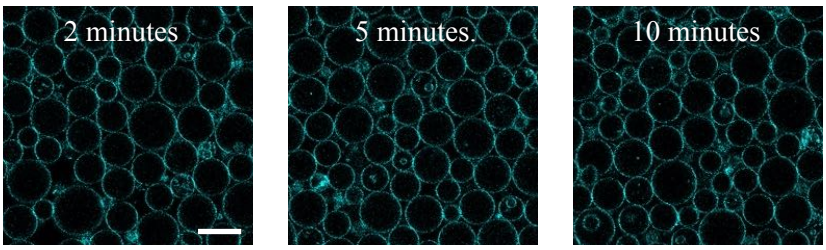

Figure 2.2: Fluorescent confocal microscopy images (Atto 633 channel) of GUVs created from the inverted emulsion method. The emulsions were incubated for 2, 5 and 10 minutes before GUV formation. GUVs were created from 99.9 mol% POPC and 0.1 mol% Atto 633 DOPE. Scale bar: 20 µm.

difficult to work with. One distinct complication is the formation of pure DOPC vesicles. When using the electroformation method, there is no problem in creating pure DOPC or pure 1-palmitoyl-2-oleoyl-glycero-3-phosphocholine (POPC) GUVs. Both lipid types are almost identical in structure and only differ in the degree of saturation of the fatty acid chains (one double bond in one of the fatty acid chains in case of POPC, one double bond in both of the fatty acid chains in case of DOPC). Unfortunately, the formation of pure DOPC vesicles from the inverted emulsion method was not possible while, when using pure POPC, vesicle production was possible (see Figure 2.3). Although, the reason for that is not clear yet and more experiments have to be conducted in the future, there seems to be a connection to the saturation of the fatty acid chains. Other lipid compositions, including only lipids with two unsaturated fatty acids carrying different polar head groups, resulted in the same dilemma of no or almost no GUVs forming. Therefore, in this study, when GUVs were formed composing almost exclusively of one lipid, POPC was used.

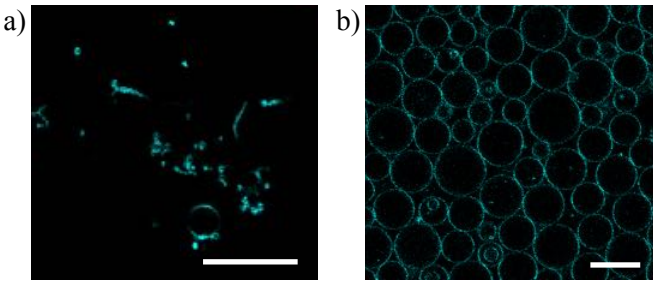

Figure 2.3: Fluorescence confocal microscopy images (Atto 633 channel) of a) pure DOPC GUVs and b) pure POPC GUVs created from the inverted emulsion method. GUVs are labelled with 0.1 mol% Atto 633 DOPE. Scale bars: 20 µm.

The next factor to influence the GUVs created from the method is the centrifugation speed. Conducted experiments at different centrifugation speeds from 100 x g up to 4000 x g and a sugar concentration of 900 mM show a decrease in size at increasing centrifugation speeds (Figure 2.4a). One has to consider here that not all GUVs (vesosomes and non - vesosomes) can be counted in a sample prepared in a microtiter plate because of overlays (see Figure 2.4b) and other imaging obstacles but it was assumed that there are between 200 - 1200 GUVs in one well. At 100 x g, the average GUV size is ~ 27 µm while at 2000 x g the size is reduced by half of that to ~ 13 µm. Using 4000 x g reduces the size again by half, resulting in GUVs of ~ 6.5 µm on average. In the range of 200 - 500 x g, the decrease in size is not as significant to actually make a difference for an

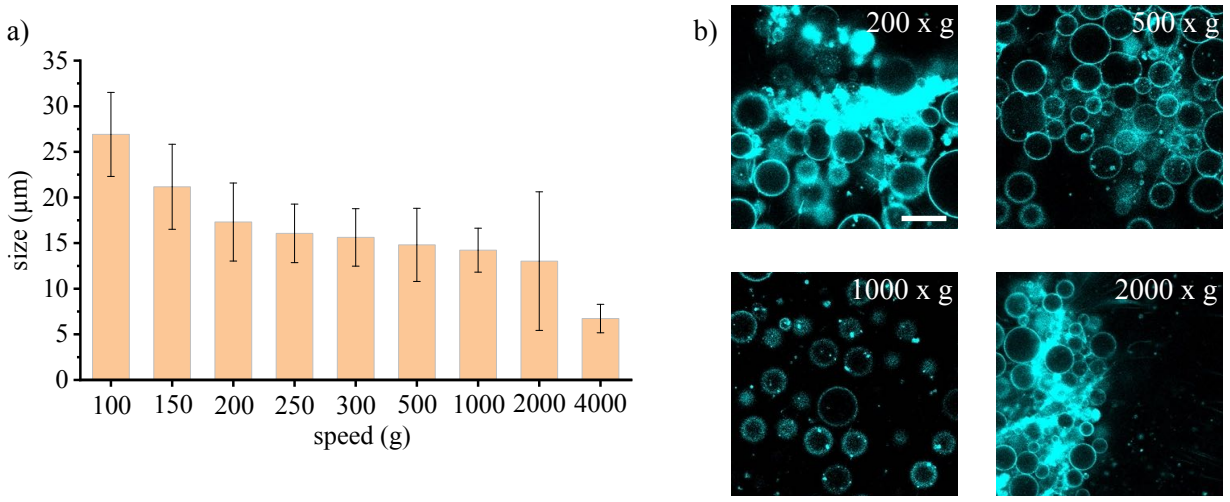

Figure 2.4: a) GUV sizes prepared from the inverted emulsion method at different centrifugation speeds. GUVs formed in a 96 well microtiter plate at 900 mM glucose and sucrose concentrations. b) Fluorescence confocal microscopy images (Atto 633 channel) of GUVs prepared at four different centrifugation speeds. GUVs created from 99.9 mol% POPC and 0.1 mol% Atto 633 DOPE. Three samples were analysed part automated, part manual (images taken automatically, GUV measurements manually) per centrifugation speed with at least 1000 GUVs counted per sample (not per well!). The error bars show the standard deviation of the mean GUV size. Scale bar: 20 µm.

experimental setup. The inverted emulsion method gives a feasible vesicle size to conduct a large variety of experiments on but they are far from being monodisperse. Although, the formation of vesosomes is not particularly size dependent, the encapsulation of electroformed GUVs is favoured at smaller ratios between the inner and outer GUVs which will be shown next. Because of that, the inverted emulsion GUVs are important to have a size which is ideally achieved from centrifugation speeds between 100 - 300 x g.

By using the inverted emulsion method to encapsulate GUVs, the resulting vesosomes vary in size especially the outer GUVs range from ~ 10.0 µm up to ~ 57.0 µm (shown in Figure 2.5a) when formed at 250 x g. Of course, electroformed GUVs vary in size too in general. Sizes of encapsulated vesicles range from ~ 3.0 - 24.0 µm (Figure 2.5a). Analysing the vesosomes more closely shows varying ratios of inner to outer GUV diameters between 0.05 - 0.8 (Figure 2.5b). The three resulting exemplary forms are shown in Figure 2.5c showing firstly the inner GUV being much smaller compared to the size of the outer one (ratio value ~ 0.05). The second microscopy image displays an inner GUV being around half the size of the outer vesicle (ratio value ~ 0.5), and the third image gives an example of the inner GUV being almost the size as the outer one (ratio value ~ 0.8). In Figure 2.5b, one can see the latter case is rather exceptional but the majority of vesosomes have ratios of 0.15 - 0.4. It is speculated that smaller electroformed GUVs are more likely to be encapsulated compared to bigger ones because they are more likely to survive the emulsion

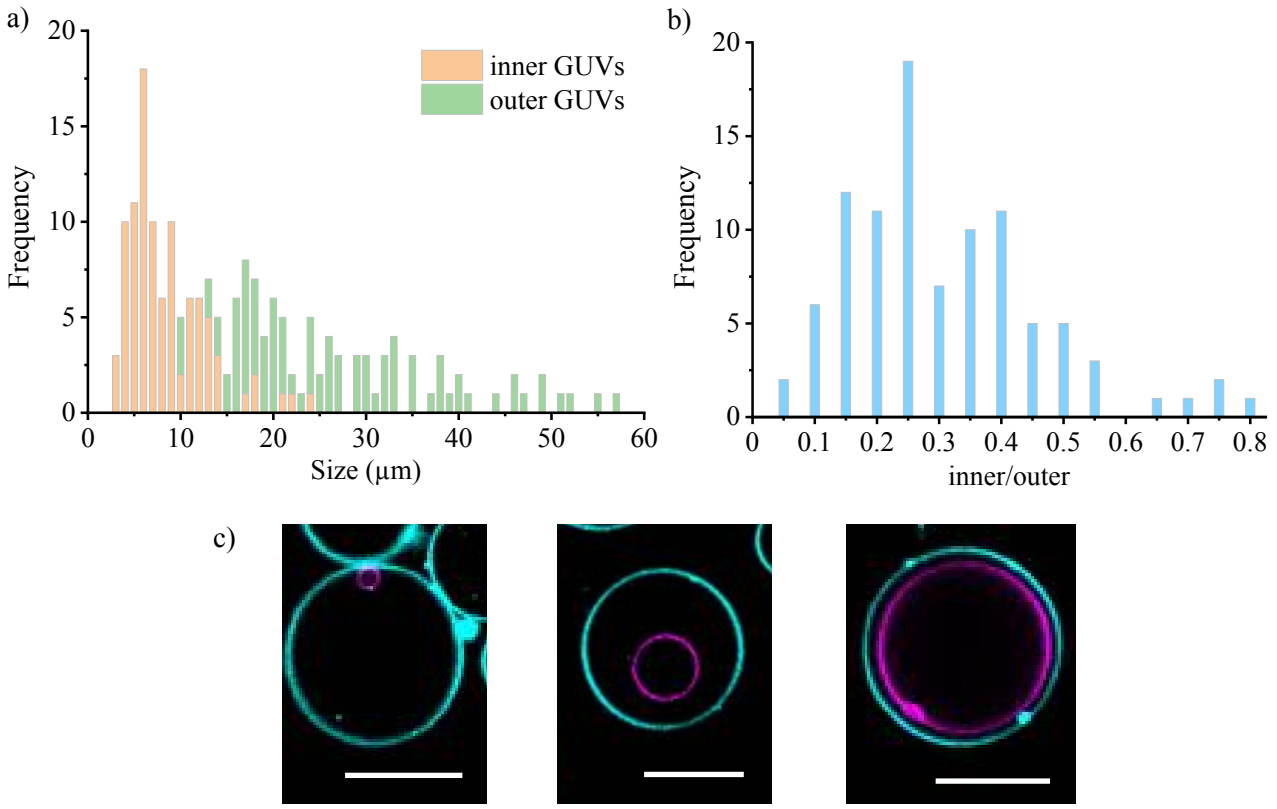

Figure 2.5: a) Histogram of vesosome sizes in total numbers. Sizes of electroformed inner GUVs depicted in orange. Sizes of inverted emulsion outer GUVs depicted in green. b) Calculated ratios between inner and outer GUVs. c) Fluorescent confocal microscopy images (merge) of vesosomes with different ratios between inner and outer GUVs. Created with a centrifugation speed of 250 x g. Electroformed inner GUVs are labelled with 0.1 mol% $DiIC_{18}$ (magenta), inverted emulsion outer GUVs are labelled with 0.1 mol% Atto 633 DOPE (cyan). Scale bars 20 µm.

preparation process and stray within the aqueous droplets during the centrifugation process i.e. the final vesosome formation. But there is more investigation needed at this point in the future.

The encapsulation of GUVs in GUVs surely depends on the centrifugation speed although, not only in terms of the sizes of the outer GUVs but the encapsulation itself which is shown in Figure 2.6a. The plot shows the number of vesosomes per sample. Three samples were analysed, each prepared in a microtiter plate with three wells per sample. The wells were thoroughly screened to count all vesosomes. It can be seen that lower centrifugation speeds (150 - 220 x g) result in higher encapsulation rates with > 60 vesosomes per sample. At speeds higher than 250 x g, the number of encapsulations decreases significantly to < 30 vesosomes. The force applied by the centrifugation and the inertia of w/o droplets in the emulsion compared to the inertia of the GUVs inside of these droplets might have an effect here. It is possible that more GUVs do not stay within the w/o droplet while crossing the interfacial lipid monolayer, or some of the inner GUVs burst during the encapsulation process. But this is just an assumption and the actual reason is still unclear and will need further investigation in the future. Another factor is the number of encapsulated GUVs per vesicle. When encapsulating GUVs using the inverted emulsion method, there is no way of

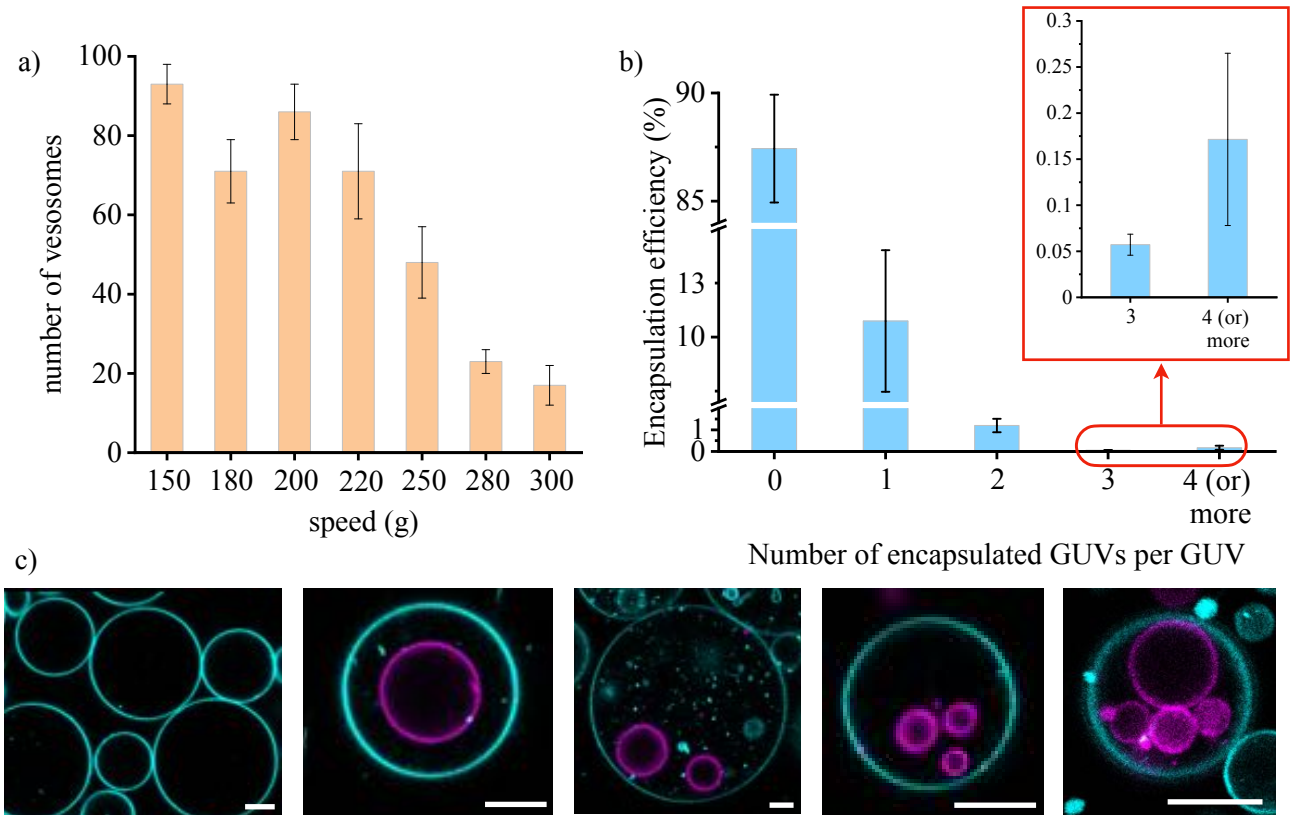

Figure 2.6: a) Number of vesosomes formed at different centrifugation speeds. Values given in total numbers. The error bars display the standard error of mean and are given by the total differences of the three samples. b) Encapsulation efficiency in percentage for ~ 500 GUVs per sample in relation to the number of encapsulated GUVs per GUV. The error bars display the standard error of mean and are given by the total differences of the three samples. c) Fluorescent confocal microscopy images (merge) of vesosomes with zero, one, two, three or more encapsulated GUVs. Electroformed inner GUVs are labelled with 0.1 mol% $DiIC_{18}$ (magenta), inverted emulsion outer GUVs are labelled with 0.1 mol% Atto 633 DOPE (cyan). Scale bars: 10 µm

controlling the number of encapsulated vesicles per GUV. Analysing three samples prepared in microtiter plates with three wells per sample and at a centrifugation speed of 250 x g show that most of the GUVs have no encapsulations (~ 87.4 %), in ~ 10.7 % of the vesosomes, there is one GUV encapsulated, two GUVs in 1.2 % and three or even more encapsulated vesicles in less than 0.4 % of the vesosomes as plotted in Figure 2.6b. Microscope images of all different configurations are displayed in Figure 2.6c. The more electroformed GUVs are encapsulated within one inverted emulsion GUV, the smaller the ratio between inner and outer GUVs become because it is more likely to encapsulate multiple small GUVs than several larger ones. As for the case of four or more encapsulated GUVs, the inner vesicles can be quite small and difficult to image. Also, not just GUVs can be encapsulated but impurities like lipid clusters too. These impurities can be from the inner GUVs or from the outer ones which can be distinguished by the membrane dye used. The middle microscopy image in Figure 2.6c with two inner GUVs shows impurities like lipid clusters originating from the outer GUV's lipid composition while the right most image comprises of impurities originating from the inner GUV's lipid composition next to the encapsulated GUVs. As

in the former experiment, the GUVs in one well could not be counted in total since a small percentage of them could not be visualised due to resolution issues. However, the analysis is still consistent across experiments.

To sum up, the strategy of encapsulating electroformed GUVs in GUVs by using the inverted emulsion method is sufficient for the creation of multi - compartment vesicles with respect to certain factors like a proper organic solvent, the lipid composition and the centrifugation speed.

2.2. Liquid Ordered - Liquid Disordered Membrane Phase Separation in GUVs Created from the Inverted Emulsion Method

With a suitable method of forming a vesosome system, in order to achieve the directed adhesion, either the membranes of the electroformed GUVs or the inverted emulsion vesicles need to be phase separated at least.

Creating liquid - liquid membrane phase separated GUVs from the electroformation method is highly dependent on choosing the right lipid composition. Phase diagrams like the one shown in Figure 1.9 are in general used here to decide on the right percentages. For the lipids forming the vesicles with L_d/L_o - phase coexistence, the lipid composition falls within the green region of the diagram, including cholesterol levels up to 40 mol%. For the low melting temperature lipid, DOPC is commonly used and for the high melting temperature lipid either DPPC or SM are suitable examples. The electroformation itself is carried out at temperatures ~ 65 °C for up to four hours. The temperature was chosen accordingly to make sure all lipids are in a liquid state ($T > T_M$ for all lipids) throughout the process of vesicle formation. For more detailed information, see methods in Chapter 7.2. After the GUVs cooled down, the coexisting phases are visible by light microscopy.

The inverted emulsion method was performed using mineral oil as organic solvent which is a mixture of several organic molecules like paraffin, cycloalkanes and different aromatic compounds. Mineral oil is used by many scientists preparing vesicles from the inverted emulsion method and other related strategies[33,53]. It can be used without problems alongside of biomolecules like proteins and DNA and often gives good results considering the GUVs, the yield, the sizes and low amounts of lipid

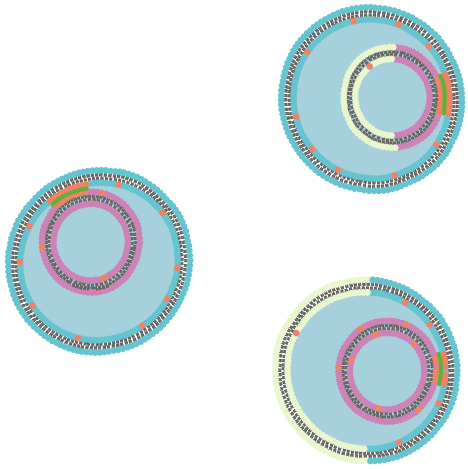

Figure 2.7: Schematic of non - directed (left) versus directed (right) internal membrane - membrane adhesion. The direction of the adhesion is achieved through the membrane phase separation of either the inner (top right) or the outer (bottom right) GUV.

impurities like tubes and small lipid aggregates. Some disadvantages are the strong tendency to oxidate when in contact with air and the absorption of water from higher humidity levels[201,202]. For that reason, it would be of great help to work and store mineral oil only within a glove box with close to no humidity. This way, the vesicles produced from it are, in general, of higher quantity and also cleaner considering lipid aggregates and tubes (data not shown). This is something that was found during the whole study while working with mineral oil at different stages of oxidisation and water content (judged by the duration of the mineral oil being used) and is often not mentioned in the literature. A second problem when using mineral oil is the varying solubility of different lipids. The average phospholipid dissolves well in mineral oil using sonication for ~ 30 minutes. When an interface with water is established, the lipids sort into the interface since the polar head group drags the lipid to the oil - water interface. Lipids that are not comprised of a strong enough polar group are more likely to remain within the oil phase and do not (or only in much lower concentration) sort into the interface in the first place which means, they are less likely to be incorporated within the forming membrane. One lipid falling within this category is cholesterol which is a key component when creating liquid - liquid membrane phase separated vesicles. So the use of pure mineral oil as organic (non polar) phase was highly problematic when used to create vesicles with lipid compositions including cholesterol. Analysing the actual membrane composition after vesicle formation is rather complex and could not be achieved by now. Because of that, it is not possible to estimate the actual cholesterol concentration a membrane is composed of, when the inverted emulsion method is used. Since, the mineral oil also displays a complex mixture of organic compounds, it is not possible to analyse the oil phase after vesicle formation (via NMR, mass spectrometry or other analytical methods), estimating the remaining cholesterol within.

A study from 2018 compared the formation of membrane phase separations in vesicles created from electroformation and the inverted emulsion method showing a liquid - liquid membrane phase separation at cholesterol concentrations between 10 mol% and 40 mol% for the electroformation method. When the inverted emulsion method was used, concentrations of 37 - 85 mol% cholesterol were needed to achieve the same outcome.[203] These results could be reproduced to some extent. A side note here, a sample was personally considered liquid - liquid membrane phase separated when ≥ 50 mol% of GUVs showed phase coexistence. For all phase separation experiments, all solutions and the microtiter plates were kept in the oven at 65 °C until centrifugation. A 600 - 900 mM sucrose solution was used as aqueous solution for the w/o emulsion. A 600 - 900 mM glucose solution was used as bottom (outer) aqueous phase were the GUVs end up after their formation. Phase separated GUVs were created with different cholesterol levels including 60 mol% cholesterol

and 70 mol% cholesterol (see Figure 2.8). Below 50 mol% cholesterol and above 70 mol% cholesterol, the formed vesicles showed no phase separation (see Figure 2.8). A liquid - liquid membrane phase separation at 50 mol% cholesterol was most of the time unreliable and it seemed to strongly depend on the quality of the mineral oil. But these effects would need further investigation. Another strategy uses different organic solvents and solvent combinations to get the required amounts of cholesterol to be incorporated into the membrane. One of those uses two different oil phases, both being mixtures of mineral oil, silicone oil and n - decane. The two distinct

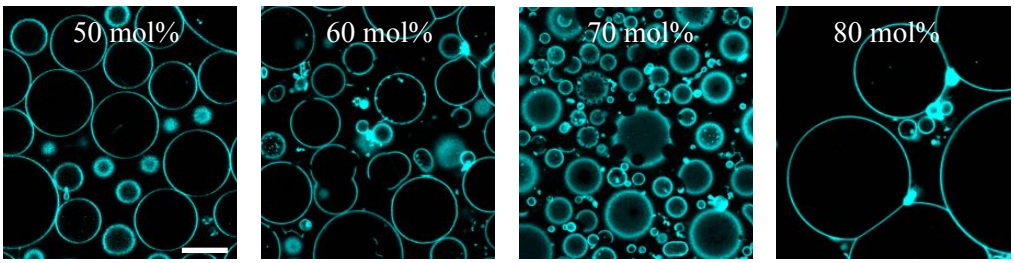

Figure 2.8: Fluorescence confocal microscopy images (Atto 633 channel) of GUVs created from the inverted emulsion method. Lipid compositions with 1:1 DOPC - SM, 0.1 mol% Atto 633 DOPE and 50 - 80 mol% cholesterol. A liquid - liquid membrane phase separation is visible for the samples including 60 - 70 mol% cholesterol. The other samples show no membrane phase separation. Scale bar: 20 µm.

oil mixtures are oil one which is used to prepare the emulsion and made from phospholipids mixed in 14 % mineral oil, 6 % n - decane and 80 % silicone oil[204] while the second oil is composed of cholesterol and phospholipids mixed in 6 % n - decane and 94 % silicone oil[204]. The second oil mixture is poured on top of the aqueous phase to form an interfacial lipid monolayer before the emulsion is added as well (see Figure 2.9). This way, the oil phase containing cholesterol does not include mineral oil and this increases the chances for cholesterol incorporation into the vesicle membrane. [204] Reproductions of this approach resulted in a liquid - liquid membrane phase separation for lipid compositions including 50 mol% cholesterol and 60 mol% cholesterol. This shows the advantage of the method, achieving a reliable liquid - liquid membrane phase separation at lower cholesterol levels compared to the pure mineral oil approach.

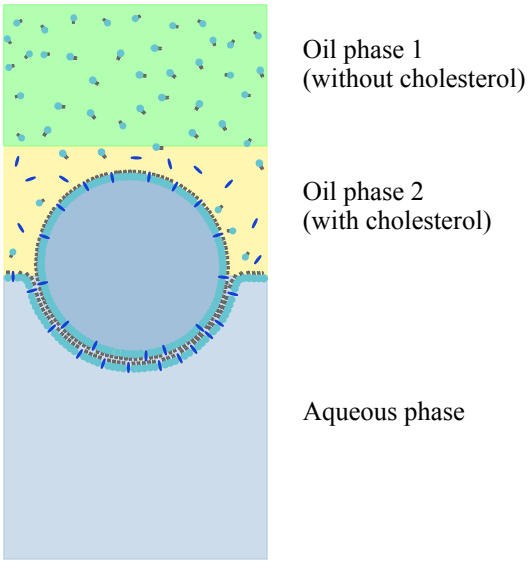

Figure 2.9: Schematic of the creation of membrane phase separated GUVs from the inverted emulsion method using two oil phases. Oil phase one is composed of lipids (no cholesterol) in mineral oil, n - decane and silicone oil (green). Oil phase two is composed of lipids (including cholesterol) in n - decane and silicone oil (yellow).

Because of all the complications with mineral oil and cholesterol, forming GUVs without cholesterol and

achieving a phase separation by adding it afterwards was also tested. Cholesterol, for this purpose, was dissolved in ethanol to be able to add it to the GUV solution. To get higher incorporation rates of cholesterol into the GUV membranes, the samples were heated to ~ 70 °C for 5 - 10 minutes after the additions. At concentrations of 70 nM cholesterol, the vesicles show S_o/L_d - membrane phase separation but every addition and heating cycle resulted in smaller GUVs (data not shown). It seems like, this is an effect of the alcohol on the GUVs. Studies on LUVs have shown a decrease in size of the liposomes after the addition of ethanol[205]. Because of the shrinking of the GUVs during the process, this strategy was not further used to create phase separations since shrinking of the outer GUVs can have unwanted negative effects on vesosomes. Therefore this strategy does not suit the study properly.

It should be mentioned that all these results here apply for ternary lipid compositions like DOPC - SM - cholesterol or DOPC - DPPC - cholesterol. As described in section 1.4., the research project has the goal of adhering two distinct membranes to each other. For that, a fourth lipid is needed in case of the biotin streptavidin system and also for the DNA strategy. Even at very low concentrations, a fourth lipid added to the composition can make a significant difference on phase coexistence, especially when the (more difficult) inverted emulsion method has to be used.

When quaternary lipid compositions (including 2 mol% biotinylated lipid) were tested with pure mineral oil, several of the samples showed a peculiar effect when imaged by light microscopy. By the influence of light irradiation, more and more GUVs burst leaving small lipid clusters and tubes as can be seen in Figure 2.10. The bursting observed in these samples is morphologically identical to the GUV bursting described in Lira et.al.[181], where this was a result from a decrease in the membrane's edge tension. The membrane's edge tension is the leading factor of pore shrinkage and closure[181,206] which can be influenced by the lipid composition (especially charged lipids)[181], the presence of ions[181] and maybe by possible traces of mineral oil within the lipid bilayer. Studies could also demonstrate pore formation induced by light irradiation[180,207]. It is possible that the vesicle bursting in this study is a combination of light induced poration and a reduced membrane edge tension which leads to vesicle rupture. All of that could be caused by the traces of mineral oil ending up in the lipid bilayer through the creation of vesicles from the inverted emulsion method. Why this effect occurs only for GUVs including 2.0 mol% PE biotin is unclear although, the acyl chains are also both unsaturated and therefore add up to the level of unsaturated lipids of the GUV membranes.

In case of the strategy of using two oil phases from n - decane, silicone oil and mineral oil, the method was slightly optimised since, the former way resulted in pure liquid disordered phased

GUVs. Instead of using two oil mixtures from three solvents, pure mineral oil was used to create the emulsion while the second oil comprised of n - decane and silicone oil. Both oil phases comprise of the same lipid compositions including cholesterol. The n - decane silicone oil phase ensures the

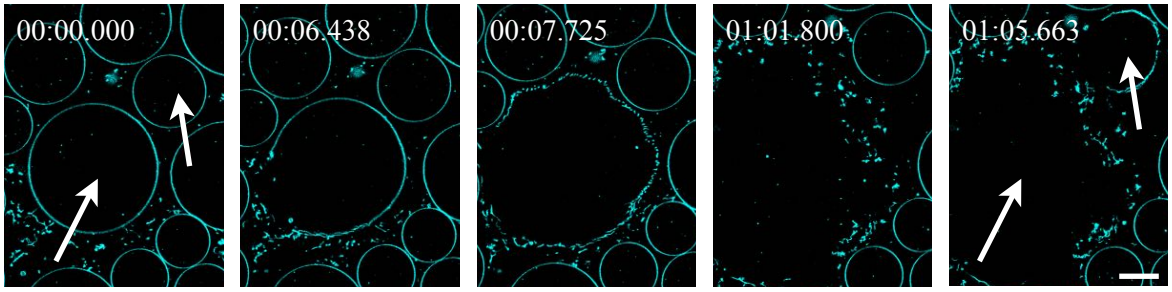

Figure 2.10: Fluorescent confocal microscopy time series (Atto 633 channel) of GUVs created using the inverted emulsion method from a quaternary lipid composition labelled with Atto 633 DOPE from pure mineral oil and 900 mM glucose and sucrose solutions. GUVs burst through light irradiation leaving small lipid clusters. The longer the light irradiation, the more GUVs burst. The lipid composition is 24 mol% DOPC, 24 mol% SM, 50 mol% cholesterol, 2.0 mol% PE biotin and 0.1 mol% Atto 633 DOPE. Time stamp is in minutes. Scale bar: 10 µm.

cholesterol incorporation into the vesicle membrane while the mineral oil phase used to create the emulsion is the main factor for vesicle formation (size, form, purity). By the use of this, it is possible to create liquid - liquid membrane phase separated GUVs at cholesterol levels of 40 mol% (see Figure 2.11). The lipid composition employed was 20 mol% POPC, 40 mol% DPPC, 2 mol% PE biotin and 40 mol% cholesterol. It is also possible to use 40 mol% SM but in this study, the best results were achieved with DPPC.

With this, the last part of the system's basis is established and the study could be proceeded with the three variations to form adhesions between inner and outer GUV membranes.

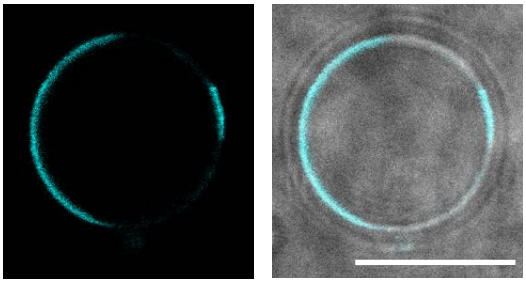

Figure 2.11: Fluorescent confocal microscopy image (first image Atto 633 channel, second image merge with brightfield) of a liquid - liquid phase separated GUV created using the inverted emulsion method from a quaternary lipid composition labeled with Atto 633 DOPE. Oil phase one used to create an interfacial lipid monolayer is made from 6 % n - decane and 94 % silicone oil. Oil phase two used to create the emulsion is made from pure mineral oil. Both oil phases comprise of the same lipid composition of 20 mol% POPC, 40 mol% DPPC, 2 mol% PE biotin and 40 mol% cholesterol. Sugar solutions of 900 mM glucose and sucrose used as aqueous phases. Image one shows the channel for Atto 633 DOPE, image two shows the merge of the fluorescence and bright field channel. Scale bar: 10 µm

3. Biotin and Streptavidin

3.1. General Overview

The use of biotin and streptavidin is a very popular option to adhere lipid bilayers[129,165] to one another making it an easy choice for the study conducted here. By using a biotinylated lipid, the incorporation of biotin moieties to the membrane of the GUVs is very simple for both vesicle types. Streptavidin needs to be encapsulated alongside the electroformed GUVs. Figure 3.1 shows the inner and outer GUV including the biotin moieties at the vesicle membranes which can bind to streptavidin. The concentrations of biotin as well as streptavidin need to be ideal for the purpose of internal adhesion of the two membranes. Because streptavidin is going to be encapsulated in this

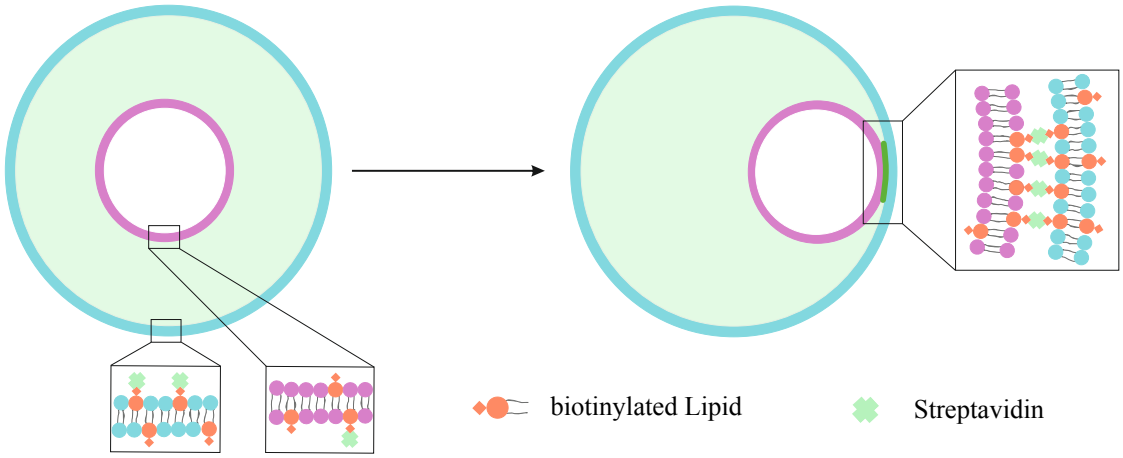

Figure 3.1: Schematic illustration of the internal adhesion of the membranes of inner and outer GUV by a biotin streptavidin bridge. Biotinylated lipids drawn in red binding streptavidin drawn in green. The enhanced streptavidin signal shown in between both vesicle membranes when adhered is a clear sign of an enrichment of streptavidin and therefore biotin molecules.

experimental setup, the concentration in the external glucose solution is supposed to be near zero although, in the case of rupturing or leaking of outer GUVs, the streptavidin also mixes with the external solution. This can lead to unwanted external adhesion of the inverted emulsion GUVs and even not encapsulated electroformed GUVs since the vesicle membranes are symmetric meaning, biotin exists in both inner and outer leaflets. The experiment is conducted so that the electroformed GUV will be mixed with a solution of streptavidin in phosphate buffered saline (PBS) buffer (see Chapter 7.2 for details on the method). There is the possibility of them already adhering to each other via a biotin streptavidin bridge and even forming bigger clusters before they are encapsulated. The only way to prevent this is to choose the concentrations of biotin and streptavidin accordingly, so as to decrease the likelihood of adhesion but at the same time not eliminating the feasibility of it.

Another factor which was mentioned in Chapter 2.1. is the centrifugation speed used to create the inverted emulsion GUVs. Since it has an influence on the encapsulation of GUVs, the efficiency of encapsulating streptavidin also needs to be ideal. Similarly, there is the possibility of leaky inverted emulsion GUVs which should be near zero for maximum efficiency and was therefore tested in context of this study. Finally, the concentration of streptavidin is optimised to complete the internal adhesion system. To acquire a directed adhesion, the completed system is executed on GUVs created from lipid compositions showing a liquid - liquid membrane phase separation. The different membrane phases contain a distinct lipid composition which leads to a spatially directed adhesion at only one of the two phases of the membrane phase separated GUVs (see Figure 2.7).

3.2. Conditions and Parameters for a Biotin Streptavidin Membrane - Membrane Adhesion

In order to find the optimal conditions for an internal adhesion using biotin and streptavidin, several factors had to be optimised.

To determine a suitable concentration for the biotinylated lipid being incorporated within the membranes of the two GUV types, an experiment with GUVs of seven different lipid compositions was conducted (non - vesosomes). At fixed streptavidin concentrations, the external adhesion of the vesicles in terms of quality and quantity were compared. The experiment was conducted in microfluidic chips to immobilise the assemblies and analyse the external adhesion areas afterwards (see Figure 3.2a). Also, by using microfluidic chips, the creation of external membrane - membrane adhesion could be controlled by flushing GUVs into the chips until the traps were properly filled (see Figure 3.2b). In comparison to the same experiment done in a microtiter plate, all GUV

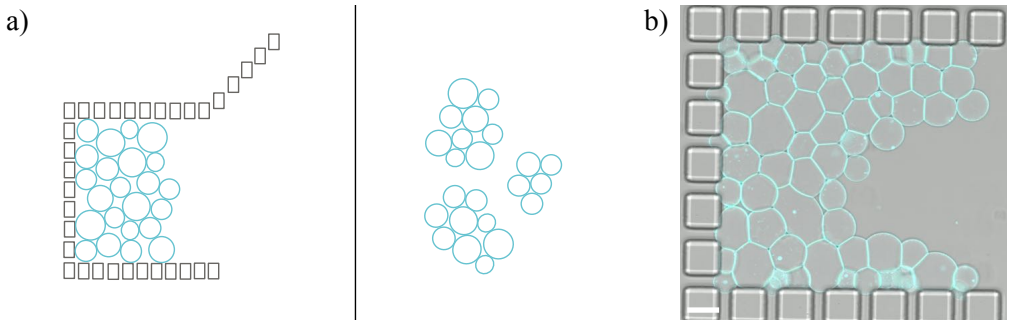

Figure 3.2: a) Schematic of a GUV experiment conducted in a microfluidic chip (left) versus in a well of a microtiter plate (right). The chip immobilises the GUVs and allows a more controlled analysis. GUVs can move freely in a well of a microtiter plate and larger GUV assemblies are more coincidental. b) Fluorescence confocal microscopy image (merge with brightfield) of a trap of a microfluidic chip filled with GUVs. Posts of the trap visible in the brightfield channel. GUVs created from the electroformation method with a lipid composition of 98.9 mol% POPC, 1.0 mol% PE biotin and 0.1 mol% Atto 633 DOPE. Scale bar: 30 µm

assemblies form less likely and would have probably given less data to analyse. The biotinylated lipid 1,2-dioleoyl-sn-glycero-3-phosphoethanolamine-N-(cap biotinyl) (PE biotin) was used at concentrations between 0.1 - 2.0 mol%. All GUV types were created from the electroformation method, mixed with streptavidin at a final concentration of 150 nM and flushed into a microfluidic chip (see Chapter 7.2 for further experimental details like flow rates etc.). The concentration of streptavidin was at this point preliminarily chosen and not optimised through other tests. The chips had been previously coated with β - casein and washed with a glucose - PBS solution before getting filled with the GUV solution. Any excess of streptavidin is removed from the GUVs through the constant fluid flow. The different concentrations of PE biotin within the GUV membranes lead to different amounts of adhesion, visible by the length of the adhesion area, the vesicle deformation and the intensity of the fluorescence signal of streptavidin which is labelled with Alexa 488 (see Figure 3.3a). At the highest concentration tested, i.e. 2.0 mol% PE biotin, the GUVs are barely spherical and adhesions are established at almost every point where the GUV membranes touch each other. The biotin concentration is high enough to provide for the adhesion while being evenly distributed throughout membranes which is visible through the streptavidin signal throughout the GUV membranes. The membranes show strong deformations to increase the adhesion area which increases the contact angle between both adhered membranes. The larger the adhesion area, the better and stronger is the adhesion for more biotin and streptavidin complexes take part in it. As the biotin concentration is decreased, the streptavidin signal disappears more and more from the areas not showing membrane adhesion. The biotinylated lipid gets accumulated within the adhesion area to provide for the adhesion, leaving the rest of the membrane deprived of it and not able to bind streptavidin and to form another adhesion with other GUVs. This is possible because of the membrane fluidity and the resulting diffusion of the lipids[69,70]. The deformation of the GUVs occurring from the adhesion of the membranes is reduced as well, so the vesicles appear more spherical the lower the biotin concentration is, leading to smaller adhesion areas. At 0.1 mol% PE biotin, the streptavidin signal is barely visible in the sample and although, some vesicles adhere to each other, streptavidin is not visible along the entire adhesion area. It seems like, there is not enough biotin to cover even the entire adhesion area despite with the accumulation of the lipid. To plot the information gathered from this experiment, the fluorescent signal of the streptavidin (labelled with Alexa 488) and the membrane dye (Atto 633 DOPE) were measured on the GUV membranes for comparison (see Figure 3.3b). Since the concentration of Atto 633 DOPE is steady (0.1 mol%) and evenly distributed throughout the membrane, the signal did not change for the different lipid compositions or is influenced by the membrane adhesion. It gives a good reference to

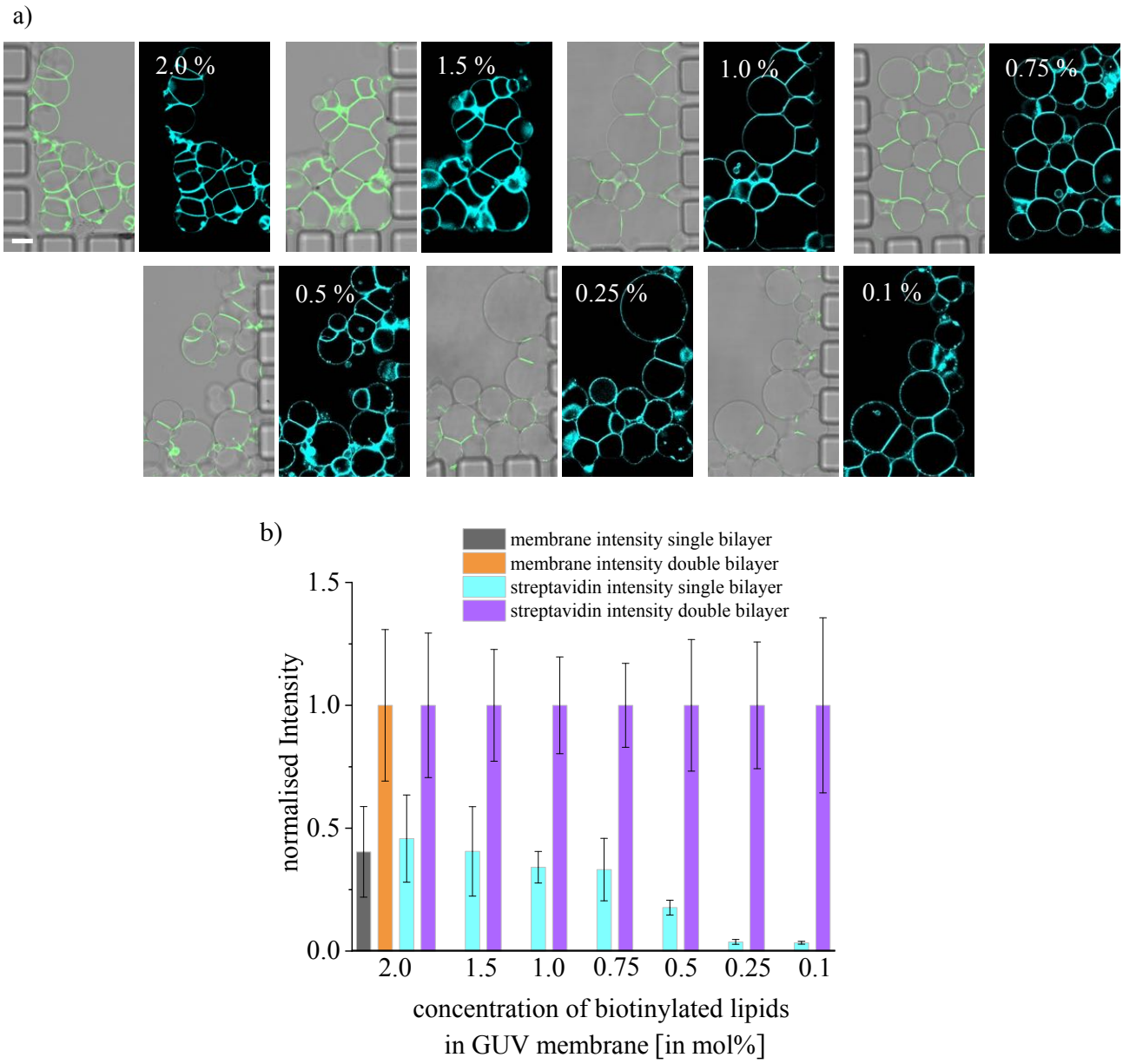

Figure 3.3: a) Fluorescence confocal microscopy images (merge of streptavidin channel and brightfield) of GUVs with concentrations of PE biotin from 2.0 mol% to 0.1 mol% and fixed streptavidin concentrations (c = 150 nM). GUVs prepared using the electroformation method from POPC, PE biotin and 0.1 mol% Atto 633 DOPE. GUVs were flushed into the chips at flow rates of 2 µl/min. Streptavidin signal visible in green. Membrane signal (Atto 633 DOPE) visible in cyan. Scale bar: 20 µm b) The average fluorescence intensity of the single bilayer intensity of the non - adhered area compared to the double bilayer intensity of the adhesion area at decreasing biotin concentrations. Fluorescence intensity normalised to the double bilayer intensity for both membrane dye and streptavidin. The decrease in intensity of the single bilayer signal results from the enrichment of PE biotin within the adhesion area and depletion within the non - adhesion area. Streptavidin gets almost completely excluded from areas of the membranes not adhering to other membranes. At higher biotin concentrations, the signal of the single bilayer signal is approximately about 50 % of that of the double bilayer signal. Membrane dye signal shown for comparison for the sample of 2.0 mol% PE biotin. For all concentrations, a number of ~ 300 GUV adhesions were measured with three points for every single bilayer intensity and three points for every double bilayer intensity. The error bars give the standard deviation of the mean fluorescence signal.

compare it with the streptavidin signal of the samples with higher concentrations of PE biotin (2.0 - 1.5 mol%). Signal measurements were taken at the two different areas of the membranes, the adhesion area (double lipid bilayer) and the non - adhesion area (single lipid bilayer). The signal

intensity ratio of both is therefore supposed to be 2 : 1. The single lipid bilayer intensity was normalised to the double bilayer intensity. This helps to show the decreasing intensity of the streptavidin signal of the single bilayer at decreasing biotin concentrations in relation to the double bilayer intensity. The plot visualises that the two highest biotin concentrations give very similar values compared to the intensity of the membrane dye, pointing to the lipid being evenly distributed. It cannot be estimated, if there is an accumulation of PE biotin at the adhesion area occurring to provide for the adhesion. Biotin accumulation at the adhesion area becomes clear for lower concentrations (≤ 0.5 mol%) when the single bilayer streptavidin signal drops to < 25 % of that of the double bilayer signal. The two lowest biotin concentrations show barely any signal in the single bilayer areas and the majority of PE biotin lies within the adhesion area. In the final experiment of adhering two GUV membranes internally to one another, the solution which gets prepared for encapsulation contains electroformed GUVs and a streptavidin solution at the same time. At this point, adhesion needs to be inhibited as much as possible. For that reason, the incubation time of the solution should be rather short and the concentration of PE biotin needs to be low to prevent clustering of the GUVs. In the case of the outer GUVs, the biotin levels can be higher also because adhesion and the formation of clusters of the outer vesicles is much more unlikely because of a lack of streptavidin within the external sugar solution (to the premise of an efficient streptavidin encapsulation). The information gathered from the chip experiment points to concentrations between 0.25 - 0.1 mol% biotinylated lipid in case of the inner GUVs for that purpose and 1.5 - 2.0 mol% PE biotin for the outer ones.

To confirm the adhesion analysis and the conclusions taken from it, samples of the highest and lowest PE biotin levels as well as a mixture of both mixed with streptavidin to a final concentration of 150 nM were flushed into microfluidic chips. After the traps were filled, the fluid flow was reversed (see Figure 3.4)(see Chapter 7.2 for further experimental details like flow rates etc.). Doing that, the GUVs will be flushed out separately whereby with an established adhesion the GUVs move out of the traps as one large aggregate of vesicles. This is the case for the GUVs containing 2 mol% PE biotin, demonstrating the efficiency of the adhesion (Figure 3.4a). In the case of the vesicles including 0.1 mol% PE biotin, the GUVs do not move as one construct but in smaller assemblies breaking apart through the pressure of the flow (Figure 3.4b). One difference, visible immediately, is the morphologies of the GUVs. Although both GUV types (of Figure 3.4a and b) were prepared from electroformation, the majority of the GUVs in Figure 3.4b look much more spherical and larger in size. It is not clear if the difference in size is due to the biotin concentration within the membranes or the biotin streptavidin adhesion causing strong deformations of the GUVs

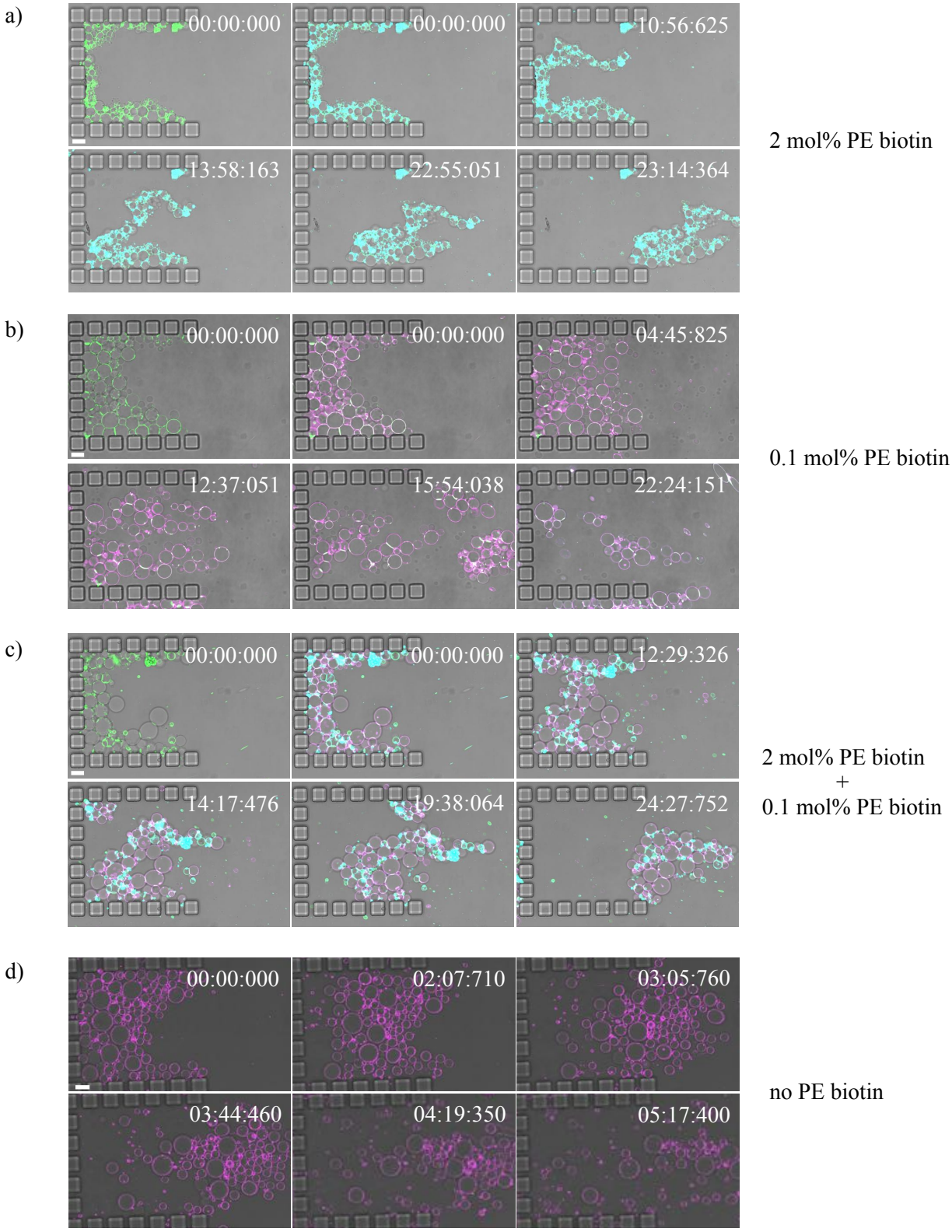

Figure 3.4: Fluorescence confocal microscope time laps images of electroformed GUVs created from a) 97.9 mol% POPC, 2.0 mol% PE biotin and 0.1 mol% Atto 633 DOPE. b) 99.8 mol% POPC, 0.1 mol% PE biotin and 0.1 mol% $DiIC_{18}$. c) 97.9 mol% POPC, 2.0 mol% PE biotin and 0.1 mol% Atto 633 DOPE mixed with GUVs created from 99.8 mol% POPC, 0.1 mol% PE biotin and 0.1 mol% $DiIC_{18}$. d) 99.9 mol% POPC and 0.1 mol% $DiIC_{18}$. Samples a - c were mixed with streptavidin to a final concentration of 150 nM. A merged image of the streptavidin channel and brightfield is shown as first image at time zero. The following images are merged of all channels. Sample d was used without streptavidin. All images are merged with brightfield. All samples were flushed into a cascade microfluidic chip at a flow rate of 2.0 µl/min. After the traps got sufficiently filled with GUVs the flow was reversed to 0.25 µl/min to flush the GUVs back out of the traps. Time is given in minutes. Scale bars: 30 µm

in case of the first sample. A third sample composes of both GUV types mixed together. Here the size variation is even more obvious (Figure 3.4c) with the 0.1 mol% PE biotin GUVs (labelled with $DiIC_{18}$ (magenta)) being nice and spherical and the 2 mol% PE biotin GUVs can mostly only be distinguished by their membrane dye (Atto 633 DOPE (cyan)) but hardly look spherical. The microscope images show, even with those GUVs displaying more as clusters compared to the 0.1 mol% PE biotin type, the adhesion within the whole structure is strong enough to not fall apart when a reversed flow is applied, why it moves like a large aggregate. These three samples support the information gained from the first chip experiment, to use a lipid composition with 2.0 mol% for the outer GUVs while 0.1 mol% is also sufficient for the inner GUVs. The last sample (Figure 3.4d) was executed for comparison (and a control) and shows the process without any PE biotin nor streptavidin and therefore no adhesion. The most significant difference to all other samples is the time needed to flush all GUVs out of the trap which is only a fraction of the time compared to the other samples since the GUVs can move individually.

The second building block in this study is streptavidin which is used as a free biomolecule, not incorporated into the membrane but added and encapsulated. Experiments were conducted on the encapsulation efficiency as well as the leakiness of the inverted emulsion GUVs considering streptavidin. The encapsulation of different streptavidin solutions at distinct concentrations was measured via the average fluorescence intensity gained from fluorescence confocal microscopy (see Figure 3.5). A calibration curve to fit the data was obtained by measuring the average fluorescence intensity of different streptavidin solutions in bulk (see Figure 3.5a, black points)(see Chapter 7.2 for further experimental details). The plot of Figure 3.5a (blue points) shows, the encapsulation of streptavidin is very efficient with ~ 100 % for concentrations up to 150 nM. Only the 200 nM concentrated solution showed a slight drop. In some cases the intensity even exceeded 100 % which is probably an artefact of uneven distribution of streptavidin (see Figure 3.5c). This is also reflected by the error bars in Figure 3.5a. The signal for every GUV can vary slightly due to minor differences of the focus plain. Two GUVs can appear to be in focus in a confocal image despite one GUV being slightly more in focus than the other one which can result in a minor intensity variation. In Figure 3.5b the corresponding exemplary confocal images are shown for the four encapsulated streptavidin solutions. It should be noted that, these experiments were conducted without PE biotin to not alter the streptavidin concentration of the vesicle lumen. The second experiment was conducted to examine any possible leaking of the GUVs which was tested in a similar way by the encapsulation of streptavidin and monitoring the average fluorescence intensity over two hours. Plot 3.5d visualises the intensity changes over time revealing no significant leakage. The variation of the

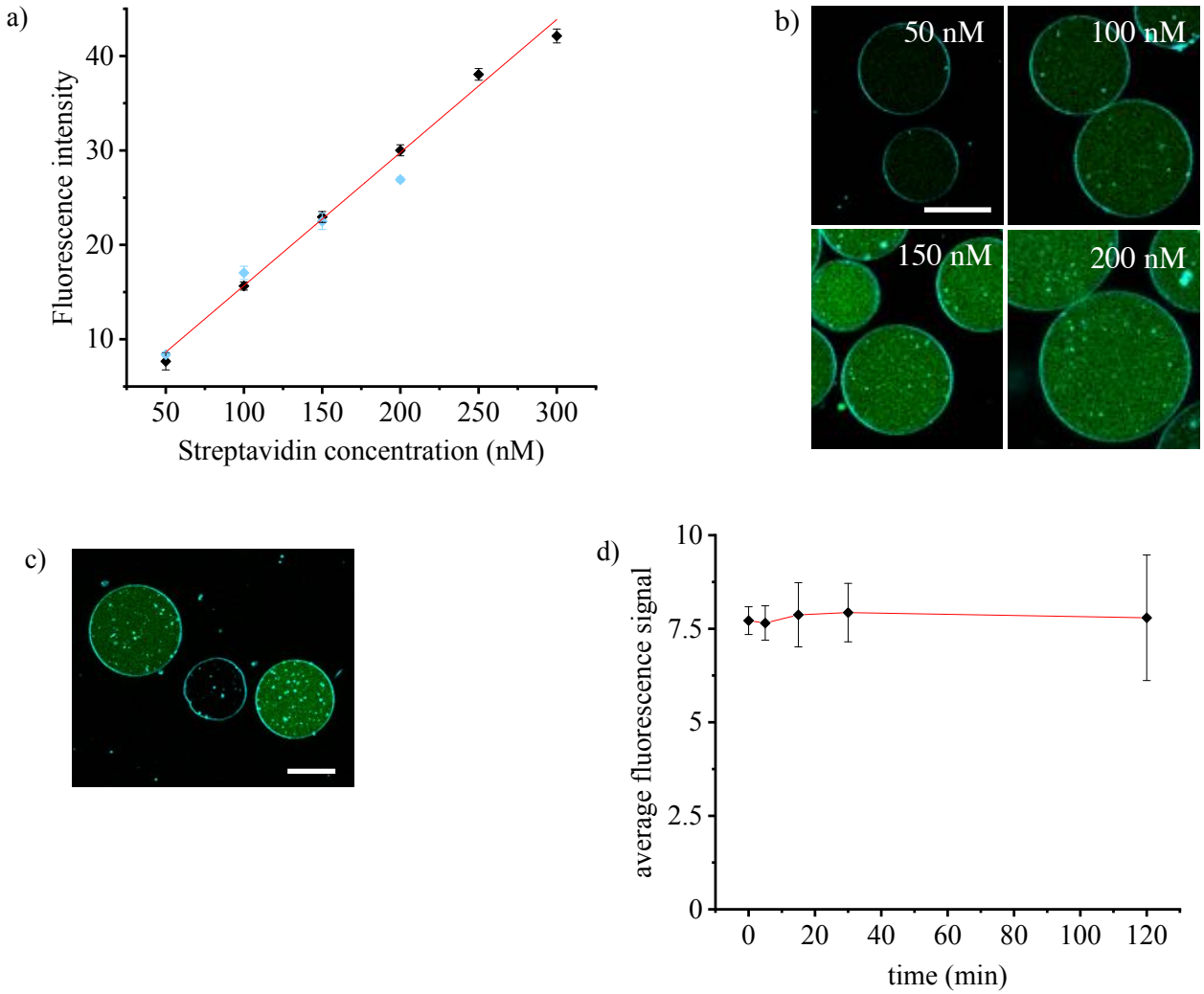

Figure 3.5: a) Average fluorescence intensity measurements of streptavidin solutions in bulk and encapsulated. Bulk measurements of solutions from 50 - 300 nM for calibration (black symbol). Encapsulation measurements of streptavidin solutions with concentrations of 50 - 200 nM in GUVs created from the inverted emulsion method (blue symbols). The error bars represent the standard deviation of the mean fluorescent intensity. b) Corresponding fluorescence confocal microscope images (merge) of inverted emulsion GUVs with 50 - 200 nM streptavidin solutions encapsulated. GUVs created from 99.9 mol% POPC and 0.1 mol% Atto 633 DOPE. Three samples with two wells per sample for every concentration were prepared and ~ 300 GUVs were measured for every sample. Scale bar: 20 µm c) Fluorescence confocal microscopy image (merge) of streptavidin encapsulated in inverted emulsion GUVs. Example for uneven distribution of streptavidin. GUVs created from 99.9 mol% POPC and 0.1 mol% Atto 633 DOPE. The final streptavidin concentration is 150 nM. Scale bar: 20 µm d) Average fluorescence intensity measurements of 50 nM streptavidin encapsulated in GUVs created from the inverted emulsion method over a time period of 120 minutes. The average fluorescence intensity of 5 GUVs within one image frame was measured. The error bars represent the standard deviation of the mean fluorescent intensity.

intensity and the errors is possibly an effect of the measurement over time. The experiment was conducted in a microtiter plate and the GUVs were not immobilised. This means over time the GUVs moved slightly over time along the x - , y - and z - axis whereby the region of interest (the region of the fluorescence intensity measurement) was constant. Especially movement along the z - axis can change the intensity of the signal without an actual change of the streptavidin concentration inside the GUVs. This experiment ensures no excess streptavidin is leaking into the external

aqueous solution which prevents clustering of the inverted emulsion GUVs. Five GUVs of one sample (one well) were analysed.

A suitable streptavidin concentration for the internal membrane - membrane adhesion was determined by internal adhesion experiments in the following.

3.3. Biotin Streptavidin: Internal Membrane - Membrane Adhesion

After being sure that the encapsulation of streptavidin is achieved without any significant loss, the next step is to study the effects when it is encapsulated along with internal GUVs. Two membranes were considered adhered when the membranes existed in close proximity without movement in relation to each other and when the streptavidin intensity was enhanced within the adhesion area (where both membranes touch) when labelled streptavidin was used. The quality of the adhesion was evaluated (assessed by eye) by the adhesion area and the contact angle (see Figure 3.6). A large adhesion area and a large contact angle point to a strong adhesion (Figure 3.6a) while a small adhesion area and a small contact angle point to a more weak adhesion (Figure 3.6b). The quantity of adhesion events is good, if most of the vesosomes of a sample show internal membrane - membrane adhesion.

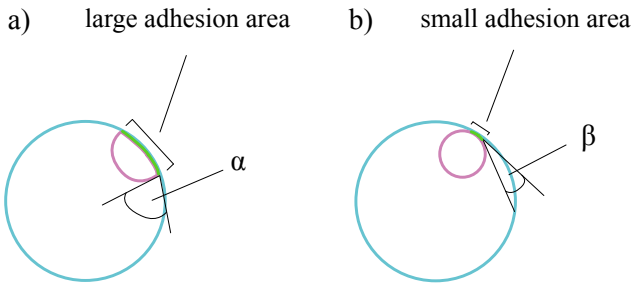

Figure 3.6: Schematic of internal membrane - membrane adhesion with a) a large adhesion area and a large contact angle α and b) a small contact area and a small contact angle β. The streptavidin signal (green) is visible throughout the whole adhesion area.

Different concentrations from 50 - 200 nM of streptavidin were encapsulated including electroformed GUVs to examine possible adhesions (see Figure 3.7)(see Chapter 7.2 for further experimental details). Figure 3.7a gives the percentages of vesosomes that show membrane - membrane adhesion at the different tested streptavidin concentrations. It shows, in the case of 50 nM streptavidin, a little over 20 % of the vesosomes of a sample show adhesion while the rest does not. When looking at 150 nM streptavidin, more than 80 % of the vesosomes include a membrane - membrane adhesion which points to being the optimal concentration for this experiment. Optimal means most of the vesosomes show adhesion and the streptavidin signal is clean without aggregates or other impurities within the samples. Using 200 nM streptavidin shows a slight drop of adhesion events of ~ 10 % compared to 150 nM streptavidin. The concentration of streptavidin influences not only the occurrence of the adhesion but as seen before in the chip experiments, the characteristics of it too. This aspect gets more clear when looking at Figure 3.7c where fluorescence confocal

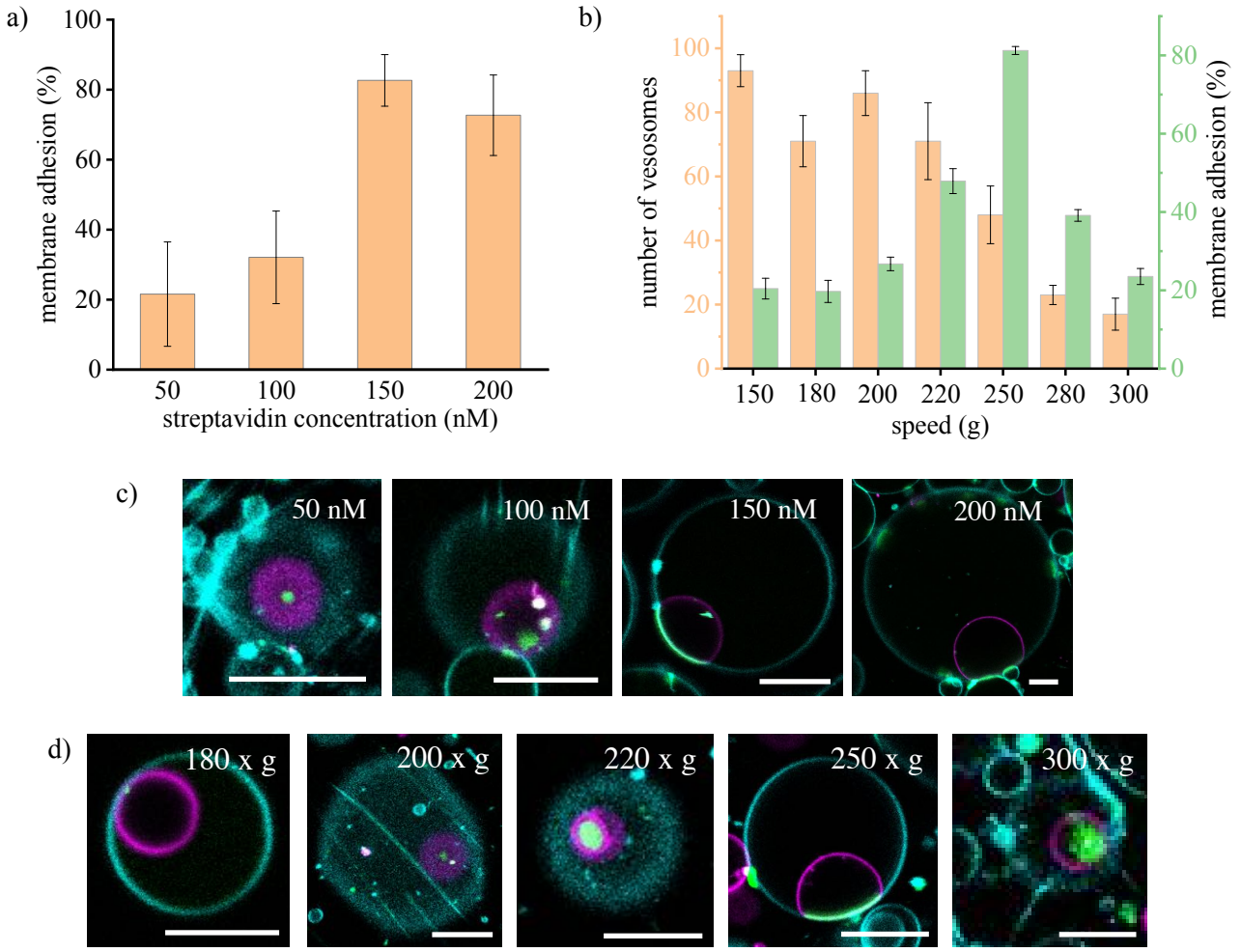

Figure 3.7: a) Histogram of the quantity of internal membrane - membrane adhesions in a vesosome system in percentage at different streptavidin concentrations. Three samples were analysed manually with at least 500 GUVs counted per sample (not per well!). Error bars represent the variation between different samples of one concentration (not wells). b) Number of encapsulations in juxtaposition to internal membrane - membrane adhesions in percentages at increasing centrifugation speeds. Values for vesosomes are given in total numbers. Error bars represent the variation between different samples (not wells). Percentages of membrane adhesions calculated from the total numbers of the vesosomes. c) Fluorescence confocal microscopy images (merge) of vesosome systems with internal membrane - membrane adhesions at different streptavidin concentrations. Centrifugation speed for all samples was 250 x g. d) Fluorescence confocal microscopy images (merge) of vesosome systems created with 150 nM streptavidin at different centrifugation speeds. All images show internal membrane - membrane adhesion. For all samples the outer GUVs (cyan) were created from the inverted emulsion method with 97.9 mol% POPC, 2.0 mol% PE biotin, 0.1 mol% Atto 633 DOPE. All inner GUVs (magenta) were created from the electroformation method with 99.8 mol% POPC, 0.1 mol% PE biotin, 0.1 mol% $DiIC_{18}$. Streptavidin labelled with Alexa 488 signal visible in green. Scale bars: 10 µm

microscopy images of the vesosomes of the four different tested concentrations are depicted. The adhesion area is in all cases visible by the enhanced streptavidin signal in green and the extent of the adhesion area gives evidence on the quality of the adhesion. In the cases of the 50 nM and 100nM examples, the adhesion is on the bottom of the outer GUV why it is not identifiable if any of the vesicles are deformed by the adhesion but it is unlikely. A deformation of the vesicle membranes occurs from the enlargement of the adhesion area and leads to a larger contact angle. Two GUVs can only have a narrow adhesion area without the deformation of either of their membranes. In

order to extent this area, one or both GUV membranes must deform. Since the adhesion area for 50 - 100 nM streptavidin is rather small, a membrane deformation can be excluded. Whereas, for the examples of 150 nM and 200 nM streptavidin, the deformation due to the adhesion is obvious and leads to an enlargement of the adhesion area as well. From this data, the concentration giving the best results is 150 nM streptavidin to achieve internal membrane - membrane adhesion of good quality as well as good quantity. Also, this concentration gives the best qualitative results. This experiment gives a good guide when it comes to tuning the adhesion in matter of the contact areas.

Former experiments discussed in Chapter 2.1., revealed also the dependency of the centrifugation speed when encapsulating GUVs by the inverted emulsion method. Because of that, another experiment was conducted to examine if the centrifugation speed might also influence the internal adhesion in the biotin streptavidin system. The experiment was executed at a 150 nM streptavidin concentration. The analysed and plotted data shown in Figure 3.7b, shows the quantity of vesosomes at the different centrifugation speeds tested as well as the quantity of vesosomes showing internal membrane - membrane adhesion for comparison. The data shows a dependency of the adhesion to the centrifugation speed unfortunately, proving that at the highest encapsulation rates the quantity of adhesions are rather low with < 30 %. Only at a speed of 220 x g, the number of adhesions rises to ~ 50 %, coming to a peak at 250 x g with slightly > 80 % of the encapsulated GUVs showing adhesion to the outer one. At higher speeds the adhesion levels drop again. One would expect that the binding of biotin and streptavidin does not depend on such a force. However, this experiment shows that this is not the case. Further investigations will be needed to clarify this. Examples for some of the vesosomes showing adhesions are depicted in Figure 3.7d with the adhesion area visible by the enhanced streptavidin signal (green). The microscope images give more evidence on the quality of the adhesions. The most obvious about the adhesion examples is the very small adhesion area in case of 180 - 200 x g. The adhesion is barely even visible in these cases. The microscope images support the data plotted in Figure 3.7b in terms of more vesosomes showing adhesions and also the adhesion being of much better quality.

Since the encapsulation is significantly better at lower centrifugation speeds but the adhesion on the other hand is of low quality and quantity, a combination of centrifugation speeds was tested to achieve high encapsulation rates combined with optimal adhesions. By using two centrifugation cycles, one at 200 x g and a second one at 250 x g, the results were hoped to be improved and more insight on the influence of the centrifugation speed gained. Unfortunately, the results were the same as if only one centrifugation cycle had been applied. The microscope images show the streptavidin signal on the membrane of the outer GUVs suggesting a saturation of all biotin moieties (see Figure

3.8a first image). On the membrane of the inner GUV the concentration of PE biotin is much lower, so the missing streptavidin signal is not uncommon (see Figure 3.3). It is still possible that there is streptavidin on the membrane. In this case, the desired internal membrane - membrane adhesion can not form for, all biotin moieties are considered bound to individual streptavidin molecules. This experiment shows that a second centrifugation cycle increases the binding of streptavidin to the outer GUV membrane which is evidence for the centrifugation force influencing the complex formation of biotin and streptavidin. But it does not benefit the membrane - membrane adhesion. For comparison, an example of inverted emulsion GUVs is shown in Figure 3.8b (no vesosome) which were formed using one centrifugation cycle at 200 x g. The first image shows the streptavidin

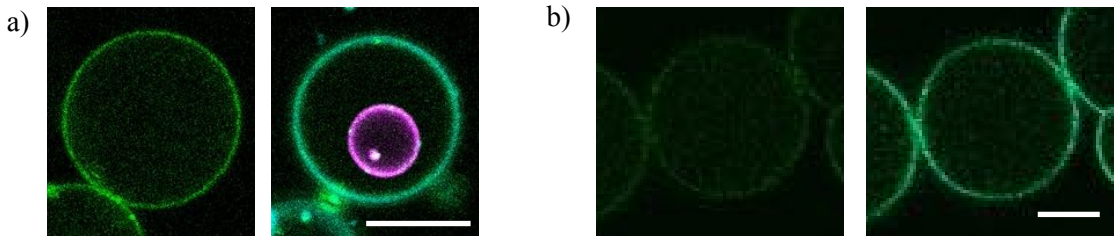

Figure 3.8: a) Fluorescence confocal microscopy images (first streptavidin channel, second merge) of a vesosome system created with two centrifugation cycles, the first at 200 x g, the second directly afterwards at 250 x g. An internal membrane - membrane adhesion is missing. Streptavidin is bound to the outer GUV membrane visible through the fluorescence signal (green). b) Fluorescence confocal microscopy images (first streptavidin channel, second merge) of inverted emulsion GUVs created with one centrifugation cycle of 200 x g. Streptavidin is barely bound to the vesicle membrane. The lipid composition for the inverted emulsion GUVs is 97.9 mol% POPC, 2.0 mol% PE biotin, 0.1 mol% Atto 633 DOPE. The lipid composition for the electroformed GUVs is 99.8 mol% POPC, 0.1 mol% PE biotin, 0.1 mol% $DiIC_{18}$. The final streptavidin concentration is 150 nM. Scale bars: 10 µm

signal which is barely visible suggesting still free biotin moieties on the vesicle membrane.

The final conditions to achieve an internal membrane - membrane adhesion, is a streptavidin concentration of 150 nM while using a centrifugation speed of 250 x g. By that, the encapsulation rate is slightly reduced for the benefit of a much higher quantity and quality of the internal membrane - membrane adhesion. The encapsulated GUVs compose of 0.1 mol% PE biotin and the outer GUVs have an amount of 2.0 mol% PE biotin next to other lipids forming their membranes.

Negative controls were conducted to exclude membrane - membrane adhesion originating from other factors like lipid stickiness. For this, different samples were prepared without biotin (for the inverted emulsion GUVs, electroformed GUVs include 0.1 mol% PE biotin) but including streptavidin (see Figure 3.9a and b) and samples with no biotin nor streptavidin (see Figure 3.9c). In both cases internal adhesion was never observed but external adhesion was in rare cases. In Figure 3.9b one can see the streptavidin intensity is enhanced at the two points where the membranes touch but is excluded from the rest of the adhesion area. A lipid transfer of small amounts of the

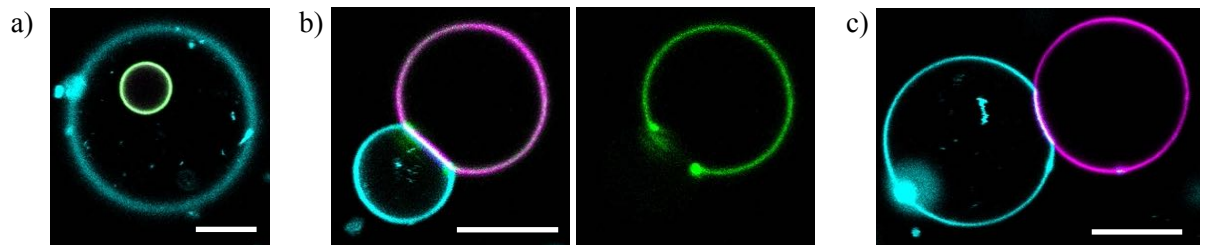

Figure 3.9: a) Fluorescence confocal microscopy image (merge) of a vesosome without internal adhesion (control sample). The lipid composition for the outer GUV is 99.9 mol% POPC and 0.1 mol% Atto 633 DOPE (cyan). The lipid composition for the inner GUV is 99.8 mol% POPC, 0.1 mol% PE biotin and 0.1 mol% $DiIC_{18}$ (magenta). The streptavidin concentration is 150 nM (green). b) Fluorescence confocal microscopy image (first merge, second streptavidin channel) of external membrane - membrane adhesion. Images a and b are from the same sample. c) Fluorescence confocal microscopy image (merge) of external membrane - membrane adhesion (control sample). The lipid composition for the outer GUV is 99.9 mol% POPC and 0.1 mol% Atto 633 DOPE (cyan). The lipid composition for the inner GUV is 99.8 mol% POPC and 0.1 mol% $DiIC_{18}$ (magenta). There is no streptavidin in this sample. All samples were created at a centrifugation speed of 250 x g. Scale bars: 10 µm

biotinylated lipid from the electroformed GUV to the inverted emulsion GUV could be the reason. The external adhesion in Figure 3.9c cannot originate from biotin and streptavidin since both agents are absent in this sample. This is evidence for the possibility of non - specific adhesion events without the adhesion agents (biotin and streptavidin). Despite no internal adhesion found in these samples, it cannot completely be excluded. Because of that, in this study, the streptavidin signal is an important factor to identify membrane - membrane adhesion originating from biotin streptavidin. Since this experiment was just a negative control, there is not enough data to do a full analysis and to conduct statistical calculations on the quantity of adhesion events.

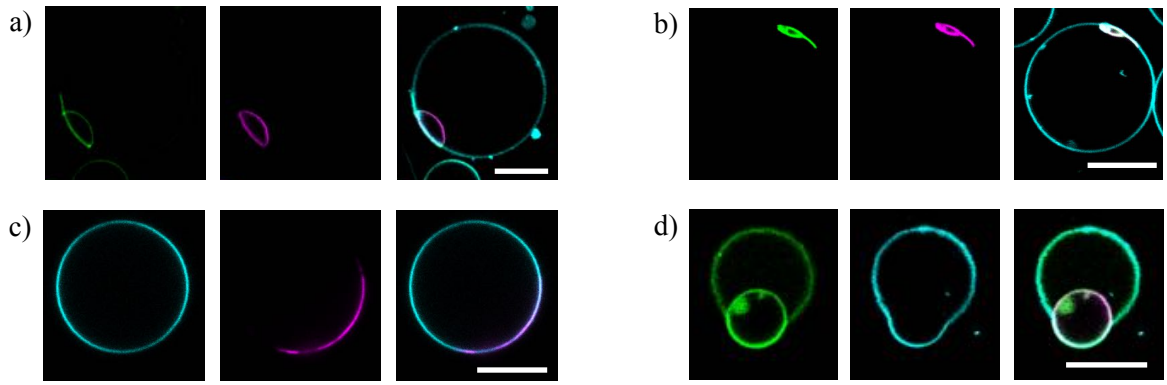

Figure 3.10: Fluorescence confocal microscopy images of vesosome systems with internal membrane - membrane adhesions including membrane deformations of a) the inner GUV (first image streptavidin channel, second image $DiIC_{18}$ channel, third image merge) b) the inner GUV (first image streptavidin channel, second image $DiIC_{18}$ channel, third image merge) c) the inner (first image Atto 633 channel, second image $DiIC_{18}$ channel, third image merge) and d) the outer GUV (first image streptavidin channel, second image Atto 633 channel, third image merge). The green channel shows the streptavidin signal (Alexa 488). The magenta channel shows the inner GUVs ($DiIC_{18}$) and the cyan channel shows the outer GUVs (Atto 633 DOPE). The last rows show the merge images of all channels. All samples were created with a final streptavidin concentration of 150 nM and at a centrifugation speed of 250 x g. The lipid composition for the outer GUVs formed by the inverted emulsion method is 97.9 mol% POPC, 2.0 mol% PE biotin, 0.1 mol% Atto 633 DOPE. The lipid composition for the inner GUVs formed by the electroformation method is 99.8 mol% POPC, 0.1 mol% PE biotin, 0.1 mol% $DiIC_{18}$. Scale bars: 10 µm

The adhesion occurring by the use of this system at these conditions can be strong enough to deform the vesicle membranes of which some examples are shown in Figure 3.10. The deformation morphologies vary significantly. Especially the inner GUVs show different degrees of deformations from disk - like geometries (Figure 3.10a) up to a form that completely loses the GUV structure and rather looks like a lipid film on the membrane of the outer GUV (Figure 3.10c). It is possible in this case that the inner GUV bursted due to the adhesion and remained on the outer GUV membrane forming a double bilayer in this specific area. Deformations of the outer GUVs are usually not as severe compared to the inner ones. The factors are not clear as to when the membrane of the inner GUV gets deformed compared to the membrane of the outer GUV. In rare cases, both membranes show mild deformations. A membrane deformation in general is influenced by an adhesion of a certain extend and area size. There might be an effect from the vesicle sizes pointing to, the bigger the size the less likely for it to deform. Another possibility is the diameter size ratio between inner and outer GUV which could have an effect here. Although, more data will be needed here. There is more investigation needed in the future. These assumptions only apply for internal membrane - membrane adhesions. It was mentioned before that the encapsulation of streptavidin is very efficient and unless some vesicles burst, the concentration of it in the external solution is supposed to be close to zero. Of course GUV bursting cannot completely be excluded or prevented and therefore the mixing of streptavidin with the external solution is probable. External membrane - membrane adhesion is therefore also possible as well as membrane deformations. In this case, the GUV sizes

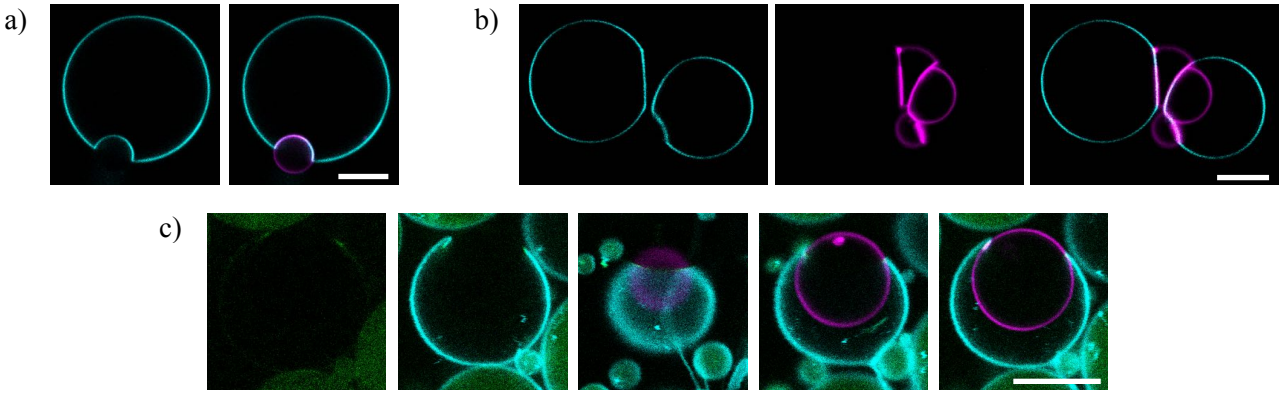

Figure 3.11: Fluorescence confocal microscopy images of GUVs showing external membrane - membrane adhesion between electroformed and inverted emulsion GUVs including a membrane deformation of a) the outer GUV (first image Atto 633 channel, second image merge) and b) both GUV types (first image Atto 633 channel, second image $DiIC_{18}$ channel, third image merge). Electroformed GUVs were created from 99.8 mol% POPC, 0.1 mol% PE biotin, 0.1 mol% $DiIC_{18}$ (magenta). Inverted emulsion GUVs were created from 97.9 mol% POPC, 2.0 mol% PE biotin, 0.1 mol% Atto 633 DOPE (cyan). The final streptavidin concentration (unlabelled) is 150 nM. c) Fluorescence confocal microscopy images (first image streptavidin channel, second image merge of streptavidin and Atto 633 channel, last three images merge) of a vesosome system showing membrane - membrane adhesion and the penetration of the the inner GUV through the membrane of the outer one. GUV types were created from the same lipid composition as were the ones used for a and b. The final streptavidin concentration (labelled with Alexa 488) is 150 nM. Scale bars: 10 µm.

seem to have no influence on whether a deformation takes place or not (see Figure 3.11a and b) but similar to the internal adhesion, it seems like the electroformed GUVs show stronger deformations compared to the inverted emulsion vesicles. This could also be an effect from differences in membrane tension or membrane rigidity between both GUV types. Because one has to assume that in the case of the inverted emulsion GUVs, there are traces of mineral oil left within the lipid bilayer, this can change membrane properties like the membrane tension and the membrane rigidity influencing the GUV behaviour. A very rare form of deformation is not actually a deformation but a penetration (see Figure 3.11c). There is only a minor enhancement of the streptavidin signal on both ends of the outer GUV where the inner one penetrates it without leaving it completely. The resulting outer GUV appears as if it has a hole within its membrane but the integrity of the system does not seem to be compromised by that.

One factor which has a definite effect on the membrane tension is a difference in osmolarity between the internal and the external sugar solutions of the GUVs. Different sugars were used for the internal and external aqueous solutions in order to form the GUVs by centrifugation and to take advantage of the density difference to make the imaging process easier. Using a density difference like that reduces GUV movement within the aqueous solutions and helps when imaging the samples. There is the issue of osmolarity balance which has a strong influence on the membrane tension. Two processes can be directed by osmolarity changes of the external sugar solution, inflation and deflation. Inflation is the addition of water externally which decreases the sugar concentration and results in a compensation of it within the internal solution leading to water entering the GUV lumen and an increase in membrane tension. A membrane area increase of 5 - 10 % will lead to vesicle bursting. A concentration difference high enough in this case will lead to membrane rupture. The corresponding deflation occurs when the sugar concentration of the external solution gets increased. In order to compensate for this, water gets released from the vesicle lumen reducing tension of the membrane. In this case, the membrane becomes more floppy and the GUVs often appear less spherical.

In an experimental approach, this alteration can be used to manipulate the membrane - membrane adhesion occurring from biotin streptavidin because of the direct influence on the membrane of the outer vesicle. Membrane deformations can be very severe with the inner GUV protruding out so drastically and almost budding off of the outer GUV (see Figure 3.12a). The adhesion area in these cases is significantly larger compared to adhesions without or with only a minor membrane deformation. It was tested, if the deflation of the system increases the deformation of the membrane at the adhesion area and therefore, leads to an enlargement of the same. Figure 3.12b shows a

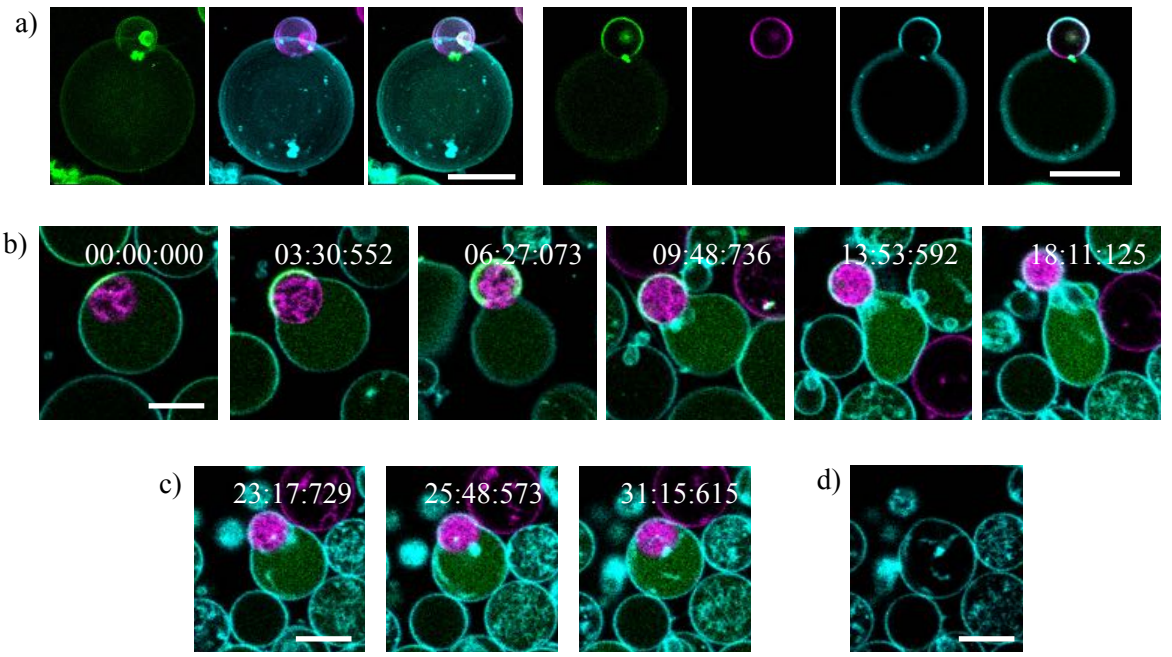

Figure 3.12: a) Fluorescence confocal microscopy z - stack projections (first image streptavidin channel, second image merge of Atto 633 and $DiIC_{18}$ channel, third image merge) and images (first image streptavidin channel, second image $DiIC_{18}$ channel, third image Atto 633 channel, fourth image merge) of a vesosome system with internal membrane - membrane adhesion with a severe membrane deformation of the outer GUV. b) Fluorescence confocal microscopy time series (merge) of the deflation process of a GUV with internal membrane - membrane adhesion with a moderate membrane deformation of the inner GUV in the beginning. External sugar solution made of a 900 mM glucose/PBS solution (1:4 v/v). Internal sugar solution made of a 900 mM sucrose solution. Increasing glucose/PBS concentrations from ~ 900 mM (osmotically balanced level) to ~ 2000 mM were added over time. Membrane deformation switches to the outer GUV and increases over time at increasing sugar concentrations. c) Fluorescence confocal microscopy time series (merge) of the inflation process of the same GUV shown in b at decreasing sugar concentrations through careful step by step water addition. Visible reversing membrane deformation at decreasing sugar concentrations. d) Fluorescence confocal microscopy image of the Atto 633 DOPE channel of the last time laps image of the inflation process. Time is given in minutes. Scale bars: 10 µm

vesosome with an internal adhesion and a slight deformation of the inner GUV membrane. At this point, the osmolarity is completely balanced (external glucose solution at 900 mM, internal sucrose solution at 900 mM). Through the addition of a glucose solution of a higher concentration over time and the stepwise increase of the glucose concentration of the external solution, the outer vesicle membrane becomes more floppy because of the reduced membrane tension which results in the desired effect. The deformation changes immediately from the inner to the outer GUV and leads over time to an enlargement of the adhesion area. Although the deformation comes close to budding, a small membrane neck remains. The membrane loses all tension and visible excess membrane area of the outer GUV forms around the neck. The excess membrane area is also evidence for the shrinkage of the outer vesicle's volume and size. The second part of the experiment is shown in Figure 3.12c, where it is demonstrated how inflation reverses the membrane deformation very fast which was caused by the initial deflation process. Due to the stepwise addition of water and the re - established membrane tension, the effect is almost completely

reversed leaving only small rests of the excess area. In Figure 3.12d which shows the Atto 633 DOPE channel displaying the outer GUV's membrane, the still remaining excess membrane area is visible especially, a part of the bilayer which is wrapping almost all the way around the encapsulated and adhered GUV. This is a clear indicator for the shrinkage of the outer GUV over the whole process and an artefact of the immense membrane deformation triggered through the deflation process. Further inflation at this point only led to vesicle rupture. See Chapter 7.2 for further experimental details.

In general, the internal membrane - membrane adhesion can be achieved easily (good reproducibility) at the right conditions. Even a minor tuning of the adhesion is possible considering the quality and quantity (see criteria mentioned above) of the adhesion although, in order to accomplish a strong adhesion, in most of the created vesosomes from the inverted emulsion method, the optimal conditions are necessary which were mentioned above.

3.4. Directed Membrane - Membrane Adhesion

Using a liquid - liquid membrane phase separation to acquire a direction of the internal adhesion takes advantage of the exclusion of certain lipids from one of two membrane phases. The different phases have specific properties defining them like, the partitioning of the lipids into them which allows it to use this feature for the needed direction of the adhesion (see Chapter 1.2.1.).

The goal here is to have the biotinylated lipid partition into one particular phase of the membrane to direct the internal biotin streptavidin adhesion to that specific membrane phase. The lipid PE which was chosen in this study in its biotinylated form, when used for the formation of membrane phase

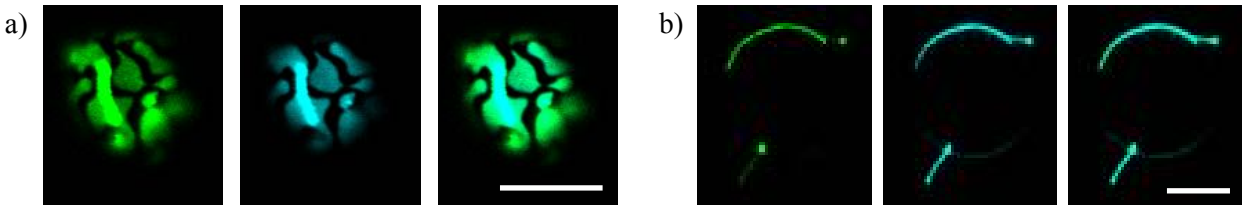

Figure 3.13: a) Fluorescent confocal microscopy images (first image streptavidin channel, second image Atto 633 channel, third image merge) of liquid disordered - solid ordered membrane phase separated GUVs created from the inverted emulsion method. The first image shows streptavidin labelled with Alexa 488 (green) binding to the liquid disordered phase. The second image shows the membrane dye Atto 633 DOPE (cyan) within the liquid disordered phase. The third one is the merged image. The used lipid composition is 20 mol% DOPC, 37.9 mol% SM, 40 mol% cholesterol, 2 mol% PE biotin and 0.1 mol% Atto 633 DOPE. b) Fluorescent confocal microscopy image (first image streptavidin channel, second image Atto 633 channel, third image merge) of liquid disordered - liquid ordered membrane phase separated GUVs created from the electroformation method. The first image shows the streptavidin labelled with Alexa 488 (green) binding to the liquid disordered phase. The second image shows the membrane dye Atto 633 DOPE (cyan) within the liquid disordered phase. The third one is the merged image. The used lipid composition is 20 mol% DOPC, 30 mol% DPPC, 47.9 mol% cholesterol, 2.0 mol% PE biotin and 0.1 mol% Atto 633 DOPE. Scale bars: 10 µm

separated GUVs, partitions into the liquid disordered phase. It was discussed before that the creation of membrane phase separated GUVs from a quaternary lipid composition using the inverted emulsion method is not as easy compared to the use of a ternary lipid mixture or the use of the electroformation method (see Chapter 2.2.). After the formation of membrane phase separated GUVs (see Chapter 7.2 for further experimental details), they were imaged via confocal microscopy to see which phase the PE biotin partitions in, via the addition of labelled streptavidin. Two lipid compositions are shown in Figure 3.13, one showing a liquid disordered - solid ordered membrane phase separation (Figure 3.13a) and one with a liquid disordered - liquid ordered membrane phase separation (Figure 3.13b). There were more lipid compositions tested (data not shown) especially, with the inverted emulsion method in order to get optimal phase separations considering the extent of the phase areas. Ideal membrane phase separation would be to have Janus - like particles with 50 % liquid ordered and 50 % liquid disordered phases. In both cases, the streptavidin signal is visible in the same phase as the membrane dye. Atto 633 DOPE partitions into the liquid disordered phase as does $DiIC_{18}$ which can be seen later in this chapter. This preliminary test showed the biotinylated lipid PE biotin will be excluded from both liquid ordered and solid ordered phases (although a solid ordered - liquid disordered phase separation is not the desired form of membrane phase separation in this study because of the sizes of the solid phases). Both the solid ordered as well as the liquid ordered phase remain unlabelled in these GUVs and therefore cannot be visualised by fluorescence microscopy. In conclusion, the biotinylated lipid partitions into the liquid disordered phase to which then streptavidin binds to. Therefore, a membrane - membrane adhesion from biotin and streptavidin should occur at the liquid disordered phase. One additional note here, it seems by the use of this method, lipid compositions using SM are more likely to form solid ordered phases while

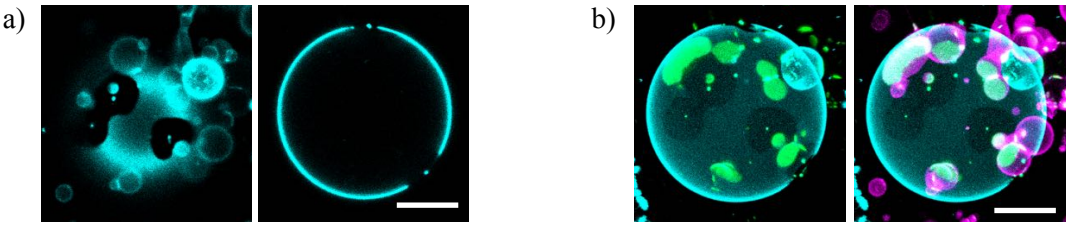

Figure 3.14: a) Fluorescence confocal microscopy images from the Atto 633 channel of a GUV with a liquid disordered - liquid ordered membrane phase separation. The membrane dye Atto 633 DOPE only partitions into the liquid disordered phase. The liquid ordered phase is not labelled and therefore not visible by fluorescence microscopy. b) Fluorescence confocal microscopy z - stack projections (first image merge of streptavidin and Atto 633 channel, second image merge) of the same GUV showing external membrane - membrane adhesion. Inverted emulsion GUV visible in cyan, electroformed GUVs in magenta and streptavidin in green. The lipid composition for the inverted emulsion vesicles is 20 mol% DOPC, 40 mol% DPPC, 37.9 mol% cholesterol, 2 mol% PE biotin and 0.1 mol% Atto 633 DOPE. The electroformed GUVs were prepared from 99.8 mol% POPC, 0.1 mol% PE biotin and 0.1 mol% $DiIC_{18}$. The final streptavidin concentration (labelled with Alexa 488) is 150 nM. Scale bars: 10 µm

compositions including DPPC form liquid ordered phases even at equal percentages. This would implicate that in case of the use of SM, higher amounts of cholesterol are needed to create a liquid - liquid phase separation compared to the use of DPPC when using the inverted emulsion method.

The directed adhesion was initially tested as external directed adhesion (see Figure 3.14). In the experiment, both GUV types (inverted emulsion GUVs and electroformed GUVs) were mixed with a final streptavidin concentration of 150 nM. The GUVs from the inverted emulsion method were prepared to include a liquid - liquid membrane phase separation since this is the desired membrane phase separation to achieve a directed adhesion (reasons for this explained in Chapter 2.2). In Figure 3.14a the unlabelled liquid ordered phases can be seen (appear as holes in the membrane due to a lack of fluorescence). There should be no membrane adhesion to these areas due to a lack of biotinylated lipid. The general conditions for both GUV types and the concentration of streptavidin are the same as for the experiments from the internal adhesion experiments before. A z - stack projection (see Figure 3.14b), including the streptavidin channel and the channel of the inverted emulsion GUVs, shows the places of the adhesions through the enhanced streptavidin signals and the slightly darker areas show the liquid ordered phases on the GUV membrane. A second projection with all three channels shows the smaller adhering vesicles only at the liquid disordered phases. This experiment of external membrane - membrane adhesion was conducted as preliminary test for the adhesion, occurring to the liquid disordered phase of the GUV membrane. It also gives a clear evidence of the absence of adhesions to the liquid ordered phases. The membrane phase separation results in smaller liquid ordered phases even though, the lipid ratio between low melting temperature lipid (DOPC) and high melting temperature lipid (DPPC or SM) points to larger ordered phases which are composed of the high melting temperature lipid and cholesterol. Because of that, the external adhesion has a higher chance for adhesion (compared to the final internal setup) due to the higher number of GUVs available for it, and was supposed to deliver reliable evidence for the exclusion of adhesions to the liquid ordered phases. A second example visible in Figure 3.15a, shows the z - stack projection of the adhesion of electroformed GUVs to an inverted emulsion GUV where in the lower left corner it seems as if the adhesion appears within an area (see white arrow in Figure 3.15a) of an ordered phase rather than a disordered phase of the membrane. Taking a closer look at this area (see Figure 3.15a second row) reveals, at the point of adhesion, there is a small region of the membrane existing in the disordered phase within a bigger ordered phase area. Also, when looking at another section of the projection (see white arrow in Figure 3.15b), the adhesion of the electroformed GUVs on the bottom of the inverted emulsion GUV seems to stretch across the boundary of the liquid disordered phase into the area of the liquid

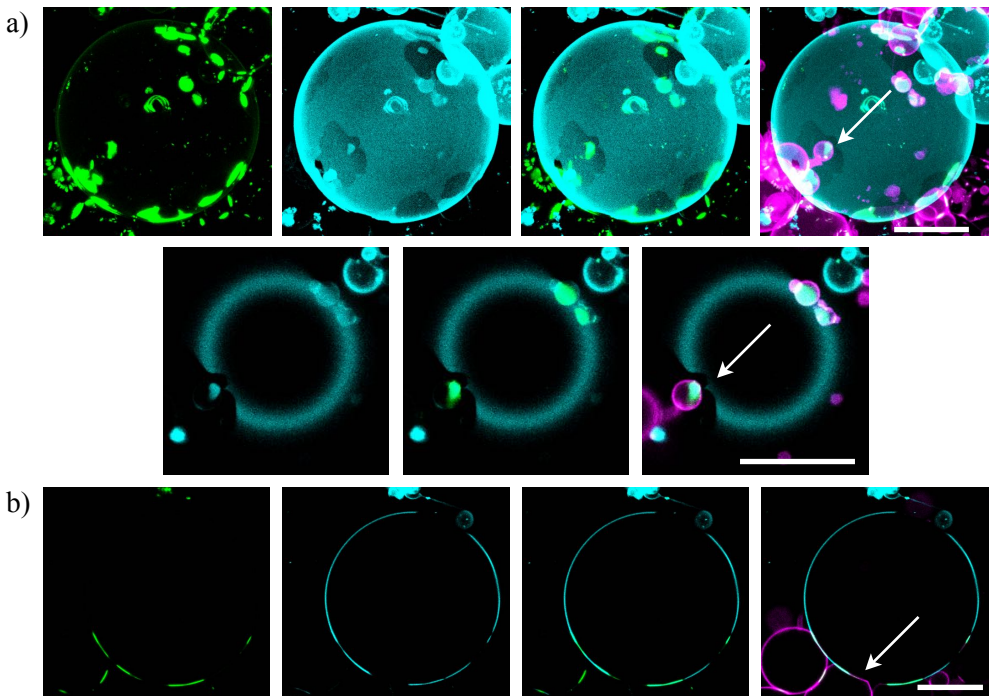

Figure 3.15: a) Fluorescence confocal microscopy z - stack projections (first image streptavidin channel, second image Atto 633 channel, third image merge of streptavidin and Atto 633 channel, fourth image merge) and images (first image Atto 633 channel, second image merge of streptavidin and Atto 633 channel, third image merge) of external membrane - membrane adhesions. The inverted emulsion GUVs (cyan) formed with a liquid - liquid membrane phase separation. The liquid ordered phase is unlabelled. The electroformed GUVs (magenta) are adhered to the liquid disordered phase of the inverted emulsion GUV. The streptavidin signal (green) is enhanced within the biotin streptavidin binding areas. The inverted emulsion GUVs were created from 20 mol% DOPC, 30 mol% DPPC, 47.9 mol% cholesterol, 2.0 mol% PE biotin and 0.1 mol% Atto 633 DOPE. The electroformed GUVs were created from 99.8 mol% POPC, 0.1 mol% PE biotin and 0.1 mol% $DiIC_{18}$. The final streptavidin concentration is 150 nM labelled with Alexa 488. b) Fluorescence confocal microscopy images (first image streptavidin channel, second image Atto 633 channel, third image merge of streptavidin and Atto 633 channel, fourth image merge) of external membrane - membrane adhesions. The inverted emulsion GUVs (cyan) formed with a liquid - liquid membrane phase separation. The electroformed GUVs (magenta) are adhered to the liquid disordered phase of the inverted emulsion GUV. The liquid ordered phase is unlabelled. The streptavidin signal (green) is enhanced within the biotin streptavidin binding areas. The inverted emulsion GUVs were created from 20 mol% DOPC, 30 mol% DPPC, 47.9 mol% cholesterol, 2.0 mol% PE biotin and 0.1 mol% Atto 633 DOPE. The electroformed GUVs were created from 99.8 mol% POPC, 0.1 mol% PE biotin and 0.1 mol% $DiIC_{18}$. The final streptavidin concentration is 150 nM labelled with Alexa 488. Scale bars: 10 µm

ordered phase. When taking a closer look at the first and third image of Figure 3.15b only showing the channels of the inverted emulsion GUVs and the streptavidin, one can see the streptavidin signal fading towards the liquid ordered phase. It is therefore possible that the adhesion, additionally visible through the deformation of the electroformed GUV, stretches across the boundary of the liquid disordered phase because of the lack of space due to crowding of several GUVs binding in close proximity to the membrane phase separated vesicle. The adhesion at this point, can include biotin streptavidin binding but the concentration of both is particularly low and the streptavidin signal is too low to be detected. It is also possible that there is no biotin streptavidin binding on the liquid ordered phase but only the visible deformation of the electroformed GUV originating from the biotin streptavidin binding within the liquid disordered part of it.

In general, these experiments clarify the partitioning of PE biotin into the liquid disordered phase and an established membrane - membrane adhesion due to biotin streptavidin also to the liquid disordered phase of a liquid - liquid membrane phase separated vesicle. According to Figure 3.13, the same applies for liquid - solid membrane phase separated GUVs which will come up later again. In the case of an internalised membrane - membrane adhesion within a vesosome system, there are additional factors affecting the adhesion now, in particular the quantity of adhesions. The change of the oil phase from pure mineral oil to two oils including mineral oil and a mixture of n - decane and silicone oil can have an effect on the formed GUVs as well as the encapsulation and the adhesion. There is evidence of silicone oil leading to the aggregation of proteins [208,209,210,211] which would directly affect streptavidin and its binding affinity to the biotin moieties of the GUV membranes. The possible area available for an adhesion is also reduced due to the membrane phase separation which can lower the quantity of adhesions. There might be a connection here to factors which were discussed in advance like the centrifugation speed (force seems to be needed to establish biotin streptavidin complex formation) and the streptavidin concentration.

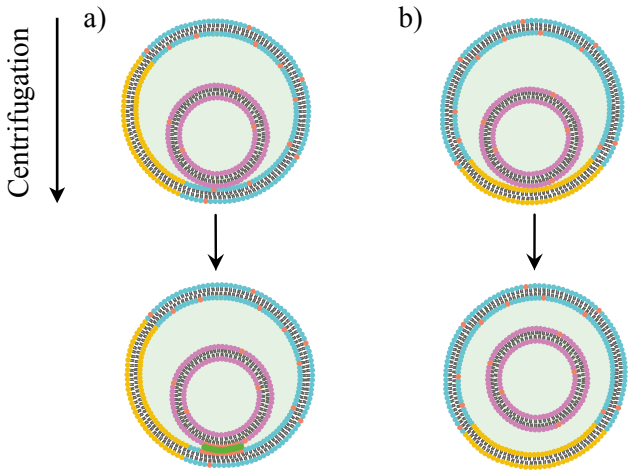

Figure 3.16: Schematic of a theoretical membrane phase separated vesosome system with a) an internal membrane - membrane adhesion being initialised through contact of the inner GUV and the liquid disordered phase of the outer GUV and b) no internal adhesion forming after a contact between the inner GUV and the liquid ordered phase of the outer GUV.

For example, if in theory the adhesion might be established in the moment both membranes touch each other when the vesosome finally gets created through the centrifugation process in the end (see Figure 3.16a) and a few initial biotin and streptavidin moieties bind, providing for the adhesion, this would mean adhesion can only occur when a biotin streptavidin bridge can be built in this initial moment. If there is no second biotin moiety because the two membranes touching at an area where one exists in the liquid ordered state, no adhesion will form (see Figure 3.16b) since there is no additional force applied (like from centrifugation). This would mean, the biotin streptavidin complex needs this initialising contact to form and afterwards the chance of binding and adhesion formation is significantly lowered. But this is just an assumption and will need more investigation in the future.

Looking at the adhesion events in case of the internalised directed adhesion, supports the former results gained from the external directed adhesion experiments. Experiments were conducted on the combinations of the inverted emulsion GUVs being membrane phase separated with the electroformed GUVs formed with only one phase and vice versa. In both cases, the quantity of adhesion events was significantly lower to less than 1.0 % compared to the undirected internal adhesion experiments. In the case of the membrane phase separated inverted emulsion GUVs, it was very complicated to find a proper sample with the adhesion being visible and both vesicles being of appropriate size and shape. Although, the amount of vesosomes did not seem to change, the experiment was repeated several times and often without any internal adhesion events. In Figure 3.17a, one can see a directed internal adhesion of an inner GUV to the liquid disordered phase close to the edge of the liquid ordered phase of the outer GUV. Unfortunately, the inner GUV is rather small and could not be clearly seen by microscopy analysis. A schematic is also shown for a better visualisation and understanding of the microscope images and the directed internal adhesion of the

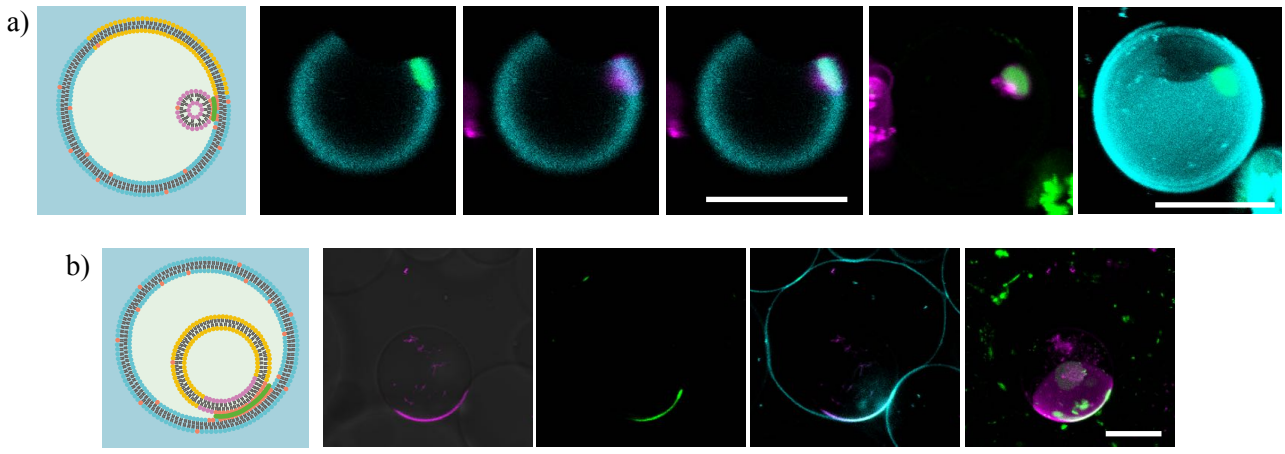

Figure 3.17: a) Schematic of the following fluorescence confocal microscopy images (first image merge of streptavidin and Atto 633 channel, second image merge of Atto 633 and $DiIC_{18}$ channel, third image merge) and z - stack projection (fourth image merge of streptavidin and $DiIC_{18}$ channel, fifth image merge) of a vesosome system. The outer GUV (cyan) formed from the inverted emulsion method with a liquid - liquid membrane phase separation. The liquid ordered phase is shown in yellow in the schematic and unlabelled in the microscopy images. The inner GUV (magenta) formed from the electroformation method is adhered to the liquid disordered phase of the outer GUV. The streptavidin signal (green) is enhanced within the biotin streptavidin binding area. Outer GUVs were created from 20 mol% DOPC, 40 mol% DPPC, 37.9 mol% cholesterol, 2.0 mol% PE biotin and 0.1 mol% Atto 633 DOPE. Inner GUVs were created from 99.8 mol% POPC, 0.1 mol% PE biotin and 0.1 mol% $DiIC_{18}$. The final streptavidin concentration is 150 nM labelled with Alexa 488. b) Schematic of the following fluorescence confocal microscopy images (first image merge of brightfield and $DiIC_{18}$ channel, second image streptavidin channel, third image merge) and z - stack projection (fourth image merge of streptavidin and $DiIC_{18}$ channel) of a vesosome system. The outer GUVs (cyan) were formed from the inverted emulsion method. The inner GUVs (magenta) were formed from the electroformation method with a liquid - liquid membrane phase separation. The liquid ordered phase is shown in yellow in the schematic and unlabelled in the microscope images. The inner GUV is adhered to the outer GUV via its liquid disordered phase. The streptavidin signal (green) is enhanced within the biotin streptavidin binding area. The outer GUVs were created from 97.9 mol% POPC, 2.0 mol% PE biotin and 0.1 mol% Atto 633 DOPE. The inner GUVs were created from 30 mol% DOPC, 44.4 mol% SM, 25 mol% cholesterol, 0.5 mol% PE biotin and 0.1 mol% $DiIC_{18}$. The final streptavidin concentration is 150 nM labelled with Alexa 488. Scale bars: 10 µm

real example. The yellow phase depicts the liquid ordered phase and the liquid disordered phase is visible in cyan. The inner GUV which only exists in one phase, is shown in magenta. The adhesion area with the enhanced streptavidin signal can be seen in green.

The second example, shown in Figure 3.17b, is the vice versa case with the inner GUV being membrane phase separated. Because the inner GUVs are created from the electroformation method but the lipid composition (except for the membrane dye) is the same as the one used for the outer GUVs in the former example (except for the amount of PE biotin), the area of the ordered phase is larger compared to the liquid disordered phase. Both methods probably give different results considering the area sizes of the two phases because the final cholesterol concentration within the GUV membranes is still very low in case of the inverted emulsion method. Even with the use of two different oil phases, cholesterol might be lost in the oil phases. The directed adhesion in this example is clearly restricted to the liquid disordered phase of the inner GUV. Both vesicles have good sizes (both GUVs can be resolved properly in confocal microscopy and their shape is clearly visible), only the shape of the outer GUV is not as spherical which could be caused by other GUVs in the direct periphery to it. Because the adhesion in this case is close to the equatorial region of both GUVs, the focus plain for both GUVs and the membrane phase separation of the inner GUV is similar which made imaging via confocal microscopy much more efficient compared to the first example were the adhesion is in the top region of the outer GUV. Both GUVs and the membrane phase separation can be seen very clearly as can be the adhesion area on the liquid disordered phase of the inner GUV, despite being very close to the liquid ordered phase. There is a clear distinction of the adhesion area being restricted to the liquid disordered phase.

More examples are given in Figure 3.18 for adhesion and non - adhesion. Figure 3.18a includes a membrane - membrane adhesion and a liquid - liquid membrane phase separation of the outer GUV but, the liquid ordered phases are rather small which is often the case for these samples. A direction of the adhesion could be argued about in this example because of the large area of the liquid disordered phase. The ordered phases are so small that the likelihood of an adhesion to these areas would be very low even if they included biotin. The second example (see Figure 3.18b) shows a non - adhering event with a liquid disordered - solid ordered membrane phase separation of the outer GUV. Solid ordered phases spread more across the membrane in flower like patches and a directed adhesion to one of the phases is more difficult to establish. For these samples, no internal adhesion was found. The last sample (Figure 3.18c) with a membrane phase separation of the inner GUV also shows no adhesion. And similar to the former example, the liquid ordered phase is turned to the membrane of the outer GUV and a biotin streptavidin bridge could not be established

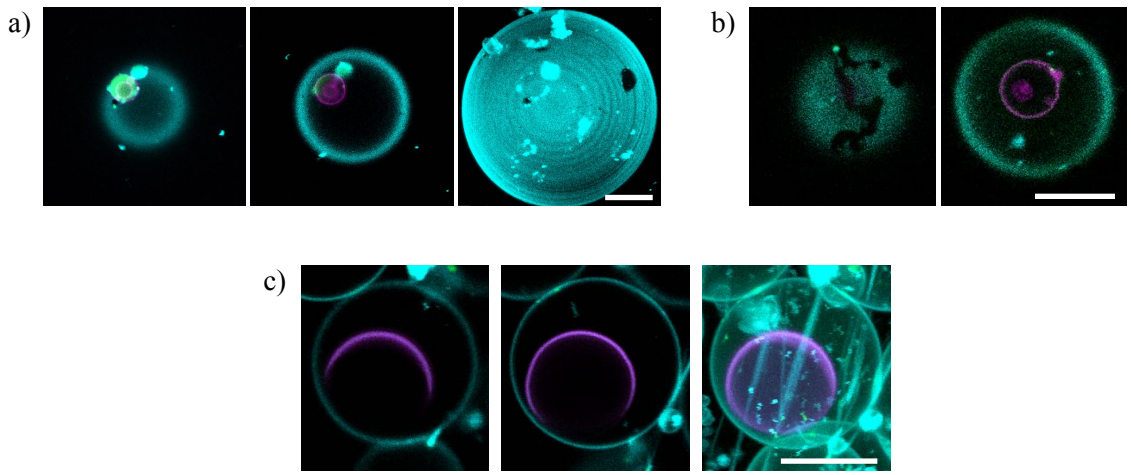

Figure 3.18: a) Fluorescence confocal microscopy images (first image merge of streptavidin and Atto 633 channel, second image merge) and z - stack projection (Atto 633 channel) of a vesosome system. The outer GUVs (cyan) were formed from the inverted emulsion method with a liquid - liquid membrane phase separation. The liquid ordered phase is unlabelled. The inner GUV (magenta) was formed from the electroformation method is adhered to the liquid disordered phase of the outer GUV. The streptavidin signal (green) is enhanced within the adhesion area. Outer GUVs were created from 20 mol% DOPC, 30 mol% DPPC, 47.9 mol% cholesterol, 2.0 mol% PE biotin and 0.1 mol% Atto 633 DOPE. Inner GUVs were created from 99.8 mol% POPC, 0.1 mol% PE biotin and 0.1 mol% $DiIC_{18}$. The final streptavidin concentration is 150 nM labelled with Alexa 488. b) Fluorescence confocal microscopy images (first image Atto 633 channel, second image merge) of a vesosome system. The outer GUV (cyan) were formed from the inverted emulsion method with a liquid - solid membrane phase separation. The solid ordered phase is unlabelled. The inner GUV (magenta) was formed from the electroformation method is not adhered to the outer GUV. The outer GUVs were created from 20 mol% DOPC, 37.9 mol% SM, 40 mol% cholesterol, 2.0 mol% PE biotin and 0.1 mol% Atto 633 DOPE. The inner GUVs were created from 99.8 mol% POPC, 0.1 mol% PE biotin and 0.1 mol% $DiIC_{18}$. The final streptavidin concentration is 150 nM labelled with Alexa 488. c) Fluorescence confocal microscopy images (first and second image merge of Atto 633 and $DiIC_{18}$ channel) and z - stack projection (merge) of a vesosome system. The outer GUV (cyan) was formed from the inverted emulsion method. The inner GUV (magenta) was formed from the electroformation method with a liquid - liquid membrane phase separation. The liquid ordered phase is unlabelled. The inner GUV is not adhered to the outer GUV. The outer GUVs were created from 97.9 mol% POPC, 2.0 mol% PE biotin and 0.1 mol% Atto 633 DOPE. The inner GUVs were created from 30 mol% DOPC, 44.4 mol% SM, 25 mol% cholesterol, 0.5 mol% PE biotin and 0.1 mol% $DiIC_{18}$. The final streptavidin concentration is 150 nM labelled with Alexa 488. Scale bars: 10 µm

probably because of a lack of biotin within the ordered phase. These two cases point towards the theory discussed before and pictured in Figure 3.16. But one has to consider that the vesicles move around and are not stationary which means both GUV types have changed their positions compared to the moment of encapsulation and formation of the outer GUV. In order to clarify this, more investigation is needed in the future.

In summary, a directed internalised adhesion is possible in a vesosome system created from electroformed vesicles encapsulated within inverted emulsion GUVs. Using biotin and streptavidin to establish the membrane - membrane adhesion, the biotin attached to a lipid can easily be incorporated into the vesicle membrane of both GUV types. The employment of the liquid - liquid membrane phase separation gives the opportunity to direct the incorporation of the biotinylated lipid into one particular phase while being excluded from the other. This allows a direction of the

internal adhesion of both membranes. Compared to the undirected adhesion, the quantity is significantly lowered. The reasons for that are unknown and it can only be speculated about possible causes. One possible cause which was discussed above is the moment for the complex formation of biotin and streptavidin (see Figure 3.16). Having membrane phase separated GUVs reduces the chance for the complex formation of the particular GUV. This would only apply if a force is needed to establish biotin streptavidin binding which seems to be the case in this study even for the non - directed adhesion. Another factor could be the second oil phase composed of n - decane and silicone oil which could influence the streptavidin and lead to possible aggregation[208,209,210,211].

3.5. Conclusion

The use of biotin and streptavidin to create a membrane - membrane adhesion in a vesosome system gives good results considering quantity (with > 80 % of vesosomes show adhesion) and quality (extent of the adhesion area and contact angle) of the adhesion. The biotinylated lipid can easily be incorporated into the vesicle membranes, independently of the used method for vesicle formation and streptavidin can be encapsulated alongside the electroformed GUVs. Different experiments were conducted to establish the ideal conditions for both the internalised adhesion as well as the directed internalised adhesion. The lipid composition for the electroformed GUVs include 0.1 - 0.5 mol% PE biotin and the inverted emulsion GUVs include 2.0 mol% PE biotin. The optimal streptavidin concentration for the adhesion is 150 nM. One factor which interferes with the size of the formed inverted emulsion GUVs as well as the encapsulation and internal adhesion of GUVs is the centrifugation speed. Why the centrifugation speed affects the adhesion is not clear. Streptavidin and biotin are used in numerous studies especially because the binding is easily established and one of the strongest known in nature. In this study, it was observed that the centrifugation affects the binding of these two partners influencing the membrane - membrane adhesion. Why that is can only be speculated about. The question is, what factors promote biotin binding to streptavidin in this setup and are there even specific factors? There is enough streptavidin within a sample to saturate all biotin moieties of both vesicle types without the formation of a membrane - membrane adhesion. What was noticeable in the external adhesion experiments in microfluidic chips was, even though the vesicles were premixed with streptavidin including several minutes of incubation time, the adhesion formed only when the vesicles were finally inside the microfluidic traps. Since the vesicles are flushed into the traps via a syringe pump, there is a force applied through the flow rate which might affect the GUV's adhesion (i.e. prolonged contact). In the case of external adhesion,

this could simply be tested by another experiment including several samples with GUVs from identical lipid compositions and flushing them into microfluidic chips (one chip per sample) at different flow rates. The experiments of this study were executed at a flow rate of 2 µl/min. The flow rate can be lowered as far as 0.02 µl/min to reduce the force within the chip as far as possible. At 0.02 µl/min, it will take significantly longer to transport the GUVs from the inlet into the traps. It is possible that this effect of needed force could only apply to the particular biotinylated lipid used here. In this study streptavidin does not bind to free biotin but to biotin attached via a short spacer to the head group of a lipid which is included in a vesicle membrane. The vesicle membrane itself could represent a certain steric hindrance. This could explain why the adhesion seems to need some sort of force (like applied by the centrifugation or a constant fluid flow maybe) to form in this study. The schematic of Figure 3.1 shows the binding of biotin to streptavidin, leading to the desired membrane adhesion. This is of course just a very simplified presentation. In reality, there are several hydrogen bonds as well as van - der - Waals interactions between a biotin molecule and one of the monomers of the tetrameric protein which results in a complex structure in which biotin is getting deeply buried within the protein interior (see Figure 3.19).[161,212,213] With the biotinylated lipid used in this study, the distance between vesicle membrane and biotin moiety is so small that a binding to streptavidin could be aggravated. There are different biotinylated lipids commercially available including different spacers connecting biotin to (in this case) the head group of the lipid. Depending on the length of the spacer, the biotin moieties stick out more or less from the membrane's surface of a vesicle. This probably changes the ability of streptavidin and biotin to establish full binding. PEG (in different lengths) which is often used as a spacer, extends the distance between lipid head group and biotin moiety significantly which can make it easier for the protein to form a complex with it. In a similar experiment as described before, this can be tested through external membrane - membrane adhesion with GUVs including distinct biotinylated lipids for every sample. Naturally, experiments should also be conducted to compare the different changes in case of the internalised membrane - membrane adhesion.

Figure 3.19: Schematic of the β sheet folding pan of a streptavidin dimer with one biotin molecule (red) bound to one monomer. Adapted from [161].

One small experiment which was supposed to overcome the discrepancy of the number of vesosomes and internal adhesions influenced by the centrifugation speed was, to use two

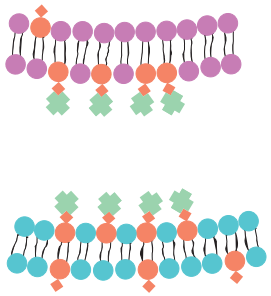

Figure 3.20: Schematic of a section of both GUV membranes (inner GUV magenta and outer GUV cyan) with all biotin moieties saturated with streptavidin. A membrane - membrane adhesion is not possible this way.

centrifugation cycles at different speeds (first cycle 200 x g, second cycle 250 x g) to benefit from both cycles. Unfortunately, this experiment did not show any improvement concerning the adhesion. Although, this experiment shows a clear improvement of streptavidin binding to the membrane of the outer GUV, there was no effect on the adhesion of the inner to the outer vesicle. The direct comparison of GUV formation with one and two centrifugation cycles, including streptavidin encapsulation, seems to imply a dependency of the biotin streptavidin complex formation from the centrifugation speed like, it was discussed in the former section. But it remains unknown why there is no improvement of the adhesion rates. It seems like all biotin moieties on the outer vesicle membranes are saturated with streptavidin which could be indicated by the fluorescence signal. It is possible that also the inner GUV's biotin moieties are completely saturated with streptavidin without visible fluorescence signal. In this case, the formation of a biotin streptavidin bridge creating the adhesion is not possible (see Figure 3.20).

Hansen et.al. published a study in 1997 about the interference of biotin streptavidin binding by the presence of sugars[214]. And a study from our own group (Moga et.al.[143]) investigated different sugar concentrations influencing the vesicle formation when using the inverted emulsion method. This study covers many parameters next to the sugar concentration like pH, lipid concentrations and others. For the sugar concentration, the optimum for the inverted emulsion method lies between 600 - 900 mM. Because of that, there were no further experiments conducted on other sugar concentrations influencing the biotin streptavidin complex formation. There is the possibility to use microfluidic systems to create the vesosomes and test the influence of sugars, since these methods also work without sugars[60,62,183].

Further optimisations here could finally also improve the encapsulation rates by simultaneously increasing the number of internal adhesion events. Because the centrifugation speed had to be increased to achieve membrane - membrane adhesion, the encapsulation rate decreased. If the adhesion of biotin and streptavidin would not depend on the centrifugation speed, the number of adhesion events could be further increased.

Taking another look at the directed internal membrane - membrane adhesion, there are several factors needing optimisation. The creation of membrane phase separated GUVs from the inverted emulsion method is a lot more complex compared to the use of the electroformation method. The incorporation of cholesterol into the vesicle membrane is rather complicated and strongly dependent

on the organic solvent (oil phase). Because the oil phase needs to have certain properties considering density, polarity, water solubility, toxicity, inertness and others, it is rather complicated to find an adequate substitute for the ones used in this study. The liquid - liquid membrane phase separated GUVs created for this study were often not ideal and although the lipid compositions used had higher amounts of SM or DPPC (high melting temperature lipid forming liquid and solid ordered phases) compared to DOPC (low melting temperature lipid forming liquid disordered phases), the vesicles showed large liquid disordered phases and mostly just small liquid ordered phases. In order to improve this and maybe even create Janus - like particles composing of ~ 50 % of both liquid phases, it would help to be able to analyse the actual lipid composition of the formed GUVs by NMR, mass spectrometry or other methods. This way, it would be possible to adjust the initial lipid composition to get the desired results. Additionally, one could analyse the vesicle membranes further to find out more about possible oil residues within the membrane bilayer which could also have an influence on membrane fluidity, curvature, bending rigidity and other features. Getting to know more about the GUVs formed by this method will lead to better and more directed optimisation measurements.

Secondly, the effect of silicone oil on streptavidin needs further clarification to make sure the protein is not aggregated and still able to bind biotin adequately. Experiments here can be conducted by external adhesion essays. It might even be possible to exchange silicone oil with another organic solvent which is by itself not able to dissolve a phospholipid film which is the reason for needing to mix silicone oil with n - decane.

The directed adhesion might also be improved by similar changes of the system discussed for improving the undirected adhesion. Choosing a different biotinylated lipid with a PEG spacer could improve complex formation and therefore the adhesion, even after the vesosomes are created. Eliminating the dependency of the centrifugation speed would be greatly beneficial.

4. Oligonucleotides

4.1. General Overview

With the fully established biotin streptavidin adhesion system, there are a few missing features. With the former method, the adhesion is established instantly after vesicle formation and cannot be observed by fluorescence microscopy in the exact moment but only afterwards. Also, the adhesion cannot be reversed. To develop the method further, a second strategy was adopted using oligonucleotides (single stranded DNA (ssDNA)). DNA binds specifically, only forming bonds between the four different nucleobases adenine (A) to thymine (T) and cytosine (C) to guanine (G). The system and the sequences used, can be customarily designed to fit a certain purpose. This includes functionalisations like fluorescent labels or biotinylations. The biotinylation makes it possible to attach oligonucleotides to a vesicle membrane by a biotin streptavidin bridge. In Figure 4.1, the strategy of initiating a membrane - membrane adhesion using oligonucleotides is shown. The plan employs two similar oligonucleotides which can be attached to the two vesicle types but do not bind to each other. A third strand bridges the two former ones creating the membrane - membrane adhesion. The later addition of a competitive DNA strand which binds to the bridging strand and leads to unbinding from the two biotinylated strands, gives the possibility of reversing the adhesion again (see Chapter 4.1, Figure 4.10, not shown in Figure 4.1).

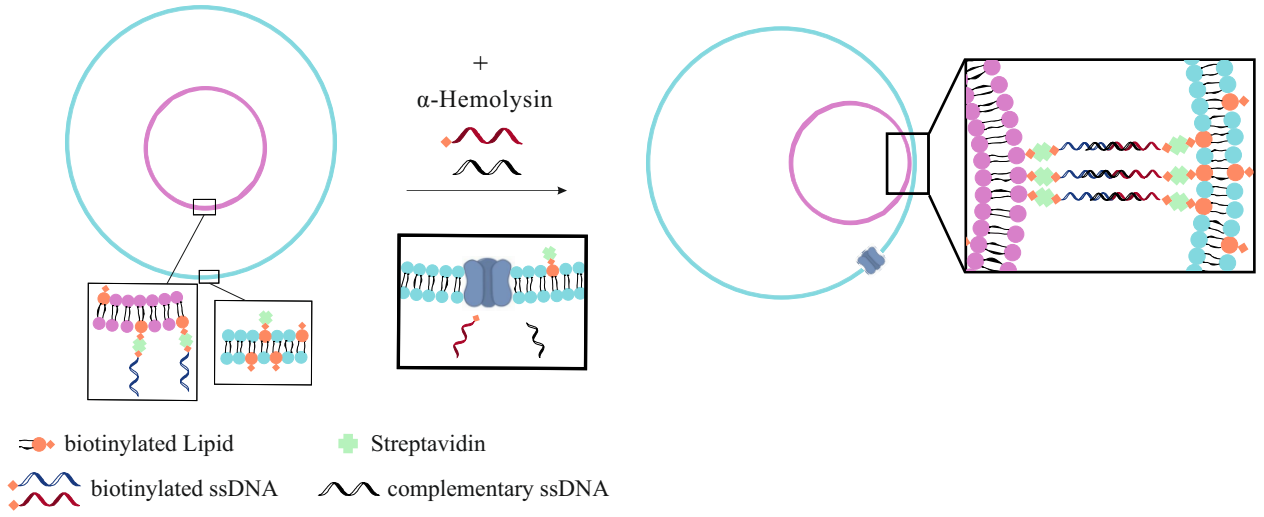

Figure 4.1: Schematic illustration of the internal adhesion of the membranes of inner and outer GUV by three oligonucleotides. Biotinylated lipids are drawn in red, streptavidin is drawn in green. The blue biotinylated oligonucleotide is incubated with streptavidin and the electroformed GUVs before the mixture being encapsulated. Additional added streptavidin which is also encapsulated, binds to the membrane of the inverted emulsion GUV. Using α - hemolysin, membrane pores are created within the outer GUV membrane. Two additional oligonucleotides (one of them biotinylated) are added successively and enter the outer GUV through the membrane pores. The third added DNA strand bridges the two biotinylated ones attached to both of the GUV membranes creating a membrane - membrane adhesion.

4.2. DNA: Internal Membrane - Membrane Adhesion

Table 1 gives the sequences of all four DNA strands used in this part of the study. Firstly, the system is using biotinylated DNA strands in order to get the oligonucleotides attached to the GUV membranes. The strategy is therefore building upon the biotin streptavidin membrane adhesion system to establish a bridge between the membrane and the oligonucleotides. The GUVs used in this part are of the same lipid compositions as used in the former strategy of internal membrane - membrane adhesion. In the case of the electroformed GUVs, they are simply mixed with streptavidin and the first oligonucleotide (DNA 1). The DNA concentration was 1.0 µM and the streptavidin concentration was also 1.0 µM. There is no way to control the biotin streptavidin complex formation therefore, it is possible that some streptavidin molecules only bind to four DNA strands instead of the GUV membrane on one side and biotinylated DNA on the other. There are studies that also used oligonucleotides attached to cholesterol[215] which is an easy way to incorporate DNA moieties to a vesicle membrane. In this study and with the use of the inverted emulsion method, this strategy was not considered because of the issues of the incorporation of cholesterol into the vesicle membrane but it could be a viable option for future trials.

Table 1: Table of the used oligonucleotide sequences.

DNA 1	biotin - 3’ - TTATTATTATTA - 5’
DNA 2	3’ - TTATTATTATTA - 5’ - Atto 488 - biotin
DNA 3	3’ - TAATAATAATAATAATAATAACTCCAG - 5’ - Atto 488
DNA 4	3’ - CTGGAGTTATTATTATTATTATTATTA - 5’

After a certain incubation time and another addition of streptavidin of the same concentration, the whole mixture was encapsulated by using the inverted emulsion method (see Chapter 7.2). The second addition of streptavidin is required to bind to the biotin moieties of the outer GUVs and has to be encapsulated during the formation of the inverted emulsion GUVs since it cannot enter the GUV lumen through membrane pores because of its size. The membrane pores formed by α - hemolysin allow a penetration of molecules of ≤ 3 kDa[216]. The size of streptavidin is ~ 52 kDa[217]. Applying the knowledge from the former adhesion system, the centrifugation speed to create the vesosomes was set to 250 x g to achieve optimal binding of the encapsulated streptavidin to the membrane of the outer GUVs since the biotinylated lipid was not changed for this system.

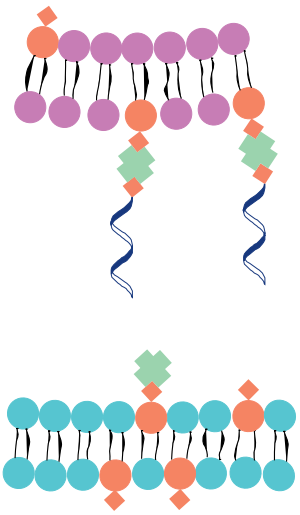

Figure 4.2: Schematic of a section of both GUV membranes (inner GUV magenta and outer GUV cyan) with all biotin moieties saturated with streptavidin and DNA 1 binding to the streptavidin moieties of the inner GUV membrane. A membrane - membrane adhesion is not possible.

At this point, an internal membrane - membrane adhesion due to a biotin streptavidin bridge does not occur if the former added streptavidin and the biotinylated DNA are attached to the GUV membranes (see Figure 4.2). In the case that there was a visible internal adhesion at this point, perhaps the first oligonucleotide did not properly bind to the vesicle membranes. After the vesosome formation, executed in a 96 - well microtiter plate, the sample is constantly observed by a fluorescence confocal microscope. To be able to introduce more oligonucleotides to the outer vesicle lumen, membrane pores are formed using α - hemolysin. For reasons not completely understood, the mixing of an aqueous α - hemolysin solution with the vesicle solution was not as efficient. The vesicles were prepared with sucrose solution inside and glucose solution outside, in order for the GUVs to sink to the bottom of the vessel for better imaging and less movement. It was assumed because of that, α - hemolysin took too much time sinking down to the bottom, reaching the GUVs. The same effect was observed when a solution from calcein or fluorescein was added. Both molecules are fluorescent and can be easily detected by the microscope. Adding one of the two in an aqueous solution to the vesicles, almost no signal was visible for more than ten minutes. Only when the agent was mixed with a sucrose solution, the fluorescence signal could be detected just a few seconds after the addition. It is assumed that the addition of the agent as a mixture with sucrose, helps the agent to sink to the bottom of the vessel faster. Preparing the α - hemolysin solution with sucrose improved the mixing within the imaging vessel greatly and added the advantage of keeping the osmolarity balanced throughout the whole experiment even if only very small volumes of solutions are being added to the GUVs. This procedure was continued for all following agents added to the vessel. The ideal method to see membrane pores being incorporated into the vesicle membranes is the loss of phase contrast when using a phase contrast objective. Unfortunately, the experiments were executed using microtiter plates which do have open wells and therefore include a liquid - air interface with the liquid, in this case water, forming a meniscus due to its surface tension. Because of that meniscus, phase contrast objectives did not work as intended and one does not get a clear image of the vesicles. So instead of using the phase contrast objective for imaging, a brightfield objective was employed. The contrast in brightfield occurs from the different refractive indices of the internal and external sugar

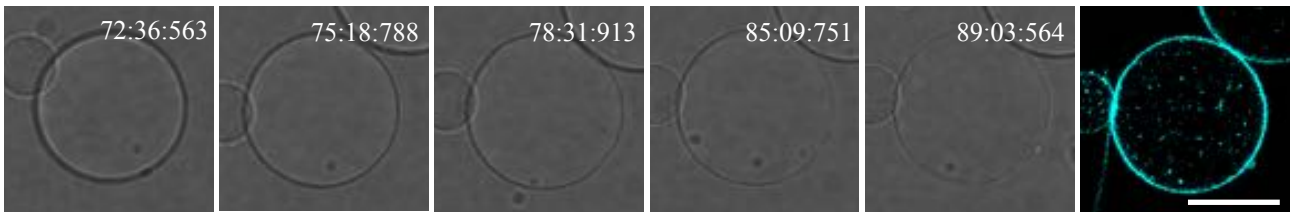

Figure 4.3: Brightfield and fluorescence confocal microscopy images (Atto 633 channel) of inverted emulsion GUVs. α - hemolysin in a sucrose solution of 900 mM was added stepwise to a final concentration of 0.25 - 0.3 µg/ml with an incubation time of 30 min after every addition (three additions in total). The GUVs were created from 97.9 mol% POPC, 2.0 mol% PE biotin, 0.1 mol% Atto 633 DOPE. Time is given in minutes. Scale bar: 20 µm

solutions. With the pore formation, the two solutions equilibrate and the density difference and difference in refractive index goes to zero (see Figure 4.3) which is why the contrast fades. The concentration of α - hemolysin used, did vary between 0.25 - 0.3 µg/ml from experiment to experiment. The concentration was not exceeded from there even if not all GUVs had pores inserted into their membranes, most of them did. If too many membrane pores form in one vesicle, it bursts (data not shown). That is why α - hemolysin was applied carefully and only in this concentration range. It is also possible that an inner GUV can be lost through pore formation (see Figure 4.4) which was one of the issues in this study when using α - hemolysin. Because of that, α - hemolysin was used very careful and in low concentrations. In this example, the pore opens where the inner GUV touches the outer one. The vesicle exits then through the pore which closes afterwards again leaving the outer GUV intact. An effect like this is very unusual and is not necessarily caused by the addition of the α - hemolysin solution. This might be induced by a combination of factors or just a

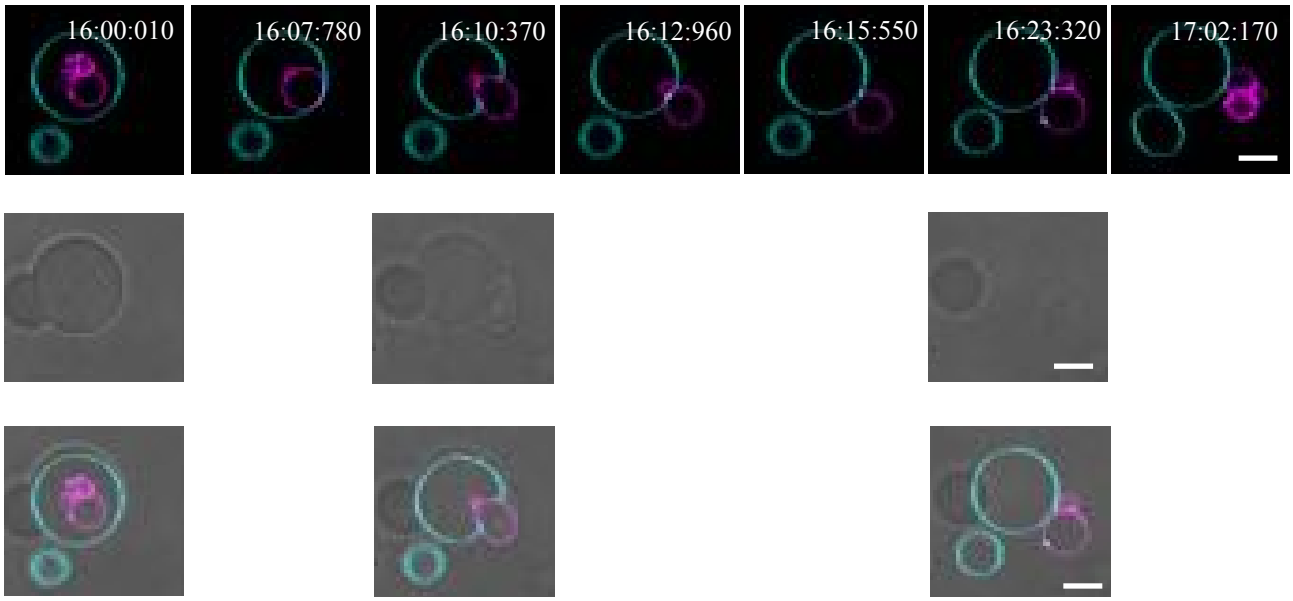

Figure 4.4: Fluorescence confocal (merge of Atto and $DiIC_{18}$ channel), corresponding brightfield and merged microscopy time - lapse images of a vesosome mixed with a solution from α - hemolysin and sucrose. The inner GUV exits through a temporary formed pore. The outer GUVs (cyan) were created from the inverted emulsion method with 97.9 mol% POPC, 2.0 mol% PE biotin, 0.1 mol% Atto 633 DOPE. The inner GUVs (magenta) were created from the electroformation method with 99.8 mol% POPC, 0.1 mol% PE biotin, 0.1 mol% $DiIC_{18}$. Scale bars: 10 µm

single one. Pore formation in GUVs (through a variety of methods; see Chapter 1.2.1.2.) is depending on various parameters. Masahito Yamazaki is researching this topic for years, identifying among others, membrane tension as an influencing factor[218,219,220,221,222]. An increase in membrane tension can be caused by numerous effects like electrostatic interactions[219] or osmotic pressure[220]. One factor influencing the tension could be oil residue within the lipid bilayer. However, it is not clear if this pore formation event and the loss of the inner GUV was caused by membrane tension. It seems like the membrane integrity of the outer GUV was compromised and without the inner GUV sealing off the pore in some way, the outer GUV might have been bursted. But without more investigation, this is highly speculative.

Aside from the actual DNA membrane adhesion experiment, membrane pores established from α - hemolysin were initially checked by adding a calcein or fluorescein solution to find out the ideal concentration for α - hemolysin used on the inverted emulsion GUVs. Both calcein and fluorescein can enter GUVs through membrane pores and can be detected via their fluorescence signal. In the adhesion experiment only the loss of contrast was observed to check the establishment of the membrane pores. The concentration of α - hemolysin was chosen according to most of the vesicles having membrane pores. The vesosomes were preselected right after their formation. This means, only the ones under observation (in a specific field of view) were needed to have membrane pores. Because of that the addition of α - hemolysin was stopped when the selected vesosomes lost their contrast. This also prevents too much solution being added to the GUVs and therefore, reduces vesicle movement.

Two of the oligonucleotides used in the following steps carry a label (Atto 488), one of them is the second strand (DNA 2) being introduced to the system. The label gives the ability to see the DNA entering the vesicles through the nanopores. In order to test the binding of the oligonucleotide DNA 2 to the vesicle membrane, a simple encapsulation experiment was conducted in advance. This way

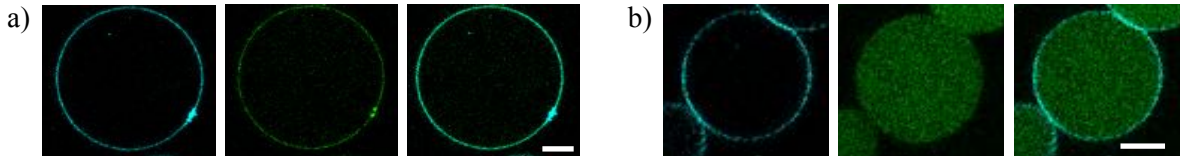

Figure 4.5: Fluorescence confocal microscope images (first image Atto 633 channel, second image streptavidin channel, third image merge) of inverted emulsion method GUVs with a) encapsulated DNA 2 labelled with Atto 488 (green) from batch one and b) encapsulated DNA 2 labelled with Atto 488 (green) from batch two. The DNA from batch one binds to the membrane which is visible through the enhanced DNA signal on the vesicle membrane. The DNA from batch two does not bind to the GUV membrane. The signal is evenly distributed in the vesicle lumen and shows no enhancement at the membrane. The GUVs (cyan) were created from the inverted emulsion method with 97.9 mol% POPC, 2.0 mol% PE biotin, 0.1 mol% Atto 633 DOPE. Streptavidin is not labelled and used at a concentration of 1.0 µM. The concentration of DNA 2 is 1.0 µM. Scale bars: 10 µm

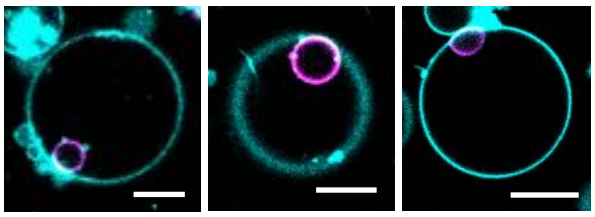

Figure 4.6: Fluorescence confocal microscopy images (merge) of three examples of vesosomes showing (probably) biotin streptavidin internal membrane - membrane adhesion. Imaged right after the formation. No α - hemolysin or labelled DNA 2 and DNA 3 were added. The outer GUVs (cyan) were created from the inverted emulsion method with 97.9 mol% POPC, 2.0 mol% PE biotin, 0.1 mol% Atto 633 DOPE. The inner GUVs (magenta) were created from the electroformation method with 99.8 mol% POPC, 0.1 mol% PE biotin, 0.1 mol% $DiIC_{18}$. The concentration of DNA 1 is 1.0 µm. The final streptavidin concentration is 2.0 µM. Scale bars: 10 µm

the binding can be directly observed by the enhanced DNA signal. During the time of the study, two DNA batches were ordered and used. Both were tested at equal conditions to see if DNA 2 binds to the membrane of the inverted emulsion vesicles. The results, visible in Figure 4.5, show that only in the first sample the oligonucleotide is binding to the vesicle membrane. This might be due to problems with the biotinylation of the DNA strands of batch two but this could not be proven. Another hint in this direction was the observation of constant biotin streptavidin membrane - membrane adhesion after the formation of the vesosomes in case of batch two (see Figure 4.6) which indicates a lack of DNA binding to the vesicle membranes.

In the next step of the adhesion experiment, the oligonucleotide is added which will bind to the membrane of the outer GUVs. It was expected to see the DNA binding to the outer vesicle membrane via the enhancement of the signal. Unfortunately, this could not be observed because the concentration of the DNA binding to the GUV membranes is too low compared to the concentration of free DNA in the aqueous solution. This will be discussed later in this chapter again. Equally to the pore formation, every addition of DNA was done by mixing it with a sucrose solution and including an incubation time of 30 minutes after every addition. Because DNA binds exclusively antiparallel with the 3' end to the 5' end[3] (see Figure 4.7), the two first strands do not have fitting sequences, preventing the GUV membranes from binding already at this point. After making sure the DNA entered the GUVs, the next DNA strand could be added as well. The third oligonucleotide's sequence (DNA 3) is designed to bridge both DNA 1 and DNA 2, finally adhering the vesicle membranes (see Figure 4.7). It comprises of eight triplets, binding to the four triplets of DNA 1 and DNA 2 and two additional triplets of random nucleobases which remain unbound at this point.

The whole experiment of pore formation and internal adhesion of the GUV membranes through ssDNA binding is shown in Figure 4.8. In Figure 4.8a, one can observe the fading of the density contrast of the GUVs over time due to membrane pore insertion. The addition of DNA 2 and its entering the GUVs over time is clearly visible in Figure 4.8b. Even at longer incubation times, there

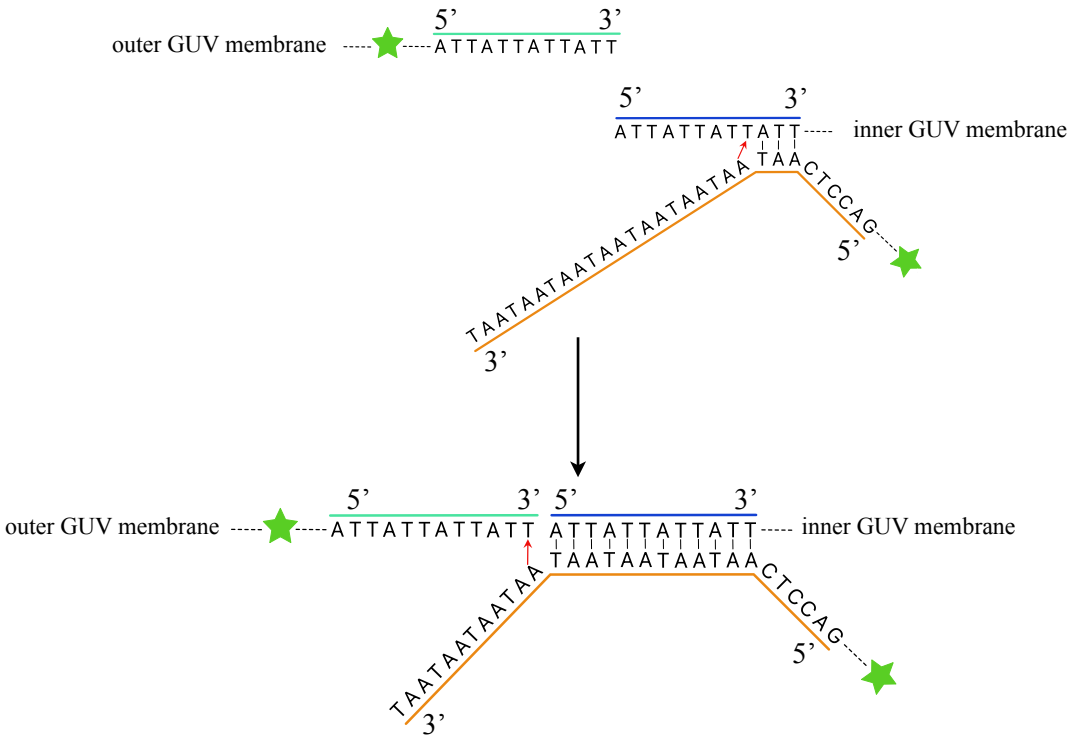

Figure 4.7: Exemplary DNA pairing schematic with DNA 1 (blue backbone) attached to the inner GUV, DNA 2 (green backbone) attached to the outer GUV and DNA 3 (orange backbone) starting to bind to DNA 1. After complete binding of DNA 1 and DNA 3 the binding to DNA 2 can start when the GUV is in close proximity. The binding is completed in a zipper - like process and the internal membrane - membrane adhesion established. The binding can also start between DNA 2 and DNA 3. The green stars represent the Atto 488 fluorescent label attached to DNA 2 and DNA 3.

was no visible enhancement of the DNA intensity on the GUV membrane as could be seen in Figure 4.5a. This is due to the significantly lower concentration of biotinylated DNA binding to the GUV membrane. Most of the DNA strands are free in the aqueous solution and not binding to GUV membranes. The following addition of the third complementary DNA 3 strand and its entering the GUV lumen cannot be seen directly since both DNA strands are labelled with Atto 488 and this leads to an increase of the intensity (see Figure 4.8c). If DNA 3 would be attached to a different fluorescent dye than DNA 2, both could be detected independently. Also, fluorescence measurements of the intensity increase overtime could not be performed because the microscope's gain had to be adjusted throughout the experiment since the Atto 488 signal increases with every addition of labelled DNA. This means, the successful entering of the last oligonucleotide to the vesicle lumen of the outer GUV and its binding to DNA 1 and DNA 2 can only be observed through the adhesion of both vesicle membranes which is shown in the time series of Figure 4.8d. After a short incubation time of less than five minutes, the inner GUV moves closer to the membrane of the outer GUV (via diffusion) and the adhesion is finally established. There is still no visible enhancement of the Atto 488 signal on the membrane at this point.

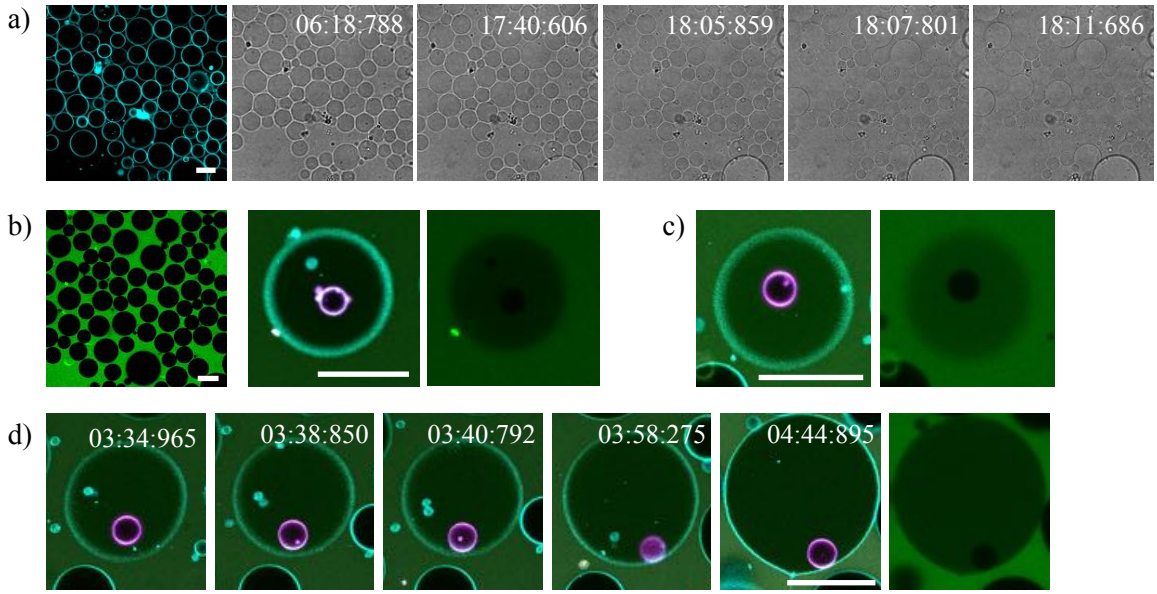

Figure 4.8: a) Fluorescence confocal microscopy image (Atto 633 channel) and brightfield microscopy time series of inverted emulsion GUVs mixed and incubated with α - hemolysin in a 900 mM sucrose solution. GUVs loose their contrast over time due to membrane pore formation. The total α - hemolysin concentration is 0.3 µg/ml. b) Fluorescence confocal microscopy images (first image streptavidin channel, second image merge, third image streptavidin channel) of the same frame as shown in a) and a selected vesosome after the first addition of DNA 2 labelled with Atto 488 (green). The single selected vesosome is shown as merged image (middle image) and the DNA 2 signal only (last image). After a few minutes the DNA signal becomes visible within the inverted emulsion GUVs as can be seen on the vesosome. The total incubation time was 30 minutes. The total DNA concentration is 1.3 µM. c) Fluorescence confocal microscopy images (first image merge, second streptavidin channel) of the same selected vesosome after the addition of DNA 3 labelled with Atto 488 (green). The final concentration of DNA 3 is 1.3 µM. The gain from the Atto 488 detector had to be lowered because of the increased fluorescence signal. The inner GUV is still moving within the outer GUV and is not adhered. d) Fluorescence confocal microscopy time series (first five images merge, last image streptavidin channel) of the same vesosome during the incubation time of DNA 3. After less than five minutes, the inner GUV moves closer to the outer GUV's membrane before the adhesion is established. The inner GUV does not change its position afterwards relatively to the outer GUV. The last image shows the DNA signal (DNA 2 and DNA 3) of the last image of the time series. The outer GUVs (cyan) were created from the inverted emulsion method with 97.9 mol% POPC, 2.0 mol% PE biotin, 0.1 mol% Atto 633 DOPE. The inner GUVs (magenta) were created from the electroformation method with 99.8 mol% POPC, 0.1 mol% PE biotin, 0.1 mol% $DiIC_{18}$. Streptavidin and DNA 1 are not labelled. The times are given in minutes. Scale bars: 20 µm

In Figure 4.9, one can see the last image from Figure 4.8d magnified on the area where the inner GUV is adhered to the membrane of the outer one (see Figure 4.9a). Fluorescence measurements of two distinct regions of interest (ROI) were taken using a line profile. The first ROI (green) represents the adhesion area crossing both the inner GUV membrane as well as the outer GUV membrane and extending further into the external solution. The external solution contains the highest concentration of DNA 2 and DNA 3 why the fluorescence intensity is at its maximum here. The second measurement (purple) was taken, only crossing the membrane of the outer GUV into the external solution. Since the first ROI's starting point lies within the internal solution of the inner vesicle, the fluorescence signal is very low but not zero because the inner GUV is not completely in focus (as can be seen in the last time series image of Figure 4.8d), leading to the background signal

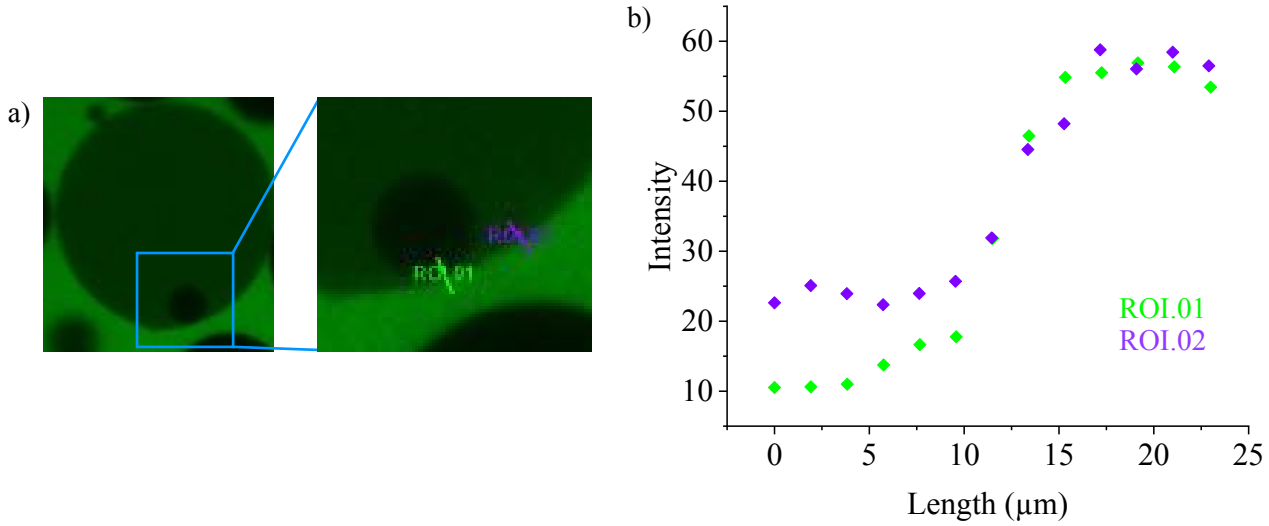

Figure 4.9: a) Fluorescence confocal microscope image (streptavidin channel) of the vesosome system of the last image of Figure 4.9d and a magnification of the marked area. Two line profiles drawn in the magnified image represent the executed fluorescence intensity measurements. ROI.01 represents the adhesion area (double lipid bilayer) and ROI.02 represents the non - adhesion area (single lipid bilayer). b) Histogram of the fluorescence intensity measurements of the signals of DNA 2 and DNA 3 (labelled with Atto 488) along the line profiles. Starting points at 0 µm within the lumen of the inner GUV (ROI.01, green) and the lumen of the outer GUV (ROI.02, purple). End points at ~ 23 µm for both within the external solution of the vesosome with the highest concentration of DNA 2 and DNA 3 and therefore the highest fluorescence intensity.

being detected. In the case of ROI.02, the signal is already higher at this point because its beginning lies within the outer GUV lumen which includes both ssDNA signals. Both intensities increase with very similar rates (see Figure 4.9b), reaching a plateau at ~ 15 µm. Between 5 - 10 µm, there is a minor slope in case of ROI.01 which is missing in case of ROI.02. This could be interpreted as an enhancement of the signal but the intensity still does not reach the level of intensity of the lumen of the outer GUV. An actual enhancement of the fluorescence intensity on the membrane could only be detected at higher DNA concentrations binding to the vesicle membranes. The fluorescence intensity of the enrichment of DNA moieties on the membrane would probably need to exceed the intensity from the internal aqueous solution of the inverted emulsion GUV to be detected properly. This does not mean, there is no DNA binding to the membrane and therefore no membrane - membrane adhesion. This only means that the concentration of DNA 2 binding to the outer GUV membrane and of the bridging DNA 3 compared to the concentration of free DNA 2 and DNA 3, is rather low so that an increased fluorescence intensity on the membrane itself cannot be detected. A low concentration of biotinylated DNA 2 binding to the membrane of the outer GUV is consistent because one has to consider that the GUVs also contain free streptavidin which was encapsulated in the beginning. Since the system is not yet optimised, the concentrations of all agents (DNA and

streptavidin) are very high. Large amounts of DNA 2 can therefore bind to free streptavidin and are no longer able to bind to the GUV membranes.

In order to be sure, there is a membrane adhesion, the vesosome was observed for a longer time period (more than ~ 1 hour). Before the adhesion event, the inner GUV moved constantly within the outer GUV creating distance between the two membranes and reducing it again. Afterwards, it is not changing its position relatively to the outer GUV any more. Both membranes stay in contact and only the outer GUV still moves over time within the aqueous solution. The adhesion does not lead to a membrane deformation, as seen very frequently in Chapter 3.2. and 3.3. when biotin and streptavidin is used to adhere membranes. In case of biotin and streptavidin, the deformation probably occurs because biotin and streptavidin accumulate within the adhesion area. The fluidity of the membrane allows the accumulation of PE biotin and therefore, leads to an enlargement of the adhesion area which again causes the membrane deformation. An accumulation of the oligonucleotides within the adhesion area seems not to happen to a similar extend or at all. The missing enhancement of the DNA signal supports this assumption. Although, it is possible that this process takes much more time and was just not observed during the experiment.

The next step in the experiment would have been the addition of DNA 4 which is the competitive strand to DNA 1 and DNA 2 and is supposed to reverse the membrane adhesion. The two unpaired triplets of the 5' end of DNA 3 are complementary to the first two triplets of the 3' end of DNA 4 (see Figure 4.10). The pairing of these nucleobases initiates the complete binding of the two strands DNA 3 and DNA 4. With the pairing of the third triplet, the unbinding between DNA 3 to DNA 1

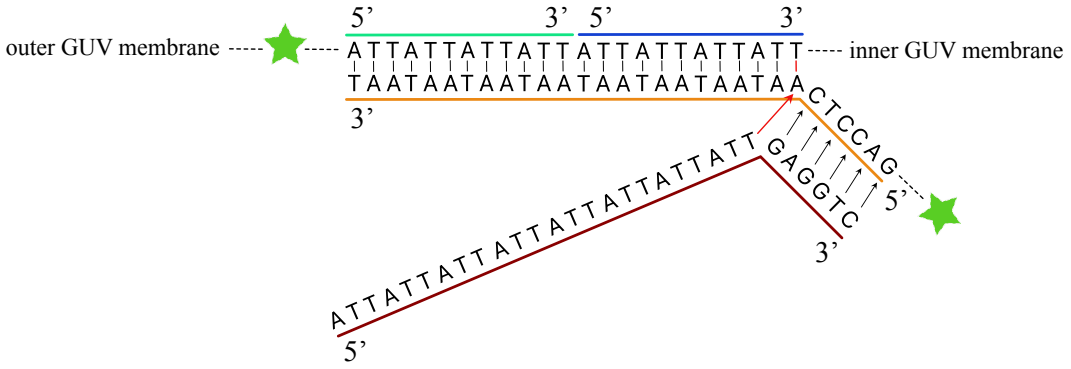

Figure 4.10: Theoretical DNA pairing schematic with DNA 1 (blue backbone) attached to the inner GUV, DNA 2 (green backbone) attached to the outer GUV and DNA 3 (orange backbone) bridging the two. The fourth strand DNA 4 (brown backbone) is complemental to strand 3 and initiates pairing at the unbound triplets at the 5' end of DNA 3 leading to the unpairing of DNA 1 and DNA 2 to DNA 3. The binding is completed in a zipper - like process and the membrane adhesion is irreversibly detached. The green stars represent the Atto 488 fluorescent label attached to DNA 2 and DNA 3.

and DNA 2 is started. After the complete pairing of the strands, DNA 3 is inactivated which means it cannot bind to DNA 1 and DNA 2 a second time to re - establish the membrane adhesion.
Unfortunately, it was not possible in the experimental setup to achieve this. Reasons were the loss of the vesosomes due to GUV movement and clustering and in rare cases loss of the electroformed GUVs during pore formation and membrane adhesion from biotin and streptavidin. A solution could be, to immobilise the GUVs using microfluidic chips or other methods.

4.2. Conclusion

The DNA internal adhesion system did not work often in the experimental approach due to various problems. It was not fully optimised and needs more investigation, parameter changing and experiments in the future which is why there is no further data on different concentrations or proven evidence for the adhesion originating from the DNA binding. Also, data on adhesion quantity (how many vesosomes show an internal membrane - membrane adhesion when the entire experiment in completed) is missing by now which is due to the way the experiments are executed. In most cases, only a single vesosome could be observed during one complete experiment, due to constant vesicle movement throughout the experiment. If in the beginning, more than one vesosome were visible in an image frame, they often moved too far apart during the experiment so only one could be imaged further. Reversing the process by the addition of a competing oligonucleotide would prove the membrane adhesion through DNA because an adhesion emerging from a biotin and streptavidin complex formation is not reversible in this setup. In general, biotinylated single stranded DNA can be attached to a GUV membrane via a biotin streptavidin bridge and can also enter the vesicle lumen through membrane pores created from α - hemolysin. It is also possible to encapsulate several different biomolecules like proteins, oligonucleotides and vesicles inside GUVs at the same time using the inverted emulsion method.
The execution of the entire experiment is rather complicated and requires a lot of time and patience. Since the vesicles are not immobilised during the experiment, one problem is vesicle movement. This is increased with every addition of solutions to the reaction vessel which can lead to clustering. Especially in the case that one particular vesosome is observed, one needs to be extremely careful to prevent the vesicles from moving too much, so not to lose it. If the vesicles moved out of the observation area after the addition of labelled DNA, the camera had to be used to follow the vesosome in order to find it again. The oculars could not be used from this step on because the fluorescence intensity of the DNA is very high and even at low concentrations visible in all

channels of the microscope setup. When a particular vesosome was lost throughout the experiment and could not be found again, the sample had to be discarded and the experiment had to be repeated with a knew sample. Because these problems occurred quite frequently, at least six samples were prepared per day. Vesicle movement should be fixed in the future by immobilising the GUVs by using microfluidic chips or maybe agarose gel[223].

Since there were two batches of all oligonucleotides ordered from the same company at different times and both showed different results in the experiment seen in Figure 4.6, the binding of the oligonucleotides to the membranes should always be tested in advance. The second batch which might not have been properly biotinylated, showed also constant internal membrane - membrane adhesion directly after vesosome formation indicating that DNA 1 did not bind to the electroformed GUVs as well. After testing the binding of DNA 2 to the vesicle membrane, the complete batch was discarded after just two months of storage. This was not the case for the first ordered batch. This one still worked properly after 1.5 years of storage. The DNA was stored at -20 °C as aqueous aliquots with a concentration of 100 µM. After one year of storage in the case of batch one, the vials were heated in a water bath to ~ 65 °C for ~ 10 minutes to make sure the DNA was still in its primary structure and therefore still usable.

The next step for the DNA system would be the reversibility of the adhesion since, it could not be tested in this study. The use of microfluidic chips could help to immobilise the GUVs and eliminate the problem of clustering and moving of the vesicles. The use of the cascade chip, used for external GUV - GUV adhesion studies, is not advisable because of the trap size and the constant fluid flow which leads to a sort of spinning motion of the vesicles within the traps. One could stop the fluid flow after adding agents to the chip which will lead to the GUVs moving slowly out of the traps. The flow would need to be stopped but started again from time to time to keep the GUVs within the traps. The trap size of the cascade chip is another problem. They can hold a large number of GUVs which can display a hindrance for the agents to reach all GUVs especially, GUVs in the middle of the traps (see Figure 4.11). An even distribution of the agents might need very long incubation times because of that or not work at all in some cases. But in order to observe the adhesion of an inner GUV to an outer one, the outer GUV should be as still as

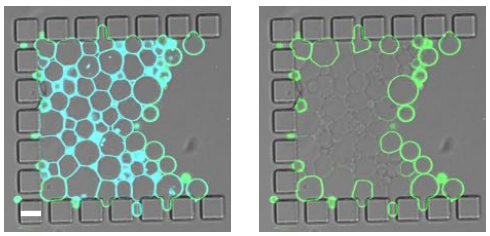

Figure 4.11: Fluorescence confocal microscopy images (first image merge, second image streptavidin channel) of GUVs in a microfluidic chip (cascade). The GUV lipid composition is 97.9 mol% POPC, 2.0 mol% PE biotin and 0.1 mol % Atto 633 DOPE (cyan). GUVs were flushed into the traps at flow rate of 3 µl/min. Labelled streptavidin (green) was flushed into the filled chip (no premixing of GUVs with streptavidin). The first image is merged. The second shows the streptavidin signal. The chip (trap) is visible in brightfield. Scale bar: 30 µm

possible. Robinson et.al. published in 2013 a chip design that can trap single GUVs which can then be isolated by a valve in donut shape[75]. With this chip, GUVs can be observed without any shear stress originating from a fluid flow. In order to effectively use microfluidic chips like the cascade chip to immobilise the vesosomes in this kind of experimental setup, it is necessary to improve the encapsulation of GUVs by the inverted emulsion method or by changing the method to create vesosomes. Flushing the samples from the used method in this study into a cascade chip, needs harvesting the GUVs and vesosomes from the microtiter plate which decreases the number of GUVs and vesosomes significantly. Also, when filling the traps of a cascade chip, not all GUVs and vesosomes end up trapped. A lot of the vesicles pass the chip completely and exit through the outlet without getting trapped. Considering that most of the GUVs within a sample are not vesosomes (~ 87 % of the GUVs have no GUV encapsulated), the likelihood of entrapping a vesosome is very low. The use of microfluidic systems to create GUVs is a viable option as mentioned in Chapter 1.2.1.3.[183] but would need further testing in experiments like the ones from this study since, several agents would need to be encapsulated at once in the GUVs.

Another part of the adhesion which could not be tested with the DNA system is the directed adhesion. The use of membrane phase separated GUVs for the DNA membrane adhesion is the same as for the directed adhesion experiments using the biotin streptavidin system. It might even be easier using the DNA system since the adhesion is not instantly established after vesosome formation. This means, the chance of membrane - membrane adhesion would in theory not change at all but only the lipid composition of either the electroformed GUVs or the inverted emulsion GUVs for the DNA membrane - membrane adhesion. Achieving the directed adhesion and reversing it afterwards again would complete the DNA internal adhesion system. A problem here could again be the usage of silicone oil for the creation of the outer GUVs being membrane phase separated which might affect the streptavidin by leading to its aggregation. This will also need further testing for the directed adhesion of the DNA strategy and possible consequences of DNA binding to the vesicle membranes.

5. Light - switchable proteins

5.1. General Overview

The last system which was used within this study is an already established one when it comes to GUV adhesion and is associated mostly with the group of Seraphine Wegner. The proteins which were used in this study were obtained by the Wegner group. The method uses special proteins which can be attached to a vesicle membrane through the lipid 1,2-dioleoyl-*sn*-glycero-3-[(N-(5-amino-1-carboxypentyl) iminodiacetic acid)succinyl] (DGS - NTA(Ni))[199]. There are some studies including membrane - substrate adhesion[224] and external membrane - membrane adhesion[200]. The two proteins used in this study which can bind to each other are called iLID and Nano. They have a specific feature of controlled binding and dissociation by using light irradiation and darkness. The process of binding and dissociation can be repeated multiple times according to Wegner et.al.[199].

5.2. iLID and Nano: Internal Membrane - Membrane Adhesion

To employ iLID and Nano for the internal membrane - membrane adhesion (see Figure 5.1), the vesosomes are created using the same method of encapsulation. The electroformed GUVs will be premixed with one of the proteins while the second is going to be encapsulated along with the GUVs (see Chapter 7.2). For this system, one can choose freely which of the proteins binds to a certain GUV type. The only difference between the two is, Nano carries the fluorescent protein mOrange and can be detected by fluorescence microscopy. After encapsulation, the second protein binds to the membrane of the outer GUV and when blue light with a wavelength of ~ 488 nm

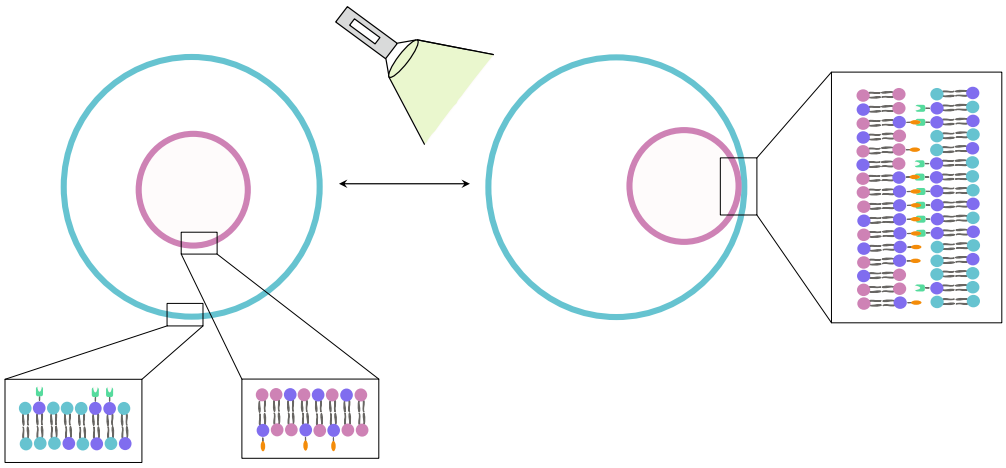

Figure 5.1: Schematic illustration of the internal adhesion of the membranes of inner and outer GUV by the use of iLID and Nano. iLID and Nano are two proteins which bind to each other under light irradiation with a wavelength of 488 nm leading to a membrane - membrane adhesion. Both proteins are encapsulated alongside the electroformed GUVs. Incubation times in the dark lead to dissociation of the membrane adhesion which can be re - established by light irradiation.

irradiates the sample, the proteins bind, creating a membrane - membrane adhesion. The inverted emulsion method could be executed, for this strategy, at lower centrifugation speeds in order to take advantage of the higher GUV encapsulation rates (see Chapter 2.1). To reverse the adhesion, the GUVs need to be cut off from the light source and left in the dark for approximately 20 minutes. After that, the adhesion can be re - established by simply shining light on the sample again. This is the only one of the three systems which is able to give control over the adhesion in form of a switch - ability.

Both iLID and Nano bind, or more correctly coordinate to DGS - NTA(Ni) via their histidine tag (His tag) (see Figure 5.2) forming a chelate complex. That way, the proteins will be attached to the membrane and similar to the biotinylated lipid, the concentration of DGS - NTA(Ni) can be chosen according to its purpose. In the case of the membrane - membrane adhesion, the lipid compositions were adopted from the publications of the Wegner group[199,224]. Although, only in the case of the electroformed GUVs, one can be sure about the actual lipid compositions of the vesicles. Since the

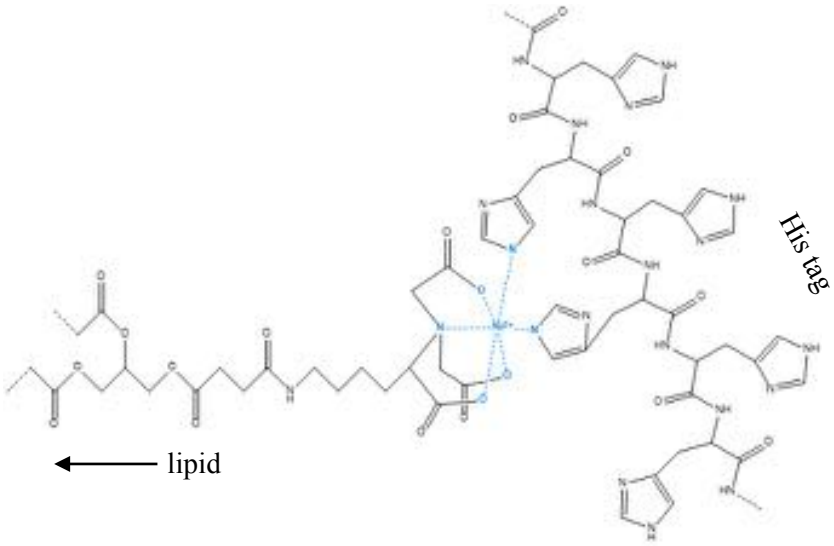

Figure 5.2: Chemical structure of the coordinative bond (marked in blue) of the Ni^{2+} - nitrilotriacetic acid head group of the lipid and the His tag of the protein. Adapted from [225] and Avanti® Polar Lipids.

lipid composition also contains cholesterol next to POPC, DOPG and DGS - NTA(Ni), the lipid composition of the inverted emulsion GUVs might differ especially, in relation to cholesterol. POPC forms the majority of the vesicle membranes while DGS - NTA(Ni) is needed to bind the proteins to the membrane. But because NTA lipids can also form complexes with each other, DOPG was included to prevent this since, it adds negative charges to the lipid bilayer which increases the electrostatic repulsion of the membranes[226]. Cholesterol is added to decrease lipid tube formation which can happen with salts present in the aqueous solution[227,228].

In the experiment, iLID was attached to the inner GUVs while Nano is coordinating to the outer GUVs. For this, the electroformed GUVs were incubated with a final concentration of 100 nM iLID in Tris(hydroxymethyl)aminomethane (TRIS) buffer. After 15 minutes, the second protein Nano is added to a final concentration of 100 nM and the mixture is used as aqueous solution to create the emulsion for the inverted emulsion method. This way, the protein Nano binds to the membrane of the outer GUVs. In Figure 5.3a - c, the first image shows the signal of Nano on the membrane of the inverted emulsion GUVs. The signal intensity is clearly visible and relatively even distributed over the membrane. The samples were incubated after their formation in the dark in order to dissociate all protein binding. Since normal daylight includes all visible light wavelengths including light of a wavelength of ~ 488 nm this means, it will lead to protein binding. Because the sample will be irradiated during the imaging process by the microscope, the membrane - membrane adhesion can be imaged while it occurs but not the dissociation process. One can observe in the examples of Figure 5.3a and b, the inner GUVs are already close to the membrane of the outer GUV but not yet adhered. Also, for both samples, the time it takes for the adhesion to be established is different which is unclear why that is. It could be that the actual time it took for the GUVs to establish the membrane - membrane adhesion is not different but only the observation time. Since both examples (Figure 5.3a and b) were from different samples, the time it took to screen the wells of the

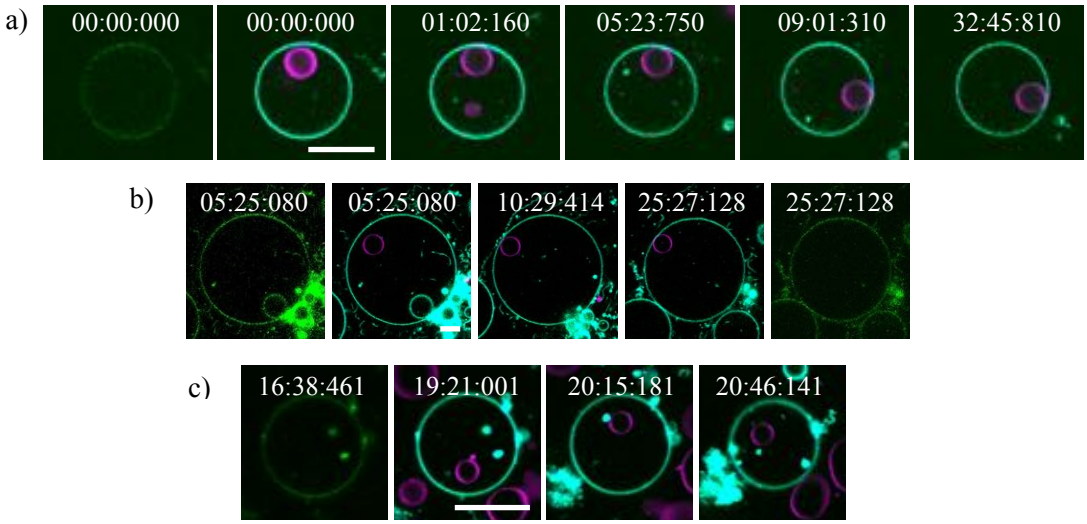

Figure 5.3: a) Fluorescence confocal microscopy images (first image streptavidin channel, following images merge) of a vesosome system with an internal membrane - membrane adhesion due to the binding of iLID and Nano. b) Fluorescence confocal microscopy images (first image streptavidin channel, second to fourth image merge, last image streptavidin channel) of a vesosome system with an internal membrane - membrane adhesion due to the binding of iLID and Nano. c) Fluorescence confocal microscopy images (first image streptavidin channel, following images merge) of a vesosome system with no internal membrane - membrane adhesion. The outer GUVs were created from the inverted emulsion method with 77.9 mol% POPC, 10.0 mol% Chol, 10.0 mol% DOPG, 1.0 mol% DGS-Ni-NTA and 0.1 mol% $DiIC_{18}$. The inner GUVs were created from the electroformation method with 78.9 mol% POPC, 10.0 mol% cholesterol, 10.0 mol% DOPG, 2.0 mol% DGS-Ni-NTA and 0.1 mol% $DiDC_{18}$. Final concentration of iLID and Nano is 100 nM. The time is given in minutes. Scale bars: 10 µm

microtiter plate can differ particularly, when the GUVs show a lot of movement which was the case for many of these samples. In the case of sample 5.3a, the vesosome barely moved over the whole time period while sample 5.3b moved the whole time and was much more complicated to follow during the imaging process. So, while the inner GUV of example 5.3a shows adhesion after ~ 1 minute, for the second example the process took more than 10 minutes. The third sample in Figure 5.3c does not show adhesion. Although, the signal of Nano is clearly visible on the membrane of the outer GUV, even after more than 20 minutes, the inner GUV is not adhered to it or made contact. In this study, the quality of the internal membrane - membrane adhesion can be compared to the internal DNA membrane - membrane adhesion. It can be observed over longer time periods without the inner GUV changing its position relative to the outer GUV. There is no membrane deformation caused by the adhesion and also, no enrichment of the proteins in the adhesion area which would be visible through an enhancement of the signal intensity of Nano. The last image of example 5.3b shows the corresponding protein signal of the last point of the time scale at which the inner GUV is adhered over several minutes. The protein distribution in this moment is still relatively even without any visible enrichment in the adhesion area. To verify this, fluorescence intensity measurements of the mOrange signal were conducted on three different points on the outer GUV's membrane (see Figure 5.4), of which the first one (ROI.01, green) displays the adhesion area and the second (ROI.02, purple) and third (ROI.03, orange) are two points without adhesion and therefore no binding of iLID and Nano (see Figure 5.4a). In Figure 5.4b, one can see that the intensity of Nano within the adhesion area (ROI.01) is on the same level as the intensity of the non - adhesion area (ROI.03). Only the intensity of ROI.02 is increased compared to the other two signals which can be caused by signal fluctuations and the just relatively even distribution of the signal of mOrange over the entire membrane. This is a clear evidence for the proteins not being enriched due to a membrane - membrane adhesion even after several minutes of adhesion. Measurements for other examples have shown the same results.

A second reason for the membranes not deforming as in the case of a biotin and streptavidin membrane - membrane adhesion, is the K_D value. As mentioned in Chapter 1.2.1.2., the K_D value or dissociation constant for biotin and streptavidin is ~ 10^{-14} M, directly reflecting on the strength of the complex's binding efficiency. The K_D value for the binding of iLID and Nano is ~ 0.28 ± 0.14 µM[192]. This significant difference is visible in the adhesions occurring from both systems, considering their quality. Quality in this context means, the stability of the adhesion over time and the size of the adhesion area and the contact angle between both adhering GUVs.

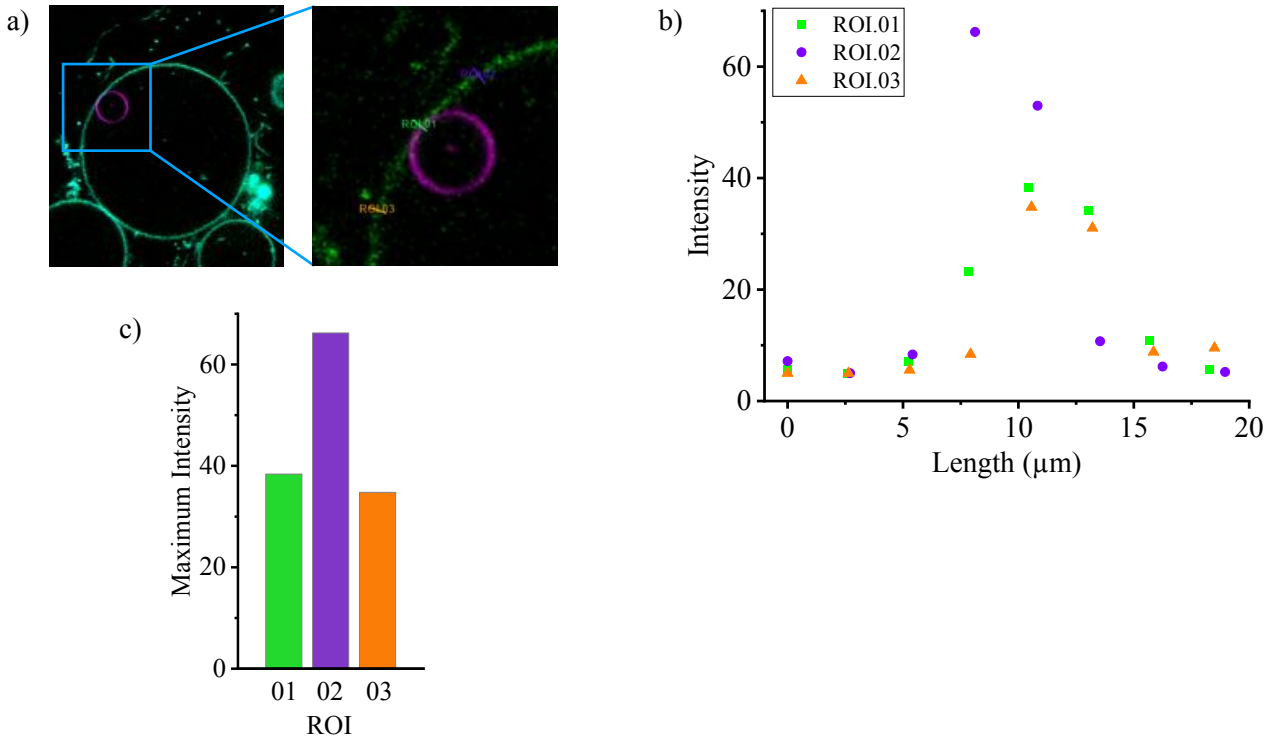

Figure 5.4: a) Fluorescence confocal microscopy images (merge) of the vesosome system from Figure 5.3b and a magnification of the marked area. Three line profiles drawn in the magnified image represent the executed fluorescence intensity measurements. ROI.01 represents the adhesion area (double lipid bilayer) and ROI.02 and ROI.03 represent the non - adhesion area (single lipid bilayer). b) Fluorescence intensity measurements of the signal of Nano (labelled with mOrange) along the line profiles. Starting points at 0 µm within the external sugar solution. End points at ~ 19 µm for ROI.01 in the lumen of the electroformed GUV and for ROI.02 and ROI.03 within the lumen of the inverted emulsion GUV. c) Maximum intensity of the fluorescence signal of all three ROIs at ~ 10 µm in comparison.

The quantity of internal adhesion events (number of adhesion events for one sample) as well as the quantity of formed vesosomes (per sample) in case of the light - switchable proteins, could not be studied in this approach as well as the repeatedly established adhesion after a second or third incubation in the dark. The cause for that lies within the stability of the inverted emulsion GUVs. The outer GUVs with the lipid composition used for this strategy of adhesion (77.9 mol% POPC, 10.0 mol% Chol, 10.0 mol% DOPG, 1.0 mol% DGS-Ni-NTA and 0.1 mol% $DiIC_{18}$), were in large amounts unstable which prevented the collection of representative data sets. The GUVs were leaky and vesosomes often lost their inner GUVs in spontaneous poration events. Bursting and transient pore formation induced also a lot of movement to the samples, disturbing the imaging processes almost constantly. Experiments with calcein encapsulated (experimental details see Chapter 7.2) along with the electroformed GUVs and the proteins in order to have the same conditions revealed, most of the outer GUVs are not stable over longer time periods. The fluorescence signal of calcein was measured for vesosomes over ~ 100 seconds. The results from this experiment are demonstrated in Figure 5.5, showing the signal declining from the beginning of the measurements

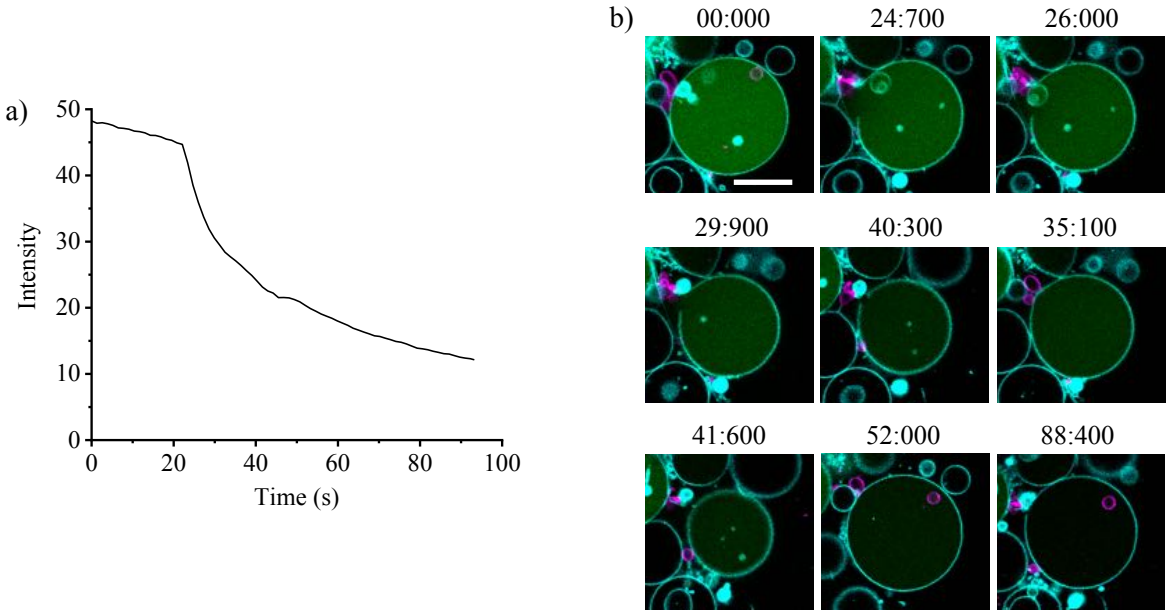

Figure 5.5: a) Fluorescence intensity measurements of an encapsulated calcein solution over a time period of ~ 95 seconds. b) Corresponding fluorescence confocal microscopy images (merge) of the vesosome system with calcein, Nano and iLID encapsulated. At 24:700 the formation of a membrane pore is visible over several seconds. The calcein solution (green) leaks from the vesicle lumen over time. The outer GUVs were created from the inverted emulsion method with 77.9 mol% POPC, 10.0 mol% Chol, 10.0 mol% DOPG, 1.0 mol% DGS-Ni-NTA and 0.1 mol% $DiIC_{18}$ (cyan). The inner GUVs were created from the electroformation method with 78.9 mol% POPC, 10.0 mol% cholesterol, 10.0 mol% DOPG, 2.0 mol% DGS-Ni-NTA and 0.1 mol% $DiDC_{18}$ (magenta). The final concentration of iLID and Nano is 100 nM. The time is given in seconds. Scale bars: 20 µm

(see Figure 5.5a). After ~ 24 seconds, a transient pore opens for the membrane of the outer GUV which can be seen in Figure 5.5b. As a result of that, the size of the outer GUV decreases and the calcein signal starts to drop more quickly. The pore closes again after a few seconds, leading to the membrane relaxing to its former size again but without stopping the fluorescence signal from decreasing further. After ~ 90 seconds the signal originating from calcein is barely visible within the vesicle lumen and the histogram shows the intensity decreased to about 1/5 of the intensity to when the measurement started. This is just one example of the inverted emulsion GUVs not being stable even, if in this example, the inner GUV remains within the outer GUV without showing adhesion. This is very often not the case when spontaneous poration occurs. In many cases, the electroformed vesicle exits when a transient pore opens (see Figure 5.6a) or even more severely, the outer GUV bursts completely (see Figure 5.6b). When looking at both events more closely, there is no visible difference in the beginning and both events can be observed within the same sample at different regions of the same well of the microtiter plate. Because these effects were observed early on for these experiments, the osmotic balance was meticulously checked to avoid any influence of it. Therefore, osmotic pressure cannot be responsible here. In the case of transient pore formation, it is possible for the pore to last for several seconds before closing again. In these cases, as discussed

before, the membrane edge tension is still large enough for the transient pore to close again[181]. GUV bursting happens in an instant, leaving lipid clusters all over the sample. The membrane edge tension was decreased so much so that the transient pore could not close again and instead the vesicles burst. The lipid clusters of GUVs were seen in all samples and are a clear evidence for vesicle bursting. Additionally, transient pore formation as well as bursting are not the only anomalies which were observed within the samples of these experiments. Figure 5.6c shows a budding event of the outer GUV happening over a time period of ~ 23 minutes. One thing that stands out here is, the signal intensity of the part of the membrane which is going to bud off. The membrane looks as if there are multiple lipid layers. The fluorescence signal of the membrane dye

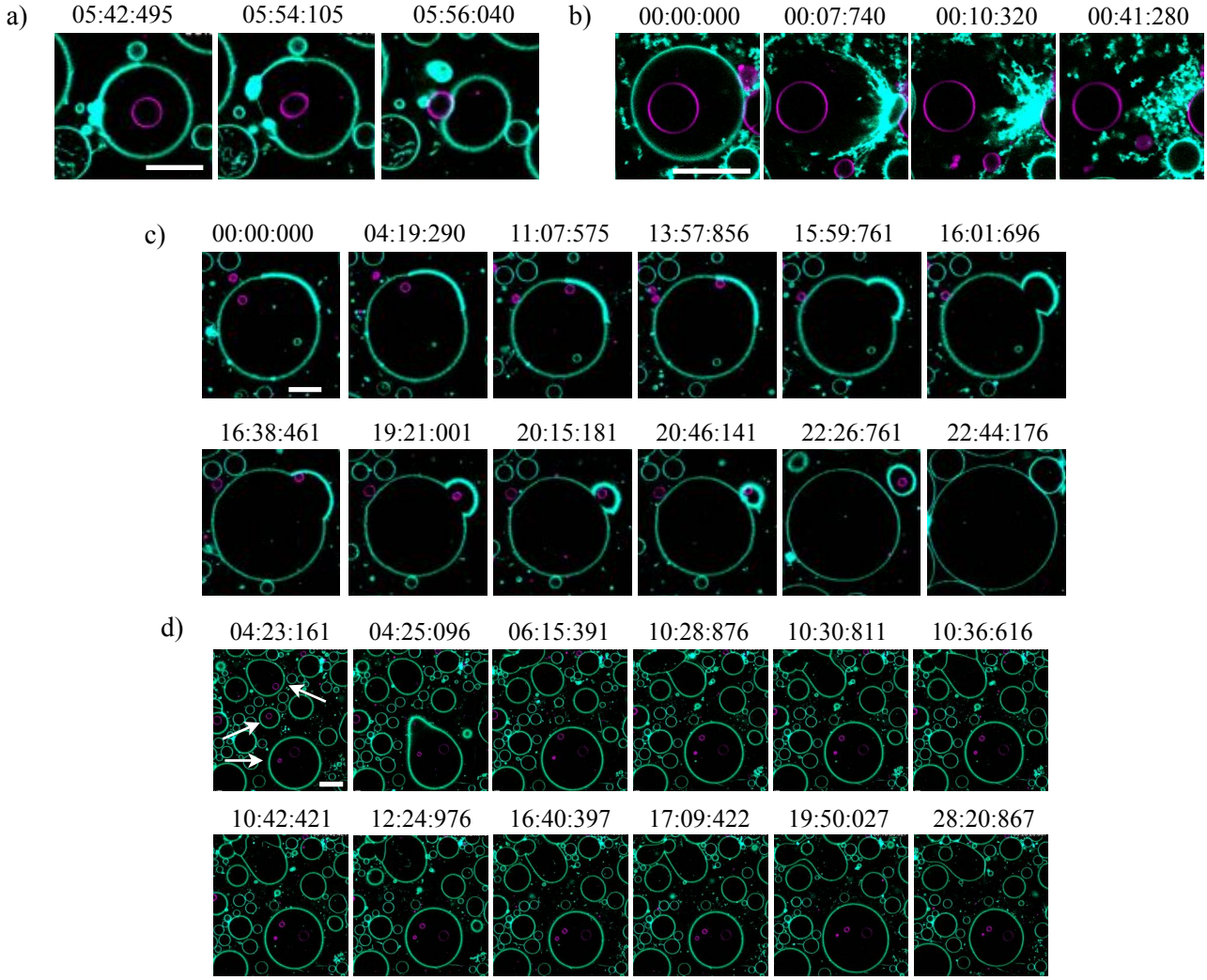

Figure 5.6: Fluorescence confocal microscope images (merge) of a vesosome system over a certain time period showing a) membrane poration of the inverted emulsion GUV and the inner GUV exiting through the pore, b) vesicle bursting of the inverted emulsion GUV, c) the budding process of the inverted emulsion GUV membrane and the formation of a second GUV and d) several fusion processes of multiple inverted emulsion GUVs. The outer GUVs were created from the inverted emulsion method with 77.9 mol% POPC, 10.0 mol% Chol, 10.0 mol% DOPG, 1.0 mol% DGS-Ni-NTA and 0.1 mol% $DiIC_{18}$. The inner GUVs were created from the electroformation method with 78.9 mol% POPC, 10.0 mol% cholesterol, 10.0 mol% DOPG, 2.0 mol% DGS-Ni-NTA and 0.1 mol% $DiDC_{18}$. Final concentration of iLID and Nano is 100 nM. The time is given in minutes. Scale bars: 20 µm

is clearly enhanced compared to the rest of the membrane and the thickness seems to be increased as well. It is not known, where this is coming from. It might be that another GUV bursted on this part of the membrane which formed a multilayer. Over the next 10 - 13 minutes, the electroformed GUV moves towards this particular area of the inverted emulsion GUV and might even form an adhesion while the budding proceeds. After ~ 21 minutes, the budding process is finished. During the recording of the time series, the z - position was then changed to see if the budding was actually completed and a complete separation took place. In fact, the image at 22:46:761 minutes shows two separate GUVs including a clear gap in between both of the two membranes. In the last image at a higher z - position, it can be seen that both GUVs are actually separated but both membranes are still in touch. Astonishingly, the electroformed GUV was included in the budding process and ends up in the new formed GUV. The opposite effect could be observed in another case, where spontaneous fusion of the inverted emulsion GUVs takes place (see Figure 5.6d). Similar to vesicle bursting, the process can happen very rapidly and even at a larger distance of the two GUV membranes (vesosome on the bottom of the image series). But it can also be more slowly and occur between several vesicles which are in close proximity (GUVs on the top of the image series). Comparing both fusion events, it can be observed that the rapid fusion happens completely without visible excess areas of the membranes while during the slow fusion event, parts of the excess membrane on the fusion side can remain for several minutes (see Figure 5.6d at 10:30:811). A second observation here is, the membrane of the rapid fused GUVs relaxed back to a circular form. This is not the case for the slow fusing GUVs which do not have a circular form. They also comprise of multiple fusion events of neighbouring GUVs. It is possible at some point, when fusion stops that the membrane of the GUV can relax into a circular form but this was not observed in this particular case.

The only thing which seemed to have an influence on these effects was, the light intensity the sample was irradiated with. The higher the intensity was, the more rapid and more severe these effects could be observed. This could indicate a direct connection to the proteins. But it should still be emphasised that these effects were only observed for the inverted emulsion GUVs and not for the electroformed vesicles. There might be a connection to the lipid composition of the inverted emulsion GUVs since similar effects like bursting were observed before in the case of the GUVs formed to include a liquid - liquid membrane phase separation which was already discussed in Chapter 2.2. A reduced membrane edge tension might cause vesicle bursting. What is not clear is, why the formation of transient pores is increased so much compared to vesicle bursting for this type of GUVs. Next to possible oil residues in the lipid bilayer, there could be a connection to the

cholesterol concentration. The lipid compositions for a liquid - liquid membrane phase separation include higher concentrations of cholesterol which leads to a higher rigidity of the membrane. The initial lipid composition for the vesicles in this part of the study, only include 10 mol% of cholesterol and it is possible that only a fraction (if any) actually gets incorporated into the membranes of the inverted emulsion GUVs. All this will need further investigation in the future in order to find the causing factor/factors and to be able to optimise this strategy for internal membrane - membrane adhesion.

5.2. Conclusion

In this part of the study, it could be demonstrated that the use of the two proteins iLID and Nano can lead to a successful internal membrane - membrane adhesion. Although, the actual light switch - ability of the system could not be tested, the adhesion process could be observed in multiple cases when the samples were irradiated by light. The problem with the observation of specific vesosomes in a sample was not just because of their stability. A vesosome which was observed might survive for a longer time period. But the transient pore formation and the busting also introduced movement of the rest of the GUVs. It was often very hard to monitor GUVs in a specific image frame without the need to change the position of any of the three axes. Because of that, observing selected vesosomes over several light and dark cycles was complicated. Immobilising the GUVs should be considered for future experiments. Changing the wavelength to observe the samples and reduce bursting and poration can also be tried although, it is possible that these effects occur independently of the wavelength of the light. This would need to be tested. In general, the whole system will need further optimisation regarding especially the inverted emulsion GUVs but also concerning the efficiency of the vesosome formation in general (mentioned before).

The inverted emulsion GUVs used for this strategy showed several different anomalies which makes them not ideal for the internal membrane - membrane adhesion. The reason for the poration, bursting, budding and fusion events are not clear. The mineral oil residues within the GUV membranes probably, play an important role in this. Osmotic pressure was ruled out as a reason because the solutions were always carefully balanced. It was not tested, if the GUVs would show similar effects without protein binding. What stands out is, the effects seemed to be triggered by light irradiation. It could be observed that when the sample was observed using the oculars of the microscope which uses a higher light intensity, these effects were accelerated and more severe. When switching to the camera, the light intensity irradiating the sample is reduced to a fraction of

the former intensity which decreased the speed, the severity as well as the occurrence of these effects. Severity means, higher light intensity lead to more bursting events while lower intensities caused more transient pore formation but less bursting. Both budding and fusion could be observed the least. This could point to the proteins being also involved in these effects. Studies have shown that some proteins, binding to the membrane of vesicles, can alter the spontaneous curvature which can even be used to fine - tune the curvature and induce specific membrane shapes, budding, fission and vesicle division[229]. However, in the case of vesicle bursting discussed in Chapter 2.3, the problem could be resolved by using a combination of mineral oil and n - decane with silicone oil. As mentioned before, silicone oil can be a problem when used with proteins. Silicone oil can lead to protein aggregation which will reduce the active protein concentration. It might be possible to observe aggregation in the case of the labelled protein Nano in form of visible protein clusters. For iLID, there is no way to determine if the protein is aggregated or not during the experiment, except when testing its binding properties to Nano.

Another possibility could be the formation of the outer GUVs using the microfluidic approach. The problem here could be that the method often uses mineral oil as well and when using the same lipid composition, there is a chance of the vesicles still showing the same effects. An exchange of the organic solvent for this strategy could be inevitable to be able to create stable outer GUVs.

Different lipid compositions could also be tested. Since the essential lipid for the membrane - membrane adhesion, DGS - NTA(Ni) is only used at concentrations of 1 - 2 mol%, the rest of the lipids could be varied in their concentration but could also be exchanged completely. DOPG is a negatively charged lipid with two unsaturated acyl chains. In Chapter 2.2. it was talked about problems when trying to create pure DOPC GUVs from the inverted emulsion method and a possible connection to the amount of oil ending up in between the lipid bilayer. Since, this is not restricted to DOPC but also the case for other lipid compositions including unsaturated acyl chains, the degree of saturation/unsaturation of the acyl chains and the amount of oil within the lipid bilayer could be linked and display a main factor for vesicle stability. The GUVs containing ~ 50 mol% of DOPC were not stable and showed heavy bursting and even concentrations of 10 mol% of an unsaturated lipid lead to poration or even bursting. If this is the reason for the instability of the GUVs from the light switchable proteins, simply exchanging DOPG with POPG could eliminate this issue. Of course, this is highly speculative and needs to be further investigated especially, the differences between the membranes formed from the inverted emulsion method compared to other methods like electroformation, with regards of the lipid bilayers.

The last part for this system is the directed adhesion which could not be tested. In order to achieve a liquid - liquid membrane phase separation more tests are needed to find a sufficient lipid composition including the necessary DGS - NTA(Ni) in adequate concentrations without disturbing the GUV formation or the membrane phase separation. The more simpler solution for this would probably be, to create liquid - liquid membrane phase separated GUVs from the electroformation method since neither the formation nor the stability should be an issue.

6. Conclusions and outlook

6.1. What the current systems are capable of

Actually mimicking the communication of cellular organelles with the plasma membrane and the involvement of membrane contact sites by using GUVs, is a very complex and diverse project. The goal of this study was to investigate possible ways to create an artificial membrane system posing for the cellular organelles and the cell's plasma membrane to mimic membrane contact sites. Clearly it is not currently possible to mimic a complete eukaryotic cell with all its different cellular organelles and all the distinct functions. Instead, only one model organelle is used in form of a GUV. A multi - compartmentalised GUV system, a vesosome, was created with two different GUV types, using two different formation methods. The first method to create the model cellular organelle, is the electroformation method which is usually simple to perform and gives very good results in terms of yield and versatility of the used lipids. The second GUV type is created from the inverted emulsion method and mimics the plasma membrane of the cell. This means, the first GUV type has to be encapsulated into the second type which has to be executed in the moment of the formation of the second GUV type.

In order to mimic membrane contact sites with these multi - compartmentalised GUVs, the membranes of both vesicle types need to come into close proximity (nm range) which is achieved by internalised membrane - membrane adhesion. Three different strategies were developed, tested and discussed in this research study to achieve internal membrane - membrane adhesion. The first strategy employed biotinylated lipids and streptavidin forming a bridge between both vesicle types and creating a strong and irreversible adhesion. The second strategy uses DNA oligonucleotides which are attached to the vesicle membranes via a biotin streptavidin bridge. The resulting membrane - membrane adhesion, established by a complementary oligonucleotide and the biotinylated DNA strands attached to the GUV membranes, enables a certain control over the establishment of the adhesion and makes it possible to observe the adhesion in the moment of its formation. A possible benefit with this strategy is a potential reversibility of the adhesion through the addition of a competitive oligonucleotide. The last one of the three strategies works with the binding of two specific proteins called iLID and Nano which can be triggered by light irradiation and dissociates again in the dark. This gives control over the adhesion, similar to the DNA strategy and an easy way to reverse it again. Even multiple binding and dissociation cycles could potentially

be possible with this strategy, giving it further advantages over the biotin streptavidin as well as the DNA system.

The methods of creating an internal membrane - membrane adhesion in order to mimic membrane contact sites is not ideal this way especially, because it is missing a key feature. The adhesions between both GUV membranes are random considering the area of the two membranes. The adhesion is not limited to a specific area regarding the size of either of the vesicle membranes nor is it directed to a certain region of the membranes and excluded from another. To adapt the model system in order to realise a directed adhesion, one of the GUV types was created to show a liquid - liquid membrane phase separation. Thereby, the membrane of the chosen GUV type would exist in two different phases of which both are composed of different lipids. The specific lipid carrying the moiety relevant for the membrane - membrane adhesion (e.g. the biotinylated lipid) will only be present in one phase and therefore, directing the adhesion to this particular area.

The general idea of these three strategies of creating internalised membrane - membrane adhesions could be executed to a certain extend. All three systems successfully lead to an adhesion between the vesicle types of which biotin and streptavidin showed the most promising results in terms of reproducibility, adhesion quality (extent of adhesion area and contact angle between adhering GUV membranes), adhesion quantity (number of adhered GUV membranes in one sample), simplicity (experimental setup and imaging process) and direction of the adhesion. A directed internal adhesion from this approach was also achieved. The DNA system although, showing adhesion, could not be properly studied in terms of quantity and quality. The major problem was the GUV movement, barely allowing to observe one vesosome over the time of one complete experiment. Reproducing results and properly optimising the system could not be achieved within this project's timescale. For the two proteins iLID and Nano, the adhesion could be observed several times. But the inverted emulsion GUVs produced at the used conditions were not stable and showed several anomalies leading often to loss of the inner GUV or complete bursting of the outer ones. This problem could not be resolved why, it was not possible to get reliable statistics concerning the quantity of the adhesion events. Unfortunately, the latter two systems could not be properly tested considering the reversibility of the adhesion.

All three strategies can be optimised in several ways in the future but already at the point of creating multi - compartmentalised GUVs, there is a lot of potential especially regarding the encapsulation efficiency. A microfluidic approach could be used to increase the encapsulation rate significantly. On the other hand, there might be ways to optimise this without the use of microfluidic equipment. Different factors like the size of the interface could be tested to study how it affects the efficiency of

vesosome formation. A second possibility is to use a stepwise approach of vesicle formation by adding the w/o emulsion in smaller portions and execute multiple centrifugation cycles. This way, the interfacial lipid monolayer could recover in between the centrifugation cycles and more electroformed GUVs could be introduced to be encapsulated. Since the GUVs are not knowingly affected by multiple centrifugation cycles, splitting this step could increase the number of vesosomes.

Changing the organic solvent which is used as oil phase is probably the factor with the highest potential for improvement of the entire method. The mineral oil which was used either exclusively or in combination with other solvents, is, for example, also available at different viscosities. A simple test of various viscosities could give more insight into the dependency of vesicle formation from the viscosity of the organic solvent and the stability of the emulsions created from the oils. But it might also influence the amount of oil residue ending up in the lipid bilayer. Mineral oil, since it is a mixture of many different components, is not an ideal nor very stable solvent in itself. High humidity levels lead to oxidisation and water uptake of mineral oil[230] which can affect GUV formation. To prevent water uptake of the oil, preliminary tests were conducted using a molecular sieve in the mineral oil aliquot. A molecular sieve is a very porous material which can be added to solvents to reduce the water content. The formation of vesicles from the inverted emulsion method using this oil, gave good results considering GUV sizes and shapes and GUV yield (data not shown). These are only some exemplary factors which might influence vesicle formation when using the inverted emulsion method.

Exchanging mineral oil with another solvent could be beneficial in several ways. One possible solvent might be diethyl carbonate which was thought of because of its properties considering polarity, density, viscosity, solubility in water, stability against humidity and temperature and toxicity. Preliminary tests with diethyl carbonate (data not shown) gave good results for vesicle formation with lipid compositions like pure POPC and also from mixtures including DOPC, SM, DPPC, biotinylated lipids and also charged lipids. Membrane phase separated GUVs although, could not be created with diethyl carbonate as organic oil phase. The reason might be a possible reaction of the hydroxyl group of cholesterol with the carbonyl group of the solvent, leading to an esterification of the cholesterol (see Figure 6.1). However, this reaction usually needs an acidic catalyst to increase the reaction rate. Reactions like this are often used to attach protection groups to molecules carrying hydroxyl groups like cholesterol.[231,232] It is unclear, if this form of cholesterol would be incorporated into the GUV membrane or stay within the organic phase which in this case would now be a mixture of diethyl carbonate and ethanol. Also, even though diethyl carbonate and

water do not mix, the polarity of diethyl carbonate is higher compared to mineral oil which could affect the formed GUVs in other ways. If and how diethyl carbonate could potentially work as an alternative oil phase will need more investigation in the future. A second possibility, when looking

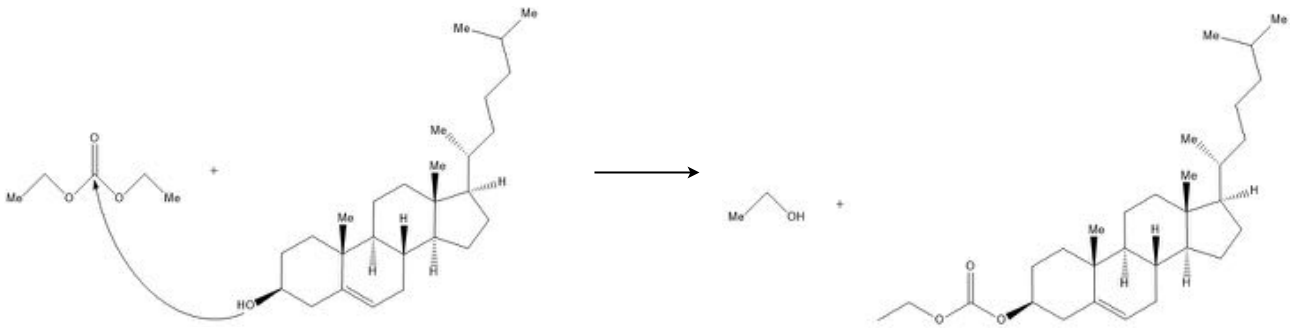

1

Figure 6.1: Hypothetical chemical reaction of diethyl carbonate with cholesterol. The hydroxyl group of cholesterol reacts with the carbonyl group of diethyl carbonate creating an ester bond while eliminating ethanol. The reaction is only hypothetical because the reactivity of both reagents is rather low. The reaction would most likely need an acid catalyst.

at the cholesterol derivate with the ester group (**1**) now attached to it would be, to use this product deliberately to create membrane phase separated GUVs from the inverted emulsion method using mineral oil as organic solvent. Because the low polarity of cholesterol displayed as an issue when using mineral oil, increasing the polarity this way might increase the likelihood of the molecule to participate in the interfacial lipid monolayer and therefore increasing the cholesterol concentration within the GUVs. A similar attempt to increase the polarity of cholesterol is to exchange it with a derivate carrying a larger group with even higher polarity, like biotin. These derivates can be purchased and often include a PEG unit as spacer between the cholesterol and the biotin moiety. The polarity of PEG is neither polar nor completely non - polar meaning, PEG dissolves in both type of solvents and can act as a so called polymer electrolyte[233]. A PEG - biotin group could introduce a high enough polarity to cholesterol, forcing it into the interfacial region. A biotinylated cholesterol would eliminate the need of a fourth lipid, when creating membrane phase separated GUVs composing biotin moieties. If this would work, the adhesion area is probably no longer at the liquid disordered phase but the liquid ordered phase since cholesterol sorts preferentially into the liquid ordered phase (for the biotin streptavidin and the DNA strategy). But exchanging the cholesterol derivate with one that includes biotin raises a different issue. The biotin concentrations used to achieve internal membrane - membrane adhesion is in general very low (2.0 mol% for the inverted emulsion GUVs). When using a biotinylated cholesterol to acquire a liquid - liquid membrane phase separation (cholesterol concentration 25 - 40 mol%) and a membrane adhesion at

the same time, the biotin concentration is increased drastically which could affect not just the membrane adhesion but even the vesicle formation. However, this method can work in lower concentrations to incorporate a suitable biotin concentration to the vesicles. The longer spacer unit in this molecule can, at the same time, improve the biotin streptavidin binding. As discussed in section 3.5., a larger spacer unit between the lipid and the biotin moiety can improve the complex formation and improve the adhesion in quality and quantity. But this only applies for the non - directed internal membrane - membrane adhesion. It is unlikely to effectively achieve a directed internal adhesion at such high biotin concentrations.

For future studies concerning the DNA strategy, there is the issue of vesicle movement. The GUVs and vesosomes should be immobilised either by using a microfluidic chip, using a design similar to the valve device which was discussed in Chapter 4.2 or using agarose gel[223]. In both cases, the GUVs have to be harvested from the formation vessel which could lead to clustering and loss of GUVs and vesosomes in particular. Because of that, the formation in a different vessel (e.g. an Eppendorf tube) could be advantageous from which the GUVs could be harvested easier. If the immobilisation could be achieved, a more detailed study of the membrane - membrane adhesion established through oligonucleotide binding can be conducted including the reversibility using a competitive oligonucleotide.

For the light protein system, membrane poration, bursting, budding and fusion of the inverted emulsion GUVs display a major problem. In the case that mineral oil traces within the bilayer are the main reason for this and if there is a direct dependency of the concentration of unsaturated lipids (DOPG here) to the amount of oil in the membrane, excluding lipids with two unsaturated acyl chains should improve the GUV stability by reducing the amount of oil within the lipid bilayer. Different lipid compositions will need testing. More analytical data on the actual membranes will be needed in the future to optimise the vesicle formation more target - oriented. This means, gaining more knowledge on, for example oil residue within the vesicle membrane in order to be able to prevent or remove it. If there is oil, what are factors influencing this effect or the amount of it? Another point would be the difference in initial lipid composition of the solutions and final lipid composition of the membrane. Is there a difference for all lipid types or just for some lipids and how can a difference of initial and final lipid composition be prevented?

There have been studies in the past on lipid bilayers to attain more knowledge on lipid distribution[234], lipid flip flop[235] and membrane phases[236,237] using for example NMR and fluorescence microscopy. But a complete analysis of the lipid composition of vesicles could not be achieved by now. Especially for the inverted emulsion method, a more detailed knowledge about

the actual lipid composition and the extend of solvent traces within the lipid bilayer would change the whole characterisation of these vesicles (also in case of other methods using organic solvents). NMR measurements on GUVs created from a single lipid could help to clarify, if there are traces of organic solvent within the lipid bilayer, to what extend and if there is a direct dependency between the type of lipid (degree of saturation) and the amount of oil in the bilayer. Not just NMR can be employed to deepen the knowledge about the actual lipid composition of a membrane including molecules that might be incorporated into the membrane or in between the two leaflets. Other promising methods are fluorescence microscopy[236], x - ray diffraction[238], infrared spectroscopy[239] and mass spectrometry[240,241] which were all employed in the past for membrane analytics to some extent.

6.2. What the future could bring

Besides the optimisation of the three strategies used in this study, there are further projects which could evolve in the future, originating from this research.

Apart from the three - stranded DNA strategy, a two - stranded DNA strategy was also developed to achieve the internal membrane - membrane adhesion but could not be included in this study due to a lack of time. In Figure 6.2, a schematic of the system is depicted. The two - stranded system is supposed to work similar to the three - stranded one by introducing the first biotinylated oligonucleotide before the formation of the outer GUVs and the second oligonucleotide which is also biotinylated is added after membrane pore formation using α - hemolysin. The second strand is labelled with Atto 488, to be able to visualise the oligonucleotide entering the lumen of the outer GUV. It is not advisable to encapsulate the second oligonucleotide along with the inner GUVs and streptavidin in order to prevent streptavidin binding exclusively to the DNA oligonucleotides. The two DNA strands are designed to bind to each other, creating the membrane - membrane adhesion without the need of a third bridging strand. The DNA sequences were chosen accordingly (see Table 2).

The third oligonucleotide for this system is the competitive strand which would be used to reverse the adhesion. The reversibility is designed in the same way as for the three - stranded system, to initiate pairing at the two unbound triplets of DNA 1. In general, this system could turn out to be easier executed since, it is missing one step of solution adding to the vesicles and therefore, reducing GUV movement. But similar to the three - stranded system, it would be best to be able to eliminate this issue completely. Other than that, the three - stranded strategy and the two - stranded strategy remain very similar.

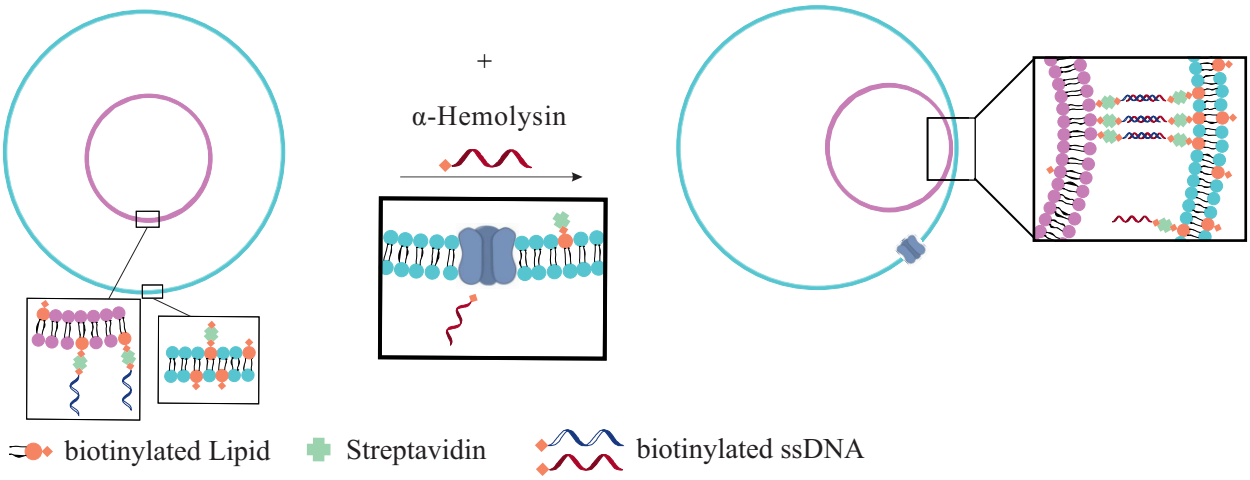

Figure 6.2: Schematic illustration of the internal adhesion of the membranes of inner and outer GUV by two oligonucleotides. Biotinylated lipids are drawn in red, streptavidin is drawn in green. The blue biotinylated oligonucleotide is encapsulated alongside the electroformed GUVs and streptavidin, and binds to the inner GUVs. Using α - hemolysin, membrane pores are created within the outer GUV membrane. The second oligonucleotide is added and enters the outer GUV through the membrane pores. The biotinylated DNA binds to the membrane of the outer GUV and binds to the oligonucleotide attached to the inner GUV creating a membrane - membrane adhesion.

Table 2: Table of the oligonucleotide sequences.

DNA 1	biotin - 5’ - AATAATAATAATCTCCAA - 3’
DNA 2	biotin - Atto 488 - 5’ - TTATTATTATTACTCCAA - 3’
DNA 3	Atto 488 - 5’ - TTGGAGAATAATAATAAT - 3’

A further extension to both of the DNA systems can be, to test the reversibility of the adhesion not by the use of a competitive oligonucleotide but through heat. Other studies which used single stranded DNA for external membrane - membrane adhesion[242,243], proved the reversibility of the adhesion by heating up their samples[242]. When the temperature was lowered again, the adhesion re - established. This means, similar to the membrane - membrane adhesion using iLID and Nano, the membrane - membrane adhesion using oligonucleotides can be switched on and off using temperature changes in comparison to light switching. Experiments on GUVs created from the inverted emulsion method and electroformation method have shown, the GUVs can withstand temperatures of ~ 75 °C (see Figure 6.3) and probably even higher temperatures. One change visible in both examples of Figure 6.3 is, heating the sample leads to the GUVs coming closer together which is an effect of evaporation of small amounts of water from the sample (even if the imaging vessels were covered during heating cycles). Alongside these trials, there is also the possibility to test the temperature resistance of the inverted emulsion GUVs in general.

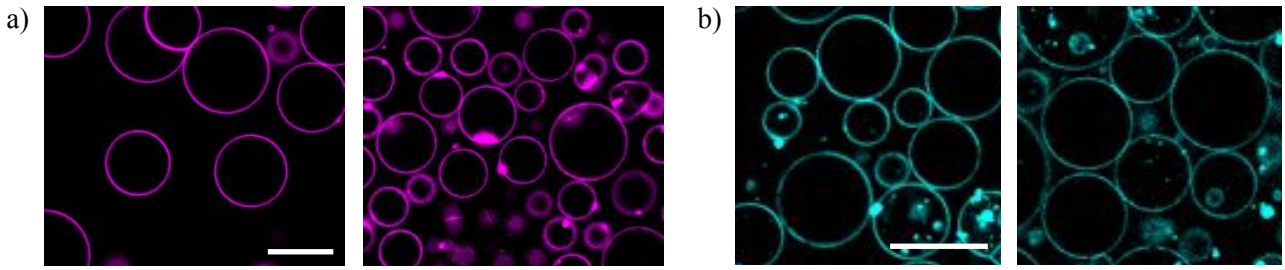

Figure 6.3: a) Fluorescence confocal microscopy images ($DiIC_{18}$ channel) of electroformed GUVs before (first image) and after heating (second image) to ~ 75 °C. The lipid composition is 1 : 1 : 1 of DOPC : SM : cholesterol with 0.1 mol% $DiIC_{18}$. b) Fluorescence confocal microscopy images (Atto 633 channel) of inverted emulsion GUVs before (first image) and after heating (second image) to ~ 75 °C. The lipid composition is 1 : 2 : 1 of DOPC : SM : cholesterol with 0.1 mol% Atto 633 DOPE. Scale bars: 20 µm

The only adhesion strategy left that seems to be not reversible is the biotin streptavidin system. A study which was published by the group around Mathias Uhlén could change this. They used aqueous solutions at temperatures of > 70 °C to reversibly break the biotin streptavidin complex[244]. Before that, when the bond between biotin and streptavidin was broken, streptavidin was denatured and therefore not reusable. With their method, using short incubation times and nonionic aqueous solutions, it might be possible to reverse the internal membrane - membrane adhesion and even re - establish the adhesion again. Similar to the DNA strategy, the biotin streptavidin adhesion could be evolved to become temperature switchable. The only issue which could intervene with this, is the problem of the dependency of certain forces to obtain biotin streptavidin binding which was discussed in Chapter 3.5. and actually applies to both the biotin streptavidin strategy and the DNA strategy. Because the DNA strategy also uses a biotin streptavidin bridge to attach the oligonucleotides to the GUV membranes, heating up the samples could not just break the DNA binding but also the biotin streptavidin bridge. In order to solve this, both systems would need initial changing. In the case of the DNA adhesion, eliminating the biotin streptavidin bridge and directly attaching the oligonucleotides to the GUV membranes would improve the whole system. Boxer et.al. used this method in 2009, where they removed the lipid head group and replaced it with the oligonucleotide[243]. It is yet unclear if lipids functionalised in this way, will be incorporated into a vesicle membrane when the inverted emulsion method is used for their formation. Although, the nucleobases provide the necessary polarity for the lipids to sort not just into the lipid layers but also to not be lost within the organic oil phase. If this attempt would be successful, the three - stranded DNA system would only need the encapsulation of the complementary strand DNA 3 to achieve membrane - membrane adhesion and no membrane pores would have to be formed. The overall complexity of the experiment would be eliminated. But in the case of reversing the adhesion by the addition of the competitive strand DNA 4, membrane pores will be necessary. In the case of a

possible temperature driven switch - ability, the system has the potential to be easily created and operated.

Turning again to the biotin streptavidin strategy and what change could improve the system in order to be able to switch the internal membrane - membrane adhesion by using temperature changes. In Chapter 3.5., it was already discussed that the problem could be solved by exchanging the biotinylated lipid with one that contains a larger spacer unit, creating a greater distance between the GUV membranes and the biotin moiety. This way, streptavidin and biotin could be able to bind easier which might eliminate the factor of the centrifugation speed influencing the membrane - membrane adhesion discussed in Chapter 3. A very prominent solution is the use of a biotinylated lipid which includes a PEG unit. The most common lipid is 1,2-distearoyl-sn-glycero-3-phosphoethanolamine-N-[biotinyl(polyethylene glycol)-2000] (DSPE - PEG (2000) biotin) which is commercially available. Another option is, to synthesise the biotinylated lipid themselves by simply attaching a biotin - PEG unit to the desired lipid. As mentioned before, a biotinylated cholesterol can also be chosen but would need more testing in advance considering the incorporation rates into the membranes. If the longer spacer unit leads to an easier complex formation in the case of the internal membrane - membrane adhesion, this could also increase the quantity of the adhesion events because lower centrifugation speeds could be used for the formation of the inverted emulsion GUVs which can increase the encapsulation rates of the electroformed GUVs. This specific change has the potential to improve the complete strategy by increasing the number of formed vesosomes as well as the number of adhesion events and introducing the possibility to activate and deactivate the adhesion through temperature changes. But there is also the possibility that an exchange of the biotinylated lipid could lead to other side effects. Using a different biotinylated lipid could lead to a biotin streptavidin binding within the aqueous droplets of the w/o emulsion and before the completed formation of outer GUVs which could interfere with the vesicle formation.

Because the biotin streptavidin strategy is the most robust in this whole study, there is also the idea to take the system a step further by trying to mimic communication between the model “plasma membrane” and the model “cellular organelle”. This would be a complex system which would need meticulous experimental planning. The idea is to introduce an agent to the inner GUV within a vesosome but avoiding at the same time, for the agent, to enter the lumen of the outer GUV. The internal membrane - membrane adhesion functions as a sort of membrane contact site, achieving a close proximity of the two membranes to each other. A communication could then be established by using membrane pores. To be able to introduce an agent, e.g. a fluorescently labelled molecule like fluorescein or calcein to the inner GUV, both vesicle types need to contain membrane pores but

only within the adhesion area. Since the creation of membrane pores cannot be restricted to certain membrane areas, both vesicle types would end up with pores all over their membranes. The deactivation of the membrane pores which are not localised within the adhesion area can be achieved by using the molecule TRIMEB which can block existing membrane pores[93,94,95]. Naturally, this blocker molecule can also not work exclusively within certain membrane areas. Because of this, it is experimentally difficult to establish a pathway through the adhesion area in order to access the inner GUV lumen. The concentration for every chemical will need to be very precise for their purpose. The experiment might be executed in the following way: Electroformed GUVs are created from the well known lipid composition used in the biotin streptavidin strategy. The GUVs are mixed with a solution of α - hemolysin to create membrane pores. Excess α - hemolysin needs to be removed for example by washing the GUVs with an adequate sugar solution (osmotically balanced). The GUVs are afterwards mixed with a solution of streptavidin and TRIMEB but not incubated. The mixture is going to be encapsulated by which the membrane - membrane adhesion is established very quickly. The concentration of TRIMEB will be needed in excess to not just block the membrane pores of the inner GUVs but also, to be available for the membrane pores which are going to be incorporated into the membranes of the outer GUVs later in the experiment. Through the membrane adhesion, the membrane pores within this area are ideally sealed off from the access of the blocker molecules within the outer vesicle lumen. In the next step, α - hemolysin will be added to the external solution to create pores within the membranes of the outer GUVs. Because the inverted emulsion GUVs have the blocker molecule encapsulated, the formed pores can be blocked from the inside immediately after their formation with the exception of the membrane pores at the adhesion area. This way a passage way is created for molecules to enter exclusively the inner GUV. The last step in the experiment would be the addition of a fluorescently labelled agent and measuring the signal intensity in the lumen of the inner GUV over time. Ideally, the fluorescent signal will be excluded from the lumen of the outer GUV or at least shows a certain time delay compared to the signal of the inner GUV. This experiment, at this time, is not been executed and will definitely need more time to be optimised and further investigated. Especially, information on thermodynamic and kinetic aspects of the function of the TRIMEB molecule are needed, to be able to optimise the system. For example, the blocking of the membrane pore could be delayed in the case of the inner GUVs at lower temperatures which could prevent pore blocking at the adhesion area. But these are all just assumptions and gaining more data will be essential to successfully mimic the communication between the model “plasma membrane” and the model “cellular organelle”.

A different project which could evolve from this study could take advantage of the directed adhesion attempt. By using the directed membrane - membrane adhesion in an external way, it might be possible to create a GUV construct composing of different GUV types which are adhered in a specific way to each other and thereby forming a specific assembly. Initially, microfluidic chips can be used to achieve a specific sorting of different GUV types, creating some sort of tissue - like assembly. Taking this idea which initially comes from Dr. Tom Robinson and combining it with the directed membrane - membrane adhesion which was achieved within this study in an internalised manner, one could build large artificial tissues (proto-tissues). By creating Janus particles with different moieties in both phases of the GUVs, a specific binding pattern is possible even when using only one type of vesicles but two different adhesion strategies. In order to be able to form assemblies like this, vesicles must be created showing a liquid - liquid membrane phase separation (Janus particles) with one adhesion moiety on the liquid ordered phase, for example biotin and another, not compatible with the first, on the liquid disordered phase like DNA oligonucleotides. This way, the ordered phases of the GUVs will need streptavidin to establish an adhesion while the disordered phases will need a compatible DNA oligonucleotide. In this way, ordered phases could only adhere to ordered phases and disordered only to disordered phases. Developing this idea even further and using multiple different GUV types and several other adhesion strategies, the creation of much more elaborate artificial tissues could be realised. It might be possible to introduce an even higher order of control by creating special designed patterns by directing the adhesions on a single GUV level. Or one could introduce a reaction cascade into the artificial tissue with a specific reaction type for every GUV type which will be triggered by the vesicle next to it, similar to the reaction cascades created within a multi - compartmentalised vesicle to synthesise two different proteins in each of its compartments[126]. This cascade could spread over three or maybe even four GUV types depending on the reactions and the adhesions[245].

During this study, the inverted emulsion method was extensively used to create GUVs and vesosomes. Distinct differences were revealed when comparing the method to others that are purely based on aqueous solutions. A severe discrepancy is the missing ability to form vesicles from lipids containing purely unsaturated acyl chains like DOPC. The formation of DOPC vesicles displays no problem when using the electroformation method. But in the case of the inverted emulsion method, unsaturated lipids seem to affect GUVs already at low concentrations. Throughout this research, numerous anomalies could be documented which could be caused by a decrease in membrane edge tension. The assumption is that there is a certain correlation of the use of unsaturated phospholipids and the amount of mineral oil within the lipid bilayer which results in an increase of transient pore formation through factors like light irradiation. Unsaturated acyl chains in a lipid bilayer are not as tightly packed as saturated lipids because double bonds are causing kinks in the carbon chains

Figure 6.4: Theoretical schematic of two membrane composed of mainly saturated phospholipids and mainly unsaturated phospholipids. Possible mineral oil within the bilayer shown in orange.

which means, the acyl chains take up more room (see Figure 1.6, Figure 1.8 and Figure 6.4). A membrane created from the inverted emulsion method and composed of mainly saturated lipids probably contains lower amounts of oil compared to a membrane composed of mainly unsaturated lipids, due to the lipid packing (see Figure 6.4). To find out more about this, an essential part would be to get to know more about possible oil residues within the lipid bilayer of the GUVs. In the former section, many analytical methods were mentioned which could help to investigate this and maybe even identify some distinct components which might interact with the lipids. The knowledge gained from the analytical data could then be used to create models and maybe even simulations of single components within the lipid bilayer. This could help to identify the differences in lipid packing or other characteristics that might lead to the effects of transient pore formation, budding, fusion and even bursting of GUVs. In GUV preparation from microfluidic systems, different strategies were developed to minimise the oil traces within the lipid bilayer[54,116,246]. Transferring this knowledge onto the inverted emulsion method, if possible, might be a way for optimising the method by effectively reducing the oil residue to a minimum. This is definitely a very complex system to analyse with multiple factors which might or might not be involved. But even small accomplishments here could help to characterise the vesicles from this method further which are already widely used in the field of bottom - up synthetic biology and to assess, if these type of GUVs are suitable to work as model membranes mimicking natural membranes from eukaryotic cells.

7. Materials and methods

7.1. Materials

All phospholipids 1-palmitoyl-2-oleoyl-sn-glycero-3-phosphocholine (POPC), 1,2-dioleoyl-sn-glycero-3-phosphocholine (DOPC), 1,2-Dioleoyl-*sn*-glycero-3-phospho-*rac*-(1-glycerol) sodium salt (DOPG), 1,2-dipalmitoyl-sn-glycero-3-phosphocholine (DPPC), Sphingomyelin (Egg, Chicken) (SM), cholesterol (ovine wool, > 98 %) (Chol), 1,2-dioleoyl-sn-glycero-3-phosphoethanolamine-N-(cap biotinyl) (sodium salt) (PE biotin), 1,2-dioleoyl-*sn*-glycero-3-[(N-(5-amino-1-carboxypentyl)iminodiacetic acid)succinyl] (nickel salt) (DGS - NTA(Ni)) were purchased from Avanti Polar Lipids.

1,1′-Dioctadecyl-3,3,3′,3′-tetramethyl-indocarbocyanine perchlorate ($DiIC_{18}$), 1,1'-Dioctadecyl-3,3,3',3'-Tetramethylindodicarbocyanine, 4-Chlorobenzenesulfonate Salt ($DiDC_{18}$) and streptavidin Alexa Fluor™ 488 conjugate were obtained from Invitrogen, Thermo Fischer Scientific.

1,2-Dioleoyl-*sn*-glycero-3-phosphoethanol-amine labeled with Atto 633 (Atto 633 DOPE), Casein from bovine milk and phosphate - buffered saline (PBS buffer) tablets, mineral oil (BioReagent, for molecular biology, light oil), α - hemolysin from s*taphylococcus aureus*, streptavidin from *streptomyces avidinii* (unlabelled), glucose, sucrose and the atmosbag glove bag were purchased from Sigma Aldrich.

Absolute ethanol was purchased from VWR International, LLC.

DNA oligunucleotides were purchased from Metabion international AG, Germany.

Nano and iLID were provided by the group of S. Wegner of from the Institute of Physiological Chemistry and Pathobiochemistry of the Westfälische Wilhelms - University Münster.

Tris(hydroxymethyl)aminomethane (TRIS) buffer, n-decane and silicone oil (M50) were purchased from Carl Roth, Germany.

Four - inch silicon wafers were purchased from Si - Mat, Kaufering, Germany.

SU8 3025 was purchased from Microchem, Newton, MA, USA.

Film masks were purchased from Micro Lithography Services, Chelmsford, UK.

The mixture for polydimethylsiloxane (PDMS) is prepared from a SYLGARD 184 Silicone Elastomer Kit and was purchased from DOW.

Chloroform stabilised with ethanol was purchased from SupraSolv.

Biopsy puncher (1.5 mm) were purchased from Kai Europe, Solingen, Germany.

Protein LoBind Eppendorf Tubes and Safe-Lock Eppendorf Tubes were purchased from Eppendorf AG, Hamburg, Germany.

High Content Imaging Plates (microtiter plates) were obtained from Corning Inc. USA.

The osmolarity of the solutions was measured using an Osmomat 3000 freezing point osmometer from Gonotec. Osmometer measuring vessels for Osmomat 3000 were purchased from Gonotec, Berlin, Germany.

An Integra UV plus Reinstwasseranlage provided MilliQ water.

The BASE 120 - neMESYS Niederdruckmodul V2 syringe pump from CETONI GmbH Germany was used for all experiments executed in microfluidic chips.

Sonication of solutions was executed using a FB15046 sonication bath from Fisherbrand.

A function generator from Keysight, Model 33220A was used for all GUV formation from the electroformation method.

A Hettich centrifuge Rotina 420R was used for centrifugation of microtiter plates, microfluidic chips and other solutions.

7.2. Methods

Sugar solutions for all experiments were prepared to a concentration of 0.6 - 0.9 M. For every experiment, the osmolarity of all sugar solutions was carefully balanced to a maximum difference of Δ 5 mOsmol/kg. All aqueous solutions were prepared using MilliQ water.

A Leica TCS SP8 CSU confocal laser scanning microscopy with a 63 x magnification objective was used. The imaging software Leica Application Suite X (LAS X) was used and in general set to sequential imaging to be able to observe all fluorescence channels and a brightfield channel in parallel. The scanning speed was set to 400 - 600 Hz and the numerical aperture was put to 1.2. Three lasers were used for the different fluorescent signals, a 638 nm diode laser, a 552 nm OP SL laser and a 488 nm OP SL laser. The used corresponding detectors were a hybrid detector HyD for the 638 nm diode laser and two photomultiplier PMT detectors for the two OP SL lasers. The PMT detector for the 488 nm signal was paired with a PTM trans detector for brightfield imaging.

Microfabrication (microfluidic chip fabrication):

For the preparation of the microfluidic chips, 4" silicon wafers with the required design were produced via soft photolithography to a height of 20 µm. Silicon wafers, coated with SU8 3025 were exposed to UV light through a film mask and un. - exposed photoresist was removed. Silanisation was performed by overnight incubation with 50 µL of 1H,1H,2H,2H-perfluorodecyl-

trichlorosilane in a desiccator. PDMS - based chips were produced by pouring the PDMS/curing agent mixture (10 : 1) on top of the silanised wafer and then curing at 80 °C for two hours. Cured PDMS was removed from the master mold and holes were punched at dedicated inlets and outlets using a 1.5 mm biopsy puncher. A small reservoir made from 200 µL pipette tips, with capacities of 150 µL, were glued to the inlet with PDMS and cured for a period of 60 minutes at 80 °C. This was followed by bonding to pre - cleaned glass coverslips using an air plasma treatment (Plasma Cleaner PDC - 002 - CE, Harrick Plasma, Ithaca, NY, USA) at 0.6 bar for 1 minute.[77]

Electroformation method:

A 2.0 mM lipid solution containing the desired lipid composition and 0.1 mol% fluorescent dye was spread on the surface of two conductive glasses which are coated with indium tin oxide (ITO). The lipid film was dried for 60 minutes under vacuum to remove the chloroform before the electroformation chamber was assembled with the conductive sides of the glasses facing each other, separated by a 2.0 mm thick Teflon spacer. The chamber was filled with a sucrose solution and connected to a function generator with an AC current of 1.6 - 2.0 V_{pp} and a frequency of 10 Hz for 2 - 4 hours. After that the GUVs were harvested for further use.[51]

Inverted emulsion method:

A volume of 50 µl of an 8 mM lipid solution with the desired lipid composition including a fluorescent dye was prepared in a glass vial and the chloroform carefully evaporated using argon gas before putting the vial in a desiccator under vacuum for 60 minutes. The dried lipid film was dissolved in 1.0 ml mineral oil (only opened at humidity levels less than 10 %, a glove box or an “atmosbag” glove bag was used). The final lipid concentration was 400 µM. The mixture was sonicated for at least 30 minutes at degas mode at room temperature. If the mixture was not completely dissolved, sonication was continued for another 30 minutes. The lipid - mineral oil solution was then incubated over night in the dark at room temperature.

The vesicle formation was performed in a 96 well microtiter plate. The wells of the plate were coated with 25 µl of a 2 mg/ml β - Casein solution and placed under vacuum for 60 minutes. Remaining traces of fluid in the wells were removed if any was left afterwards. 50 µl of glucose solution was added to the well before 20 µl of the lipid - mineral oil solution is carefully added on top to form the interfacial lipid monolayer. The plate was covered and incubated for 30 minutes. 5 µl of sucrose solution were mixed with 200 µl lipid - mineral oil solution in a 1.5 ml Safe Lock Eppendorf Tube and rubbed a few times over an Eppendorf rack to form a w/o emulsion. 50 µl of

this emulsion were carefully added on top of the well of the microtiter plate and centrifuged for 3 minutes. Afterwards GUVs were imaged directly in the microtiter plate.

Size analysis for inverted emulsion GUVs:

The lipid - oil solutions for the inverted emulsion method was prepared as stated above. All samples were prepared using the same lipid composition and sugar concentrations. The GUVs were prepared in the usual way using centrifugation speeds from 100 - 4000 x g. For every sample, three wells were prepared and analysed by imaging the entirety of every well remotely and measuring at least 1000 GUVs manually per sample to acquire the mean GUV size for every prepared sample. Size measurements were executed using the Leica LAS X software.

Creation of multi compartmentalised GUV using the inverted emulsion method:

Electroformed GUVs were prepared as stated above as were the lipid - oil solutions for the inverted emulsion method. To encapsulate electroformed GUVs, 5 µl of the GUV solutions were mixed with 200 µl of the lipid - oil solution and rubbed to a maximum of three times over an Eppendorf rack to form a w/o emulsion. 50 µl of this emulsion was carefully added on top of the well of the microtiter plate and centrifuged for 3 minutes. Afterwards, GUVs were imaged directly in the microtiter plate.
A statistic on the size ratios between inner and outer GUVs was set up from three samples (with three wells per sample) prepared from a centrifugation speed of 250 x g. All vesosomes were counted and ratios calculated. Imaging of the entirety of the wells were conducted manually. A second statistic was set up from samples prepared at centrifugation speed ranging from 150 - 300 x g with three wells per sample. All vesosomes per sample were counted and error bars (standard deviation of mean) calculated from the differences in number of vesosomes per sample. Imaging of the entirety of the wells were conducted manually. A third statistic from the samples prepared at a centrifugation speed of 250 x g was set up. 500 GUVs were counted in total and the percentages calculated of the GUVs without encapsulations, with one GUV encapsulated, two GUVs, three GUVs and more (more than three GUVs and impurities).

General chip experiments:

The micro - channels of the chip were coated with β - casein by adding 80 µl to the reservoir and centrifuging the chip at 900 x g for 10 minutes. After another 30 minutes of incubation at room temperature, the chip was connected via the outlet to the syringe pump in withdraw mode and 80 - 100 µl of a glucose solution was added to the inlet. The glucose solution was used to wash the

excess β-casein from the channels. The pump was set to a flow rate of 8 - 10 µl/min. A 20 x magnification objective is used for imaging.The GUVs are not created on chip but harvested after formation and 50 - 100 µl were flushed into the chip afterwards at flow rates around 1 - 3 µl/min.

External adhesion on chip:

For the external adhesion experiments, the GUVs were prepared from the electroformation method with increasing concentrations of PE biotin (0.1 - 2.0 mol%). As the main lipid, POPC was used. Atto 633 DOPE (0.1 mol%) was used in all cases as membrane dye. GUVs and streptavidin - Alexa 488 were mixed in a Protein LoBind Eppendorf Tube 1:1 v/v to a final streptavidin concentration of 150 nM and incubated for about 15 minutes at room temperature. 50 - 100 µl of the mixtures were flushed into the microfluidic chip at a flow rate of 2 µl/min. One chip was used per sample. For all concentrations, a number of ~ 300 GUV adhesions were measured with three points for every single bilayer intensity and three points for every double bilayer intensity. The error bars give the standard deviation of the mean fluorescence signal.

Reversed flow chip experiment:

Electroformed GUVs were prepared as stated above including 0.1 mol% PE biotin. The inverted emulsion GUVs were prepared as stated above including 2.0 mol% PE biotin. The inverted emulsion GUVs and streptavidin - Alexa 488 were mixed in a Protein LoBind Eppendorf Tube 1:1 v/v to a final streptavidin concentration of 150 nM and incubated for about 15 minutes at room temperature. 50 - 100 µl of the mixtures were flushed into the microfluidic chip at a flow rate of 2 µl/min until the traps were adequately filled. The fluid flow was reversed to a rate of 0.25 µl/min and the sample monitored until the traps are empty. The same procedure was executed with a sample of the electroformed GUVs as well as a mixture of inverted emulsion GUVs and electroformed GUVs. A fourth sample was processed in the same way, from a mixture of both GUV types without streptavidin.

Streptavidin encapsulation efficiency:

The inverted emulsion GUVs were prepared as stated above from pure POPC and 0.1 mol% Atto 633. Streptavidin concentrations from 50 - 200 nM were encapsulated. Intensity measurements were conducted on bulk streptavidin in xzy scan mode to get a more accurate value for the intensity(in xyz scan mode, the fluorescence intensity varies when the z - position is altered) and encapsulated streptavidin in xyz scan mode. For every GUV sample, 500 GUVs were measured.

A second experiment was conducted with a streptavidin solution (final concentration 50 nM) encapsulated in inverted emulsion GUVs from pure POPC and 0.1 mol% Atto 633. The fluorescence intensity of 5 GUVs within one image frame was measured over a time period of 120 minutes. The minor difference in fluorescence intensity compared to the former experiment is a result the preparation of a fresh sample and of a change in imaging settings considering the gain of the detector used for the streptavidin signal (experiments were conducted on different days).

Internal adhesion of membranes using biotin - streptavidin:

Depending on the concentration of the sucrose solution used to create the electroformed GUVs, an equi - molar glucose/PBS solution (ratio 4:1 v/v) was prepared. A streptavidin solution of 750 nM in PBS buffer was used. The emulsion was prepared from electroformed GUVs and a 750 nM streptavidin solution (final concentration 150 nM, if not stated otherwise) at a 4:1 v/v ratio (no incubation time). 5 µl of the mixture and 200 µl of the lipid - mineral oil solution were mixed in a 1.5 ml Protein LoBind Eppendorf Tube. The Eppendorf Tube was rubbed to a maximum of three times over an Eppendorf rack to form a w/o emulsion. Centrifugation is performed at 250 x g for 3 minutes (if not stated otherwise). Afterwards, the GUVs were imaged directly in the microtiter plate.

A statistic on the membrane - membrane adhesion quantity was conducted from three samples (with three wells per sample) prepared from a centrifugation speed of 250 x g and varying streptavidin concentration (50 - 200 nM). At least 500 GUVs were counted aper sample (not per well!). Error bars represent the variation between the three samples per concentration. Imaging of the entirety of the wells were conducted manually. A second statistic was conducted on the number of encapsulations in juxtaposition to the internal membrane - membrane adhesions in percentages at increasing centrifugation speeds (150 - 300 x g). Values for vesosomes are given in total numbers. Error bars represent the variation between different samples (not wells). Percentages of membrane adhesions calculated from the total numbers of the vesosomes.

Liquid - liquid membrane phase separated GUVs from the inverted emulsion method:

The mineral oil solution was prepared in the usual way with a lipid composition of 20.0 mol% DOPC, 30.0 mol% DPPC, 47.9 mol% cholesterol, 2.0 mol% PE biotin and 0.1 mol% Atto 633 DOPE (also with 40.0 mol% DPPC and 37.9 mol% cholesterol). A second oil solution was prepared using the same lipid composition. After drying the lipid solution in chloroform using argon gas and drying the lipid film in the vacuum for 60 minutes, the lipid film was dissolved in n-decane and

afterwards silicone oil was added stepwise to the solution and vortexed in between for better mixing. The final solution was made from 6.0 % n-decane and 94.0 % silicone oil. Both, the mineral oil - lipid mixture and the n-decane/silicone oil - lipid mixture were incubated overnight in the dark at room temperature.

All steps from this point on were executed in an oven, set to ~ 65 °C and all solutions were kept at the same temperature. The wells of the microtiter plate were coated with 25 µl β-casein in the usual way. After drying the plate in the desiccator under vacuum, 50 µl glucose/PBS solution were added to the wells. The interfacial lipid monolayer was created using 40 µl of the n-decane/silicone oil - lipid mixture added on top. After an incubation time of 30 minutes at ~ 65 °C, the emulsion prepared in the usual way using the mineral oil - lipid mixture, was poured on top of the well and centrifuged for 3 minutes at room temperature before imaging the sample.

Deflation and Inflation experiment:

The vesosome internal membrane - membrane adhesion system using biotin - streptavidin was prepared as above. The oil layer on top of the well was removed by taking off 70 µl from the top before adding 20 µl of glucose/PBS solution. The microtiter plate was centrifuged again and another 30 µl were taken from the top again. Afterwards the sample was monitored with the microscope for the rest of the experiment. A ~ 3000 mM glucose/PBS solution was added stepwise in volumes of 5 µl per portion to deflate the GUVs/vesosomes. After every addition, the sample was incubated for 10 - 15 minutes. The final sugar concentration of the vesicle solution was ~ 2000 mM. In the next part, water was added stepwise in 5 µl portions to reverse the deflation.

DNA oligonucleotide test binding to inverted emulsion GUVs:

The inverted emulsion method was prepared as stated above including 2.0 mol% PE biotin. A final concentration of 1.0 µM DNA 2 and 1.0 µM streptavidin was encapsulated. Two different DNA batches were tested to visualise the DNA binding to the membrane of the inverted emulsion GUVs.

Internal adhesion of membranes using DNA oligonucleotides:

Electroformed GUVs were prepared as stated above including 0.1 mol% PE biotin. The lipid - oil solution for the inverted emulsion method was prepared as stated above including 2.0 mol% PE biotin. Depending on the concentration of the sucrose solution used to create the electroformed GUVs, an equi - molar glucose/PBS solution (ratio 4:1 v/v) was prepared. A streptavidin solution of 4 mg/ml (unlabelled) in PBS buffer was used. DNA stock solutions were prepared by dissolving the

solid DNA powder in MilliQ water to a final concentration of 100 µM. The vials were vortexed for 2 minutes before centrifugation for ~ 10 seconds at 150 x g. 100 µl electroformed GUVs were incubated with 1.0 µl DNA 1 stock (unlabelled) and 1.5 µl streptavidin stock for 30 minutes. After a second addition of 1.5 µl streptavidin to the mixture without incubation, 5 µl of the mixture and 200 µl of the lipid - mineral oil solution were mixed in a 1.5 ml Protein LoBind Eppendorf Tube. The Eppendorf Tube was rubbed to a maximum of three times over an Eppendorf rack to form a w/o emulsion. Centrifugation was performed at 250 x g for 3 minutes. The oil layer on top of the well was removed by taking off 70 µl from the top before adding 20 µl of glucose/PBS solution. The microtiter plate was centrifuged again and another 30 µl were taken from the top again. Afterwards the sample was closely monitored with the microscope for the rest of the experiment. A mixture from an equi - osmolar sucrose solution with a final concentration of 0.5 mg/ml α - hemolysin was prepared and added very carefully in 5 µl steps with an incubation time of 30 minutes to the GUV solution until the GUVs lost their contrast within the brightfield channel. A mixture of 1 µl DNA 2 stock (labelled) and 4 µl sucrose solution was added next with an incubation time of 30 minutes or until the DNA signal is visible within the GUV lumen. DNA 3 (labelled) was added in the same way to the GUV solution and incubated until an internal membrane - membrane adhesion was visible. Fluorescence measurements were conducted using the Leica LAS X software.

Internal adhesion of membranes using iLID and Nano:

The first type of GUVs was created from the electroformation method from a lipid composition of 78.9 mol% POPC, 10.0 mol% DOPG, 10.0 mol% Chol, 1.0 mol% DGS - NTA(Ni) and 0.1 mol% $DiDC_{18}$. The second GUV type was formed from the inverted emulsion method using the same lipid composition just with 0.1 mol% $DiIC_{18}$ as membrane dye. Before the encapsulation process a 1.0 µM solution of iLID and Nano in TRIS buffer was prepared.

8 µl of the electroformed GUVs were mixed with 1 µl of iLID solution and incubated for 15 minutes before adding 1 µl of Nano solution. Afterwards, 5 µl of the mixture were added to 200 µl of the lipid - mineral oil solution in a 1.5 ml Protein LoBind Eppendorf Tube. The Eppendorf Tube was rubbed to a maximum of three times over an Eppendorf rack to form a w/o emulsion. Centrifugation is performed at 180 x g for 3 minutes before incubating the sample in the dark for ~ 20 minutes. Afterwards, the GUVs were imaged directly in the microtiter plate. Fluorescence measurements were conducted using the Leica LAS X software.

Internal adhesion of membranes using iLID and Nano with additional calcein encapsulated:

The vesosome system with the proteins iLID and Nano was prepared as stated above. A 100 nM calcein solution was additionally encapsulated alongside the proteins. The final sample was monitored with the microscope over the time period of the experiment and fluorescence measurements were conducted using the Leica LAS X software afterwards.

Bibliographies:

1. Cooper, G. M. & Hausman, R. E. The Cell: A Molecular Approach 2nd Edition. Sinauer Associates (2007).
2. Alberts, B.; Johnson, A.; Lewis, J.; Morgan, D.; Raff, M.; Roberts, K.; Walter, P. Molecular biology of the cell, 6th edition. (Garland Science,Taylor & Francis Group,LLC, 2015).
3. Lodish H, Berk A, Zipursky SL, et al. Molecular Cell Biology 5th Ed. W.H. Freeman (2000). doi:10.1016/S1470-8175(01)00023-6
4. Porat-Shliom, N., Milberg, O., Masedunskas, A. & Weigert, R. Multiple roles for the actin cytoskeleton during regulated exocytosis. Cell. Mol. Life Sci. 70, 2099–2121 (2013).
5. Raiborg, C., Wenzel, E. M. & Stenmark, H. ER – endosome contact sites: molecular compositions and functions. EMBO J. 34, 1848–1858 (2015).
6. Scorrano,L. et. al. Coming together to define membrane contact sites. Nat. Commun. 10, 1-11 (2019).
7. Prinz, W. A. Bridging the gap: Membrane contact sites in signaling, metabolism, and organelle dynamics. J. Cell Biol. 205, 759-769 (2014).
8. Shaw, A. S. Lipid rafts: Now you see them, now you don't. Nat. Immunol. 7, 1139-1142 (2006).
9. George, K. S. & Wu, S. Lipid raft: A floating island of death or survival. Toxicol. Appl. Pharmacol. 259, 311-319 (2012)
10. Lebiedzinska, M., Szabadkai, G., Jones, A. W. E., Duszynski, J. & Wieckowski, M. R. Interactions between the endoplasmic reticulum, mitochondria, plasma membrane and other subcellular organelles. Int. J. Biochem. Cell Biol. 41, 1805–1816 (2009).
11. Jing, J., Liu, G., Huang, Y. & Zhou, Y. A molecular toolbox for interrogation of membrane contact sites. J. Physiol. 598, 1725–1739 (2020).
12. Klein, T. J. & Mlodzik, M. Planar cell polarization: An emerging model points in the right direction. Annu. Rev. Cell Dev. Biol. 21, 155–176 (2005).
13. Goñi, F. M. The basic structure and dynamics of cell membranes: An update of the Singer-Nicolson model. Biochim. Biophys. Acta - Biomembr. 1838, 1467–1476 (2014).
14. Krause, M. R. & Regen, S. L. The structural role of cholesterol in cell membranes: From condensed bilayers to lipid rafts. Acc. Chem. Res. 47, 3512–3521 (2014).
15. Fahy, E. et al. A comprehensive classification system for lipids. Eur. J. Lipid Sci. Technol. 107, 337–364 (2005).
16. Zhukovsky, M. A., Filograna, A., Luini, A., Corda, D. & Valente, C. Phosphatidic acid in membrane rearrangements. FEBS Lett. 593, 2428–2451 (2019).
17. Kooijman, E. E. & Burger, K. N. J. Biophysics and function of phosphatidic acid: A molecular perspective. Biochim. Biophys. Acta - Mol. Cell Biol. Lipids 1791, 881–888 (2009).
18. Kooijman, E. E. et al. What makes the bioactive lipids phosphatidic acid and lysophosphatidic acid so special? Biochemistry 44, 17007–17015 (2005).
19. Zegarlińska, J., Piaścik, M., Sikorski, A. F. & Czogalla, A. Phosphatidic acid - A simple phospholipid with multiple faces. Acta Biochim. Pol. 65, 163–171 (2018).
20. Di Paolo, G. & De Camilli, P. Phosphoinositides in cell regulation and membrane dynamics. Nature 443, 651–657 (2006).
21. Falkenburger, B. H., Jensen, J. B., Dickson, E. J., Suh, B. C. & Hille, B. Phosphoinositides: Lipid regulators of membrane proteins. J. Physiol. 588, 3179–3185 (2010).
22. Schink, K. O., Tan, K. W. & Stenmark, H. Phosphoinositides in Control of Membrane Dynamics. Annu. Rev. Cell Dev. Biol. 32, 143–171 (2016).
23. Marsh, D. Structural and thermodynamic determinants of chain-melting transition temperatures for phospholipid and glycolipids membranes. Biochim. Biophys. Acta - Biomembr. 1798, 40–51 (2010).
24. Cevc, G. How Membrane Chain-Melting Phase-Transition Temperature Is Affected by the Lipid Chain Asymmetry and Degree of Unsaturation: An Effective Chain-Length Model. Biochemistry 30, 7186–7193 (1991).
25. Schrader, M., Godinho, L. F., Costello, J. L. & Islinger, M. The different facets of organelle interplay: An overview of organelle interactions. Front. Cell Dev. Biol. 3, 1-22 (2015)
26. Henne, W. M. Organelle remodeling at membrane contact sites. J. Struct. Biol. 196, 15-19 (2016)
27. Woese, C. R. & Fox, G. E. The Concept of Cellular Evolution. J. Mol. Evol. 10, 1–6 (1977).
28. Woese, C. R. & Fox, G. E. Phylogenetic structure of the prokaryotic domain: The primary kingdoms. Proc. Natl. Acad. Sci. U. S. A. 74, 5088–5090 (1977).
29. Woese, C. R., Kandler, O. & Wheelis, M. L. Towards a natural system of organisms: Proposal for the domains Archaea, Bacteria, and Eucarya. Proc. Natl. Acad. Sci. U. S. A. 87, 4576–4579 (1990).
30. Glass, J. I., Merryman, C., Wise, K. S., Iii, C. A. H. & Smith, H. O. Minimal Cells — Real and Imagined. Cold Spring Harb. Perspect. Biol. (2017). doi:10.1101/cshperspect.a023861
31. Xu, C., Hu, S. & Chen, X. Artificial cells: from basic science to applications. Materials Today 19, (2016).
32. Jewett, M. C. & Forster, A. C. Update on designing and building minimal cells. Curr. Opin. Biotechnol. 21, 697–703 (2010).
33. Gibson, D. G. et al. Creation of a bacterial cell controlled by a chemically synthesized genome. Science (80). 329, 52–56 (2010).
34. Hutchison, C. A. et al. Design and synthesis of a minimal bacterial genome. Science (80). 351, (2016).
35. Lagny, T. J. & Bassereau, P. Bioinspired membrane-based systems for a physical approach of cell organization and dynamics: Usefulness and limitations. Interface Focus 5, (2015).

36. Litman, B. J. Lipid Model Membranes. Characterization of Mixed Phospholipid Vesicles. Biochemistry 12, 2545-2554 (1973).
37. Eeman, M. & Deleu, M. From biological membranes to biomimetic model membranes. Biotechnol. Agron. Société Environ. 14, 719–736 (2010).
38. Rosetti, C. M., Mangiarotti, A. & Wilke, N. Sizes of lipid domains: What do we know from artificial lipid membranes? What are the possible shared features with membrane rafts in cells? Biochim. Biophys. Acta - Biomembr. 1859, 789-802 (2017).
39. de Franceschi, N., Alqabandi, M., Weissenhorn, W. & Bassereau, P. Dynamic and Sequential Protein Reconstitution on Negatively Curved Membranes by Giant Vesicles Fusion. Bio-Protocol 9, (2019).
40. Miklavcic, D. Electrodeformation, Electroporation, and Electrofusion of Giant Unilamellar Vesicles. in Handbook of Electroporation (2016). doi:10.1007/978-3-319-26779-1
41. Stengel, G., Zahn, R. & Höök, F. DNA-induced programmable fusion of phospholipid vesicles. J. Am. Chem. Soc. 129, 9584–9585 (2007).
42. Nordlund, G., Brzezinski, P. & Von Ballmoos, C. SNARE-fusion mediated insertion of membrane proteins into native and artificial membranes. Nat. Commun. 5, 1–8 (2014).
43. Cuvelier, D., Vezy, C., Viallat, A., Bassereau, P. & Nassoy, P. Mimicking cell/extracellular matrix adhesion with lipid membranes and solid substrates: Requirements, pitfalls and proposals. J. Phys. Condens. Matter 16, (2004).
44. Steinkühler, J., Agudo-Canalejo, J., Lipowsky, R. & Dimova, R. Modulating Vesicle Adhesion by Electric Fields. Biophys. J. 111, 1454–1464 (2016)
45. Cuvelier, D. & Nassoy, P. Hidden dynamics of vesicle adhesion induced by specific stickers. Phys. Rev. Lett. 93, 1–4 (2004).
46. Bernard, A. L., Guedeau-Boudeville, M. A., Jullien, L. & Di Meglio, J. M. Strong adhesion of giant vesicles on surfaces: dynamics and permeability. Langmuir 16, 6809–6820 (2000).
47. Menger, F. M. & Zhang, H. Self-adhesion among phospholipid vesicles. J. Am. Chem. Soc. 128, 1414–1415 (2006).
48. Reeves, J. P. & Dowben, R. M. Formation and properties of thin−walled phospholipid vesicles. J. Cell. Physiol. 73, 49–60 (1969).
49. P. Mueller, T.F. Chien & B. Rudy. Formation and Properties of Cell-Size Lipid Bilayer Vesicles. Biophys. J. 44, 375–381 (1983).
50. Lira, R. B., Dimova, R. & Riske, K. A. Giant unilamellar vesicles formed by hybrid films of agarose and lipids display altered mechanical properties. Biophys. J. 107, 1609–1619 (2014).
51. Angelova, M. I. & Dimitrov, D. S. Liposome Electroformation. Faraday Discuss. Chem. Soc. 303–311 (1986).
52. Montes, L. R., Alonso, A., Goñi, F. M. & Bagatolli, L. A. Giant unilamellar vesicles electroformed from native membranes and organic lipid mixtures under physiological conditions. Biophys. J. 93, 3548–3554 (2007).
53. Pautot, S., Frisken, B. J. & Weitz, D. A. Production of unilamellar vesicles using an inverted emulsion. Langmuir (2003). doi:10.1021/la026100v
54. Abkarian, M., Loiseau, E. & Massiera, G. Continuous droplet interface crossing encapsulation (cDICE) for high throughput monodisperse vesicle design. Soft Matter 7, 4610–4614 (2011).
55. Blosser, M. C., Horst, B. G. & Keller, S. L. cDICE method produces giant lipid vesicles under physiological conditions of charged lipids and ionic solutions. Soft Matter 12, 7364–7371 (2016).
56. Funakoshi, K., Suzuki, H. & Takeuchi, S. Formation of giant lipid vesiclelike compartments from a planar lipid membrane by a pulsed jet flow. J. Am. Chem. Soc. 129, 12608–12609 (2007).
57. Yamada, A., Lee, S., Bassereau, P. & Baroud, C. N. Trapping and release of giant unilamellar vesicles in microfluidic wells. Soft Matter 10, 5878–5885 (2014).
58. Hu, P. C., Li, S. & Malmstadt, N. Microfluidic fabrication of asymmetric giant lipid vesicles. ACS Appl. Mater. Interfaces 3, 1434–1440 (2011).
59. Teh, S. Y., Khnouf, R., Fan, H. & Lee, A. P. Stable, biocompatible lipid vesicle generation by solvent extraction-based droplet microfluidics. Biomicrofluidics 5, (2011).
60. Van Swaay, D. & Demello, A. Microfluidic methods for forming liposomes. Lab Chip 13, 752–767 (2013).
61. Morita, M. et al. Droplet-Shooting and Size-Filtration (DSSF) Method for Synthesis of Cell-Sized Liposomes with Controlled Lipid Compositions. ChemBioChem 16, 2029–2035 (2015).
62. Weiss, M. et al. Sequential bottom-up assembly of mechanically stabilized synthetic cells by microfluidics. Nat. Mater. 17, 89–95 (2018).
63. Sato, Y. & Takinoue, M. Creation of artificial cell-like structures promoted by microfluidics technologies. Micromachines 10, (2019).
64. Yandrapalli, N., Seemann, T. & Robinson, T. On-chip inverted emulsion method for fast giant vesicle production, handling, and analysis. Micromachines 11, (2020).
65. Elani, Y., Law, R. V. & Ces, O. Vesicle-based artificial cells as chemical microreactors with spatially segregated reaction pathways. Nat. Commun. 5, 1–5 (2014).
66. Stano, P. & Luisi, P. L. Achievements and open questions in the self-reproduction of vesicles and synthetic minimal cells. Chem. Commun. 46, 3639–3653 (2010).
67. Nichols, J.W.; Pagano, R. E. Kinetics of Soluble Lipid Monomer Diffusion between Vesicles. Am. Chem. Soc. 2783–2789 (1981).
68. Derzko, Z. & Jacobson, K. Comparative Lateral Diffusion of Fluorescent Lipid Analogues in Phospholipid Multibilayers. Biochemistry 19, 6050–6057 (1980).

69. Przybylo, M. et al. Lipid Diffusion in Giant Unilamellar Vesicles Is More than 2 Times Faster than in Supported Phospholipid Bilayers under Identical Conditions. Langmuir 22, 9096–9099 (2006).
70. Macháň, R. & Hof, M. Lipid diffusion in planar membranes investigated by fluorescence correlation spectroscopy. Biochim. Biophys. Acta - Biomembr. 1798, 1377–1391 (2010).
71. Wick, R., Angelova, M. I., Walde, P. & Luisi, P. L. Microinjection into giant vesicles and light microscopy investigation of enzyme-mediated vesicle transformations. Chem. Biol. 3, 105–111 (1996).
72. Bartelt, S. M., Chervyachkova, E., Ricken, J. & Wegner, S. V. Mimicking Adhesion in Minimal Synthetic Cells. Adv. Biosyst. 3, 1–10 (2019).
73. Bolognesi, G. et al. Sculpting and fusing biomimetic vesicle networks using optical tweezers. Nat. Commun. 9, 1–11 (2018).
74. Menger, F. M. & Keiper, J. S. Giant vesicles: Micromanipulation of membrane bilayers. Adv. Mater. 10, 888–890 (1998).
75. Robinson, T., Kuhn, P., Eyer, K. & Dittrich, P. S. Microfluidic trapping of giant unilamellar vesicles to study transport through a membrane pore. Biomicrofluidics 7, (2013).
76. Robinson, T. Microfluidic Handling and Analysis of Giant Vesicles for Use as Artificial Cells: A Review. Advanced Biosystems (2019). doi:10.1002/adbi.201800318
77. Yandrapalli, N. & Robinson, T. Ultra-high capacity microfluidic trapping of giant vesicles for high-throughput membrane studies. Lab Chip 19, 626–633 (2019).
78. Pokorna, S., Jurkiewicz, P., Cwiklik, L., Vazdar, M. & Hof, M. Interactions of monovalent salts with cationic lipid bilayers. Faraday Discuss. 160, 341–358 (2013).
79. Balleza, D. et al. Effects of neurosteroids on a model membrane including cholesterol: A micropipette aspiration study. Biochim. Biophys. Acta - Biomembr. 1848, 1268–1276 (2015).
80. Georgiev, V. N. et al. Area Increase and Budding in Giant Vesicles Triggered by Light: Behind the Scene. Adv. Sci. 5, (2018).
81. Menger, F. M. & Keiper, J. S. Chemistry and physics of giant vesicles as biomembrane models. Curr. Opin. Chem. Biol. 2, 726–732 (1998).
82. Hadorn, M. et al. Defined DNA-Mediated Assemblies of Gene-Expressing Giant Unilamellar Vesicles. Langmuir 29, 15309–15319 (2013).
83. Villringer, S. et al. Lectin-mediated protocell crosslinking to mimic cell-cell junctions and adhesion. Sci. Rep. 8, (2018).
84. Watanabe, M., Tomita, T. & Yasuda, T. Membrane-damaging action of staphylococcal alpha-toxin on phospholipid-cholesterol liposomes. 898, 257–265 (1987).
85. Menestrina, G. Escherichia coli hemolysin permeabilizes small unilamellar vesicles loaded with calcein by a single-hit mechanism. FEBS Lett. 232, 217–220 (1988).
86. Ostolaza, H., Bartolomé, B., de Zárate, I. O., de la Cruz, F. & Goñi, F. M. Release of lipid vesicle contents by the bacterial protein toxin α-haemolysin. BBA - Biomembr. 1147, 81–88 (1993).
87. Gouaux, E. α-Hemolysin from Staphylococcus aureus: An archetype of β-barrel, channel-forming toxins. J. Struct. Biol. 121, 110–122 (1998).
88. Fussle, R. et al. On the mechanism of membrane damage by Staphylococcus aureus α-toxin. J. Cell Biol. 91, 83–94 (1981).
89. Elsner, M. Membrane channels built from DNA. Nat. Biotechnol. 31, 125 (2013).
90. Krishnan, S. et al. Molecular transport through large-diameter DNA nanopores. Nat. Commun. 7, 1–7 (2016).
91. Burns, J. R., Seifert, A., Fertig, N. & Howorka, S. A biomimetic DNA-based channel for the ligand-controlled transport of charged molecular cargo across a biological membrane. Nat. Nanotechnol. 11, 152–156 (2016).
92. Diederichs, T. et al. Synthetic protein-conductive membrane nanopores built with DNA. Nat. Commun. 10, 1–11 (2019).
93. Thomas, J. M., Friddin, M. S., Ces, O. & Elani, Y. Programming membrane permeability using integrated membrane pores and blockers as molecular regulators. Chem. Commun. 53, 12282–12285 (2017).
94. Gu, L. Q., Braha, O., Conlan, S., Cheley, S. & Bayley, H. Stochastic sensing of organic analytes by a pore-forming protein containing a molecular adapter. Chemtracts 13, 198-202 (2000).
95. Heron, A. J., Thompson, J. R., Cronin, B., Bayley, H. & Wallace, M. I. Simultaneous measurement of ionic current and fluorescence from single protein pores. J. Am. Chem. Soc. 131, 1652-1653 (2009).
96. Discher, B. M. et al. Polymersomes: Tough vesicles made from diblock copolymers. Science (80-.). 284, 1143–1146 (1999).
97. Discher, D. E. & Ahmed, F. Polymersomes. Annu. Rev. Biomed. Eng. 8, 323–341 (2006).
98. Chandrawati, R. & Caruso, F. Biomimetic liposome- and polymersome-based multicompartmentalized assemblies. Langmuir 28, 13798–13807 (2012).
99. Le Meins, J. F., Schatz, C., Lecommandoux, S. & Sandre, O. Hybrid polymer/lipid vesicles: State of the art and future perspectives. Mater. Today 16, 397–402 (2013).
100. Che, H. & Van Hest, J. C. M. Stimuli-responsive polymersomes and nanoreactors. J. Mater. Chem. B 4, 4632–4647 (2016).
101. Rideau, E., Dimova, R., Schwille, P., Wurm, F. R. & Landfester, K. Liposomes and polymersomes: a comparative review towards cell mimicking. Chem. Soc. Rev. 47, 8572–8610 (2018).
102. Mason, A. F. & Thordarson, P. Polymersomes as protocellular constructs. J. Polym. Sci. Part A Polym. Chem. 55, 3817–3825 (2017).

103. Wong, C. K. et al. Polymersomes Prepared from Thermoresponsive Fluorescent Protein-Polymer Bioconjugates: Capture of and Report on Drug and Protein Payloads. Angew. Chemie 127, 5407–5412 (2015).
104. Qin, S., Geng, Y., Discher, D. E. & Yang, S. Temperature-controlled assembly and release from polymer vesicles of poly(ethylene oxide)-block-poly(N-isopropylacrylamide). Adv. Mater. 18, 2905–2909 (2006).
105. Zhu, L., Zhao, L., Qu, X. & Yang, Z. PH-sensitive polymeric vesicles from coassembly of amphiphilic cholate grafted poly(l-lysine) and acid-cleavable polymer-drug conjugate. Langmuir 28, 11988–11996 (2012).
106. Kim, K. T., Cornelissen, J. J. L. M., Nolte, R. J. M. & Van Hest, J. C. M. A polymersome nanoreactor with controllable permeability induced by stimuli-responsive block copolymers. Adv. Mater. 21, 2787–2791 (2009).
107. Xu, H., Meng, F. & Zhong, Z. Reversibly crosslinked temperature-responsive nano-sized polymersomes: Synthesis and triggered drug release. J. Mater. Chem. 19, 4183–4190 (2009).
108. Cheng, R. et al. Glutathione-responsive nano-vehicles as a promising platform for targeted intracellular drug and gene delivery. J. Control. Release 152, 2–12 (2011).
109. Mabrouk, E., Cuvelier, D., Brochard-Wyart, F., Nassoy, P. & Li, M. H. Bursting of sensitive polymersomes induced by curling. Proc. Natl. Acad. Sci. U. S. A. 106, 7294–7298 (2009).
110. Abdelmohsen, L. K. E. A. et al. Formation of Well-Defined, Functional Nanotubes via Osmotically Induced Shape Transformation of Biodegradable Polymersomes. J. Am. Chem. Soc. 138, 9353–9356 (2016).
111. Luo, L. & Eisenberg, A. One-step preparation of block copolymer vesicles with preferentially segregated acidic and basic corona chains. Angew. Chemie - Int. Ed. 41, 1001–1004 (2002).
112. Mason, A. F. & Thordarson, P. Polymersomes with Asymmetric Membranes Based on Readily Accessible Di- and Triblock Copolymers Synthesized via SET-LRP. ACS Macro Lett. 5, 1172–1175 (2016).
113. Wong, D., Jeon, T. J. & Schmidt, J. Single molecule measurements of channel proteins incorporated into biomimetic polymer membranes. Nanotechnology 17, 3710–3717 (2006).
114. Hammer, D. A. et al. Leuko-polymersomes. Faraday Discuss. 139, 129–141 (2008).
115. Elani, Y., Gee, A., Law, R. V. & Ces, O. Engineering multi-compartment vesicle networks. Chem. Sci. 4, 3332–3338 (2013).
116. Deng, N.-N., Yelleswarapu, M. & Huck, W. T. S. Monodisperse Uni- and Multicompartment Liposomes. J. Am. Chem. Soc. 138, 7584–7591 (2016).
117. Göpfrich, K. et al. One-Pot Assembly of Complex Giant Unilamellar Vesicle-Based Synthetic Cells. ACS Synth. Biol. 8, 937–947 (2019).
118. Oberholzer, T., Meyer, E., Amato, I., Lustig, A. & Monnard, P. A. Enzymatic reactions in liposomes using the detergent-induced liposome loading method. Biochim. Biophys. Acta - Biomembr. 1416, 57–68 (1999).
119. Oberholzer, T., Albrizio, M. & Luisi, P. L. Polymerase chain reaction in liposomes. Chem. Biol. 2, 677–682 (1995).
120. Lee, S. et al. DNA amplification in neutral liposomes for safe and efficient gene delivery. ACS Nano 8, 4257–4267 (2014).
121. Walde, P., Monnard, P. A., Wessicken, M., Goto, A. & Luisi, P. L. Oparin's Reactions Revisited: Enzymatic Synthesis of Poly (adenylic acid) in Micelles and Self-Reproducing Vesicles. J. Am. Chem. Soc. 116, 7541–7547 (1994).
122. Oberholzer, T., Wick, R., Luisi, P. L. & Biebricher, C. K. Enzymatic RNA replication in self-reproducing vesicles: An approach to a minimal cell. Biochemical and Biophysical Research Communications 207, 250–257 (1995).
123. Sunami, T., Ichihashi, N., Nishikawa, T., Kazuta, Y. & Yomo, T. Effect of Liposome Size on Internal RNA Replication Coupled with Replicase Translation. ChemBioChem 1282–1289 (2016).
124. Oberholzer, T., Nierhaus, K. H. & Luisi, P. L. Protein expression in liposomes. Biochem. Biophys. Res. Commun. 261, 238–241 (1999).
125. Kuruma, Y., Stano, P., Ueda, T. & Luisi, P. L. A synthetic biology approach to the construction of membrane proteins in semi-synthetic minimal cells. Biochim. Biophys. Acta - Biomembr. 1788, 567–574 (2009).
126. Elani, Y., Law, R. V. & Ces, O. Protein synthesis in artificial cells: Using compartmentalisation for spatial organisation in vesicle bioreactors. Phys. Chem. Chem. Phys. 17, 15534–15537 (2015).
127. Adamala, K. P., Martin-Alarcon, D. A., Guthrie-Honea, K. R. & Boyden, E. S. Engineering genetic circuit interactions within and between synthetic minimal cells. Nat. Chem. 9, 431–439 (2017).
128. Trantidou, T. et al. Engineering Compartmentalized Biomimetic Micro- and Nanocontainers. ACS Nano 11, 6549–6565 (2017).
129. Dimova, Rumiana and Marques, C. The Giant Vesicled Book. (2020).
130. Giocondi, M. C. et al. Surface topography of membrane domains. Biochim. Biophys. Acta - Biomembr. 1798, 703–718 (2010).
131. Heberle, F. A. & Feigenson, G. W. Phase separation in lipid membranes. Cold Spring Harb. Perspect. Biol. 3, 1–13 (2011).
132. Kenworthy, A. K., Petranova, N. & Edidin, M. High-Resolution FRET Microscopy of Cholera Toxin B-Subunit and GPI-anchored Proteins in Cell Plasma Membranes. 11, 1645–1655 (2000).
133. Kahya, N., Scherfeld, D., Bacia, K. & Schwille, P. Lipid domain formation and dynamics in giant unilamellar vesicles explored by fluorescence correlation spectroscopy. J. Struct. Biol. 147, 77–89 (2004).
134. Gracià, R. S., Bezlyepkina, N., Knorr, R. L., Lipowsky, R. & Dimova, R. Effect of cholesterol on the rigidity of saturated and unsaturated membranes: Fluctuation and electrodeformation analysis of giant vesicles. Soft Matter 6, 1472-1482 (2010).
135. Y. Pang, Kam-Yee ; Miller, K. W. Cholesterol modulates the effects of Membrane pertubers in Phospholipid vesicles and Biomembranes. Biochim. Biophys. Acta - Biomembr. 511, (1978).

136. Xiang, T. X., Chen, J. & Anderson, B. D. A quantitative model for the dependence of solute permeability on peptide and cholesterol content in biomembranes. J. Membr. Biol. 177, 137–148 (2000).
137. Testerink, C. & Munnik, T. Molecular, cellular, and physiological responses to phosphatidic acid formation in plants. J. Exp. Bot. 62, 2349–2361 (2011).
138. Bangham, A. D., Standish, M. M. & Watkins, J. C. Diffusion of univalent ions across the lamellae of swollen phospholipids. J. Mol. Biol. 13, 238–252 (1965).
139. Papahadjopoulos D, M. N. Phospholipid model membranes. I. Structural characteristics of hydrated liquid crystals. Biochim Biophys Acta Biomembr 135, 624–638 (1967).
140. Lefrançois, P., Goudeau, B. & Arbault, S. Electroformation of phospholipid giant unilamellar vesicles in physiological phosphate buffer. Integr. Biol. (United Kingdom) 10, 429–434 (2018).
141. Natsume, Y. et al. Preparation of giant vesicles encapsulating microspheres by centrifugation of a water-in-oil emulsion. J. Vis. Exp. 2017, 1–8 (2017).
142. Lopez, S. et al. Biochimica et Biophysica Acta Membrane composition and dynamics : A target of bioactive virgin olive oil constituents ☆. BBA - Biomembr. 1838, 1638–1656 (2014).
143. Moga, A., Yandrapalli, N., Dimova, R. & Robinson, T. Optimization of the Inverted Emulsion Method for High-Yield Production of Biomimetic Giant Unilamellar Vesicles. ChemBioChem 20, 2674–2682 (2019).
144. Magnusson, E., Nilsson, L. & Bergenståhl, B. Effect of the dispersed state of phospholipids on emulsification— Xiao, Z.; Huang, N.; Xu, M.; Lu, Z.; Wei, Y. Novel Preparation of Asymmetric Liposomes with Inner and Outer Layer of Different Materials. Chem. Lett. 27, 225–226 (1998). Part 1. Phosphatidylcholine. Colloids Surfaces A Physicochem. Eng. Asp. 506, 794–803 (2016).
145. Xiao, Z.; Huang, N.; Xu, M.; Lu, Z.; Wei, Y. Novel Preparation of Asymmetric Liposomes with Inner and Outer Layer of Different Materials. Chem. Lett. 27, 225–226 (1998).
146. Xiao, Z., Xu, M., Li, M., Lu, Z. & Wei, Y. Preparation of asymmetric bilayer-vesicles with inner and outer monolayers composed of different amphiphilic molecules. Supramol. Sci. 5, 619–622 (1998).
147. Takiguchi, K., Yamada, A., Negishi, M., Tanaka-Takiguchi, Y. & Yoshikawa, K. Entrapping desired amounts of actin filaments and molecular motor proteins in giant liposomes. Langmuir 24, 11323–11326 (2008).
148. Takiguchi, K., Negishi, M., Tanaka-Takiguchi, Y., Homma, M. & Yoshikawa, K. Transformation of ActoHMM assembly confined in cell-sized liposome. Langmuir 27, 11528–11535 (2011).
149. Yanagisawa, M., Iwamoto, M., Kato, A., Yoshikawa, K. & Oiki, S. Oriented reconstitution of a membrane protein in a giant unilamellar vesicle: Experimental verification with the potassium channel KcsA. J. Am. Chem. Soc. 133, 11774–11779 (2011).
150. Carrara, P., Stano, P. & Luisi, P. L. Giant Vesicles 'Colonies': A Model for Primitive Cell Communities. ChemBioChem 13, 1497–1502 (2012).
151. Peters, R. J. R. W., Nijemeisland, M. & van Hest, J. C. M. Reversibly Triggered Protein-Ligand Assemblies in Giant Vesicles. Angew. Chemie 127, 9750–9753 (2015).
152. Campillo, C. et al. Unexpected membrane dynamics unveiled by membrane nanotube extrusion. Biophys. J. 104, 1248-1256 (2013).
153. Litschel, T. & Schwille, P. Protein Reconstitution Inside Giant Unilamellar Vesicles. Annu. Rev. Biophys. 50, (2021).
154. Hein, C. D., Liu, X. M. & Wang, D. Click chemistry, a powerful tool for pharmaceutical sciences. Pharm. Res. 25, 2216–2230 (2008).
155. Hanashima, S., Yano, Y. & Murata, M. Enantiomers of phospholipids and cholesterol: A key to decipher lipid-lipid interplay in membrane. Chirality 32, 282–298 (2020).
156. Frank, J. A. et al. Photoswitchable fatty acids enable optical control of TRPV1. Nat. Commun. 6, (2015).
157. Kol, M. et al. Optical manipulation of sphingolipid biosynthesis using photoswitchable ceramides. Elife 8, 1–30 (2019).
158. Perttu, E. K., Kohli, A. G. & Szoka, F. C. Inverse-phosphocholine lipids: A remix of a common phospholipid. J. Am. Chem. Soc. 134, 4485–4488 (2012).
159. Dean, J. M. & Lodhi, I. J. Structural and functional roles of ether lipids. Protein Cell 9, 196–206 (2018).
160. Kepczynski, M. & Róg, T. Functionalized lipids and surfactants for specific applications. Biochim. Biophys. Acta - Biomembr. 1858, 2362–2379 (2016).
161. Weber, P. C., Ohlendorf, D. H., Wendoloski, J. J. & Salemme, F. R. Structural origins of high-affinity biotin binding to streptavidin. Science (80-.). 243, 85–88 (1989).
162. Livnah, O., Bayer, E. A., Wilchek, M. & Sussman, J. L. Three-dimensional structures of avidin and the avidin-biotin complex. Proc. Natl. Acad. Sci. U. S. A. 90, 5076–5080 (1993).
163. Mpye, K. L., Gildenhuys, S. & Mosebi, S. The effects of temperature on streptavidin-biotin binding using affinity isothermal titration calorimetry. AIMS Biophys. 7, 236–247 (2020).
164. De Lange, N., Leermakers, F. A. M. & Kleijn, J. M. Self-limiting aggregation of phospholipid vesicles. Soft Matter 16, 2379–2389 (2020).
165. Maan, R., Loiseau, E. & Bausch, A. R. Adhesion of Active Cytoskeletal Vesicles. Biophys. J. 115, 2395–2402 (2018).
166. Noppl-Simson, D. A. & Needham, D. Avidin-biotin interactions at vesicle surfaces: Adsorption and binding, cross-bridge formation, and lateral interactions. Biophys. J. 70, 1391–1401 (1996).
167. De Lange, N., Leermakers, F. A. M. & Kleijn, J. M. Step-wise linking of vesicles by combining reversible and irreversible linkers-towards total control on vesicle aggregate sizes. Soft Matter 16, 6773–6783 (2020).

168. Haluska, C. K. et al. Photo-activated phase separation in giant vesicles made from different lipid mixtures. Biochim. Biophys. Acta - Biomembr. 1818, 666–672 (2012).
169. Schwarz, G., Zong, R. ting & Popescu, T. Kinetics of melittin induced pore formation in the membrane of lipid vesicles. BBA - Biomembr. 1110, 97–104 (1992).
170. Ladokhin, A. S., Selsted, M. E. & White, S. H. Sizing membrane pores in lipid vesicles by leakage of co-encapsulated markers: Pore formation by melittin. Biophys. J. 72, 1762–1766 (1997).
171. Fuertes, G. et al. Pores formed by Baxα5 relax to a smaller size and keep at equilibrium. Biophys. J. 99, 2917–2925 (2010).
172. Bleicken, S., Landeta, O., Landajuela, A., Basañez, G. & García-Sáez, A. J. Proapoptotic Bax and Bak proteins form stable protein-permeable pores of tunable size. J. Biol. Chem. 288, 33241–33252 (2013).
173. Rausch, J. M., Marks, J. R., Rathinakumar, R. & Wimley, W. C. β-Sheet pore-forming peptides selected from a rational combinatorial library: Mechanism of pore formation in lipid vesicles and activity in biological membranes. Biochemistry 46, 12124–12139 (2007).
174. Riske, K. A. Optical Microscopy of Giant Vesicles as a Tool to Reveal the Mechanism of Action of Antimicrobial Peptides and the Specific Case of Gomesin. in Advances in Planar Lipid Bilayers and Liposomes (2015).
175. Mattei, B., Lira, R. B., Perez, K. R. & Riske, K. A. Membrane permeabilization induced by Triton X-100: The role of membrane phase state and edge tension. Chem. Phys. Lipids 202, 28–37 (2017).
176. Zhelev, D. V. & Needham, D. Tension-stabilized pores in giant vesicles: determination of pore size and pore line tension. BBA - Biomembr. 1147, 89–104 (1993).
177. Riske, K. A. & Dimova, R. Electro-deformation and poration of giant vesicles viewed with high temporal resolution. Biophys. J. 88, 1143–1155 (2005).
178. Peterlin, P. & Arrigler, V. Electroformation in a flow chamber with solution exchange as a means of preparation of flaccid giant vesicles. Colloids Surfaces B Biointerfaces 64, 77–87 (2008).
179. Emami, S., Su, W. C., Purushothaman, S., Ngassam, V. N. & Parikh, A. N. Permeability and Line-Tension-Dependent Response of Polyunsaturated Membranes to Osmotic Stresses. Biophys. J. 115, 1942–1955 (2018).
180. Sandre, O., Moreaux, L. & Brochard-Wyart, F. Dynamics of transient pores in stretched vesicles. Proc. Natl. Acad. Sci. U. S. A. 96, 10591–10596 (1999).
181. Lira, R. B., Leomil, F. S. C., Melo, R. J., Riske, K. A. & Dimova, R. To close or to collapse: The role of charges on membrane stability upon pore formation. bioRxiv 1–17 (2020).
182. Okumura, Y., Nakaya, T., Namai, H. & Urita, K. Giant vesicles with membranous microcompartments. Langmuir 27, 3279–3282 (2011).
183. Deng, N. N., Yelleswarapu, M., Zheng, L. & Huck, W. T. S. Microfluidic assembly of monodisperse vesosomes as artificial cell models. J. Am. Chem. Soc. 139, 587–590 (2017).
184. Mohanan, G., Nair, K. S., Nampoothiri, K. M. & Bajaj, H. Engineering bio-mimicking functional vesicles with multiple compartments for quantifying molecular transport. Chem. Sci. 11, 4669–4679 (2020).
185. Wubbels, T. et al. Introduction to Biophotonics. Interpersonal Relationships in Education (2012).
186. Schmitz, S. & Desel, C. Der Experimentator Zellbiologie. (2018).
187. Kubitscheck, U. Biomedical Imaging Fluorescence Applications in Biotechnology and Life Sciences Handbook of Fluorescence Spectroscopy and Imaging. (2013).
188. Holgate, J. H., Webb, J. Encyclopedia of Food Sciences and Nutrition. (2003).
189. Atkins, Peter; de Paula, J. Physical Chemistry. (2010).
190. Mondal, P. P. & Diaspro, A. Fundamentals of Fluorescence Microscopy. Fundamentals of Fluorescence Microscopy (2014).
191. Zimmermann, T., Marrison, J., Hogg, K. & O'Toole, P. Methods in Molecular Biology: Confocal Microscopy Methods and Protocols. (2014).
192. Nwaneshiudu, A. et al. Introduction to confocal microscopy. J. Invest. Dermatol. 132, 1–5 (2012).
193. Schönfeld, S.; Hardt, F. Microfluidic Technologies for Miniaturized Analysis Systems. (Springer, 2007).
194. Whitesides, G. M. The origins and the future of microfluidics. Nature 442, 368–373 (2006).
195. Robinson, T. Microfluidics and giant vesicles: creation, capture, and applications for biomembranes. Adv. Biomembr. Lipid Self-Assembly. (2019)
196. Ivanov, A. I. Exocytosis and endocytosis. Preface. Methods Mol. Biol. 440, 643–659 (2008).
197. Hadorn, M. & Hotz, P. E. DNA-mediated self-assembly of artificial vesicles. PLoS One 5, (2010).
198. Johnson-Buck, A., Jiang, S., Yan, H. & Walter, N. G. DNA-cholesterol barges as programmable membrane-exploring agents. ACS Nano 8, 5641–5649 (2014).
199. Bartelt, S. M. et al. Dynamic blue light-switchable protein patterns on giant unilamellar vesicles. Chem. Commun. 54, 948–951 (2018).
200. Chakraborty, T., Bartelt, S. M., Steinkühler, J., Dimova, R. & Wegner, S. V. Light controlled cell-to-cell adhesion and chemical communication in minimal synthetic cells. Chem. Commun. 55, 9448–9451 (2019).
201. Perrier, C., Beroual, A. & Bessede, J. L. Improvement of power transformers by using mixtures of mineral oil with synthetic esters. IEEE Trans. Dielectr. Electr. Insul. 13, 556-564 (2006).
202. Zmarzły, D. & Dobry, D. Analysis of properties of aged mineral oil doped with C60 fullerenes. IEEE Trans. Dielectr. Electr. Insul. 21, 1119-1126 (2014).
203. Karamdad, K. et al. Engineering thermoresponsive phase separated vesicles formed: Via emulsion phase transfer as a content-release platform. Chem. Sci. 9, 4851–4858 (2018).
204. Dürre, K. & Bausch, A. R. Formation of phase separated vesicles by double layer cDICE. Soft Matter 15, 9676–9681 (2019).

205. Pal, A., Sunthar, P. & Khakhar, D. V. Effects of Ethanol Addition on the Size Distribution of Liposome Suspensions in Water. Ind. Eng. Chem. Res. 58, 7511–7519 (2019).
206. Akimov, S. A. et al. Pore formation in lipid membrane I: Continuous reversible trajectory from intact bilayer through hydrophobic defect to transversal pore. Sci. Rep. 7, 1-20 (2017).
207. Karatekin, E. et al. Cascades of transient pores in giant vesicles: Line tension and transport. Biophys. J. 84,1734-1749 (2003).
208. Jones, L. S., Kaufmann, A. & Middaugh, C. R. Silicone oil induced aggregation of proteins. J. Pharm. Sci. 94, 918–927 (2005).
209. D. Brett Ludwig, John F. Carpenter, Jean-Bernard Hamel, T. W. Randolph. Protein Adsorption and Excipient Effects on Kinetic Stability of Silicone Oil Emulsions. J. Pharm. Sci. 99, 1721–1733 (2010).
210. Li, J. et al. Mechanistic understanding of protein-silicone oil interactions. Pharm. Res. 29, 1689–1697 (2012).
211. Probst, C. Characterization of Protein Aggregates, Silicone Oil Droplets, and Protein-Silicone Interactions Using Imaging Flow Cytometry. J. Pharm. Sci. 109, 364–374 (2020).
212. González, M. et al. Interaction of biotin with streptavidin. Thermostability and conformational changes upon binding. J. Biol. Chem. 272, 11288–11294 (1997).
213. Freitag, S., Trong, I. L. E., Klumb, L., Stayton, P. S. & Stenkamp, R. E. Structural studies of the streptavidin binding loop. Protein Sci. 6, 1157–1166 (1997).
214. Houen, G. & Hansen, K. Interference of sugars with the binding of biotin to streptavidin and avidin. J. Immunol. Methods 210, 115–123 (1997).
215. Beales, P. A. & Vanderlick, T. K. DNA as membrane-bound ligand-receptor pairs: Duplex stability is tuned by intermembrane forces. Biophys. J. 96, 1554–1565 (2009).
216. Fujii, S., Matsuura, T. & Yomo, T. Membrane Curvature Affects the Formation of α-Hemolysin Nanopores. ACS Chem. Biol. 10, 1694–1701 (2015).
217. Fan, X. et al. Single particle cryo-EM reconstruction of 52 kDa streptavidin at 3.2 Angstrom resolution. Nat. Commun. 10, 1–11 (2019).
218. Karal, M. A. S., Levadnyy, V., Tsuboi, T. A., Belaya, M. & Yamazaki, M. Electrostatic interaction effects on tension-induced pore formation in lipid membranes. Phys. Rev. E - Stat. Nonlinear, Soft Matter Phys. 92, 1–7 (2015).
219. Karal, M. A. S. & Yamazaki, M. Communication: Activation energy of tension-induced pore formation in lipid membranes. J. Chem. Phys. 143, (2015).
220. Alam Shibly, S. U., Ghatak, C., Sayem Karal, M. A., Moniruzzaman, M. & Yamazaki, M. Experimental Estimation of Membrane Tension Induced by Osmotic Pressure. Biophys. J. 111, 2190–2201 (2016).
221. Hasan, M., Saha, S. K. & Yamazaki, M. Effect of membrane tension on transbilayer movement of lipids. J. Chem. Phys. 148, (2018).
222. Hasan, M., Moghal, M. M. R., Saha, S. K. & Yamazaki, M. The role of membrane tension in the action of antimicrobial peptides and cell-penetrating peptides in biomembranes. Biophys. Rev. 11, 431–448 (2019).
223. Lira, R. B., Steinkühler, J., Knorr, R. L., Dimova, R. & Riske, K. A. Posing for a picture: Vesicle immobilization in agarose gel. Sci. Rep. 6, 1–12 (2016).
224. Bartelt, S. M., Steinkühler, J., Dimova, R. & Wegner, S. V. Light-Guided Motility of a Minimal Synthetic Cell. Nano Lett. 18, 7268–7274 (2018).
225. Magdeldin, S. & Moser, A. Affinity Chromatography: Principles and Applications. Affin. Chromatogr. (2012).
226. Tareste, D., Pincet, F., Brellier, M., Mioskowski, C. & Perez, É. The binding energy of two nitrilotriacetate groups sharing a nickel ion. J. Am. Chem. Soc. 127, 3879–3884 (2005).
227. Ali Doosti, B. et al. Membrane Tubulation in Lipid Vesicles Triggered by the Local Application of Calcium Ions. Langmuir 33, 11010–11017 (2017).
228. Karimi, M. et al. Asymmetric Ionic Conditions Generate Large Membrane Curvatures. Nano Lett. 18, 7816–7821 (2018).
229. Steinkühler, J. et al. Controlled division of cell-sized vesicles by low densities of membrane-bound proteins. Nat. Commun. 11, 1–11 (2020).
230. Martin, D. Evaluation of the Dielectric Capability of Ester Based Oils for Power Transformers, A thesis submitted to The University of Manchester (2007).
231. Parham, W. E. & Anderson, E. L. The Protection of Hydroxyl Groups. J. Am. Chem. Soc. 70, 4187–4189 (1948).
232. Schelhaas, M.; Waldmann, H. Schutzgruppenstrategien in der organischen Synthese. Angew. Chemie 2192–2219 (1996).
233. Bunker, A. Poly(Ethylene Glycol) in Drug Delivery, Why Does it Work, and Can We do Better? All Atom Molecular Dynamics Simulation Provides Some Answers. Phys. Procedia 34, 24–33 (2012).
234. Radda, G.K.; Berden, J.A.; Barker, R. W. NMR Studies on Phospholipid Bilayers. Biochim. Biophys. Acta - Biomembr. 375, 186–208 (1975).
235. Marquardt, D. et al. 1H NMR Shows Slow Phospholipid Flip-Flop in Gel and Fluid Bilayers. Langmuir 33, 3731–3741 (2017).
236. Veatch, S. L., Polozov, I. V., Gawrisch, K. & Keller, S. L. Liquid Domains in Vesicles Investigated by NMR and Fluorescence Microscopy. Biophys. J. 86, 2910–2922 (2004).
237. Husen, P., Arriaga, L. R., Monroy, F., Ipsen, J. H. & Bagatolli, L. A. Morphometric image analysis of giant vesicles: A new tool for quantitative thermodynamics studies of phase separation in lipid membranes. Biophys. J. 103, 2304–2310 (2012).

238. Uppamoochikkal, P., Tristram-Nagle, S. & Nagle, J. F. Orientation of tie-lines in the phase diagram of DOPC/ DPPC/cholesterol model biomembranes. Langmuir 26, 17363–17368 (2010).
239. Hull, M. C., Cambrea, L. R. & Hovis, J. S. Infrared spectroscopy of fluid lipid bilayers. Anal. Chem. 77, 6096–6099 (2005).
240. Kraft, M. L., Weber, P. K., Longo, M. L., Hutcheon, I. D. & Boxer, S. G. Phase separation of lipid membranes analyzed with high-resolution secondary ion mass spectrometry. Science (80-.). 313, 1948–1951 (2006).
241. Gunnarsson, A., Kollmer, F., Sohn, S., Höök, F. & Sjövall, P. Spatial-resolution limits in mass spectrometry imaging of supported lipid bilayers and individual lipid vesicles. Anal. Chem. 82, 2426–2433 (2010).
242. Beales, P. A. & Kyle Vanderlick, T. Specific binding of different vesicle populations by the hybridization of membrane-anchored DNA. J. Phys. Chem. A 111, 12372–12380 (2007).
243. Chan, Y. H. M., Van Lengerich, B. & Boxer, S. G. Effects of linker sequences on vesicle fusion mediated by lipid-anchored DNA oligonucleotides. Proc. Natl. Acad. Sci. U. S. A. 106, 979–984 (2009).
244. Holmberg, A. et al. The biotin-streptavidin interaction can be reversibly broken using water at elevated temperatures. Electrophoresis 26, 501–510 (2005).
245. Shetty, S., Yandrapalli, N., Pinkwart, K., Krafft, D., Vidaković-Koch, T., Ivanov, I., and Robinson, T. (2021). Directed Signaling Cascades in Monodisperse Artificial Eukaryotic Cells. (pre - print)
246. Yandrapalli, N., Petit, J., Bäumchen, O., and Robinson, T. (2020). Surfactant-free production of biomimetic artificial cells using PDMS-based microfluidics. bioRxiv, 2020. (pre - print)

List of Figures

List of Tables

Abbreviations

AC	alternating current
BSA	bovine serum albumin
CCD	charge - coupled device
cDICE	continuous droplet interface crossing encapsulation
Chol	cholesterol
CMC	critical micelle concentration
DGS-Ni-NTA	1,2-dioleoyl-*sn*-glycero-3-[(N-(5-amino-1-carboxy-pentyl) iminodiacetic acid)succinyl] (nickel salt)
DIC	differential interference contrast microscopy
DiI	dialkylcarbocyanine
DNA	deoxyribonucleic acid
DOPC	1,2-dioleoyl-sn-glycero-3-phosphocholine
DOPG	1,2-Dioleoyl-*sn*-glycero-3-phospho-*rac*-(1-glycerol)
DPPC	1,2-dipalmitoyl-sn-glycero-3-phosphocholine
ER	endoplasmic reticulum
FCS	fluorescence correlation spectroscopy
FRET	foerster resonance energy transfer
GUV	giant unilamellar vesicle
iLID	improved light - induced dimer protein
iPC	inverted phosphocholine
ITO	indium tin oxide
kbp	kilobase pair
LUCA	last universal common ancestor
LUV	large unilamellar vesicle
M	mol/l
MLV	multilamellar vesicle
MVV	multivesicular vesicle (vesosome)
NA	numerical aperture
Nano	wild - type SspB
NMR	nuclear magnetic resonance
NNR	nearest - neighbour recognition
PBS	phosphate buffered saline
PDMS	poly(dimethylsiloxane)
PE biotin	1,2-dioleoyl-sn-glycero-3-phosphoethanolamine-N-(cap biotinyl)
PEG	polyethylene glycol
PI	phosphoinositol/phosphoinositide
PLA	polylactic acid
POPC	1-palmitoyl-2-oleoyl-glycero-3-phosphocholine
RNA	ribonucleic acid
SM	sphingomyelin
ssDNA	single - stranded DNA
SUV	small unilamellar vesicle
T_M	transition temperature (melting temperature)
TRIMEB	heptakis(2,3,6 - tri - O - methyl) - β - cyclodextrin
TRIS	tris(hydroxymethyl)aminomethane